ULTRASONIC ABSORPTION BY LIPOSOMES NEAR THE PHASE TRANSITION AS A FUNCTION OF DIAMETER

BY

VALERIE MARIE MAYNARD

B.A., Bradley University, 1974

THESIS

Submitted in partial fulfillment of the requirements
for the degree of Doctor of Philosophy in Biophysics
in the Graduate College of the
University of Illinois at Urbana-Champaign, 1984

Urbana, Illinois

ACKNOWLEDGEMENTS

The author is deeply grateful for the sustentative support of Professor Floyd Dunn. Assistance from and collaboration with Professor Richard Magin in the study of liposomes are also greatly appreciated. In addition, gratitude is extended to Dr. Frieder Eggers for helpful suggestions, Billy McNeil for building the interferometer, Dr. Phil Strom-Jensen for dealing successfully with a number of experimental problems, Michael Niesman for liposome synthesis, Robert Cicone for the excellent illustrations, Wanda Elliot for much assistance with a task second in frustration only to doing experiments, viz., the final preparation, and Dr. Ron Johnston, for whose help and friendship no description is attempted.

This work was supported by the following grants: 5 T32 CA09067 and CA1-1-20910-01 of the National Cancer Institute, DHHS; GM12281 of the National Institutes of Health; and 82-9 of the American Cancer Society, Illinois Division.

TABLE OF CONTENTS

CHAPTER 1

INTRODUCTION

Ultrasound is a pressure wave with frequencies above the human perception limit, viz., about 20 kHz. Its propagation through various kinds of media depends upon the densities and compressibilities of these media. At megahertz frequencies these properties of biological media are particularly well suited to an interaction with ultrasound, allowing it to be used diagnostically or therapeutically, depending mainly upon amplitude. The investigation described herein is concerned only with those interactions which may accompany the diagnostic application of ultrasound. The mechanisms by which ultrasonic energy is lost to the media are poorly understood. It is known, however, that the interactions are complex, involving the simultaneous perturbation of at least several equilibria.

An approach to the study of such complex systems is the study of individual components of the system. Pauly and Schwan (1970) have shown that for liver tissue, the large scale tissue structure does not contribute significantly to attenuation. Thus attention should be focused upon some aspect of cellular structure; in this study, it is the membrane. Erythrocyte ghost membranes contribute to absorption in a quantitatively similar manner to that of liver tissue (Kremkau & Carstensen, 1972). Simplification of the biological system also permits greater control of the ambient conditions such as temperature and composition of the associated solution. Focusing on individual components of a system can increase the choices of investigative techniques to be utilized,

which may improve the optimal conditions which can be achieved for the study of particular phenomena. However, when the process is reversed, i.e., when interpretations are extrapolated from the simplified system to that with full complexity, the implications of the simplification process must be considered.

In addition to the study of membranes as a step in the elucidation of the interaction of ultrasound with tissue, the investigation of membranes, per se, is important. The growing knowledge of cellular function has been accompanied by discoveries of the involvement of membranes in many of those functions. Ultrasound can make unique contributions to such studies because it can yield information about the mechanical properties. For example, compressibility is related to membrane permeability, and bulk viscosity, which influences ultrasonic absorption, is related to membrane fluidity (Mitaku & Okano, 1981).

As biological membranes are very complex structures, it is possible that certain aspects can be understood better by modeling structural and functional characteristics, and pursuing the study of such models. Such studies have contributed significantly to the understanding of biomembrane structure and function (Jain, 1983). The basic structural characteristics of biomembranes which were known before the introduction of the models used in the present study include the following. The two major molecular components are proteins and phospholipids. The phospholipids are arranged in a bilayer. It was found that proteins associate with the membrane in various ways, ranging from the occupation of positions entirely external to the bilayer, i.e., associating only with the surface, to their insertion entirely through the bilayer.

The bilayer aspect of the structure is due to the amphipathic nature of the constituent molecules, mainly the phospholipids (fig. 1.1). The two basic regions of their structure are a phosphate-containing polar region, referred to as the head group, and a hydrophobic region, which consists usually of two roughly parallel hydrocarbon chains. (Figure 1.2 illustrates the two types of phospholipid molecules used in this study.) Their arrangement is probably a minimum energy condition for the polarity of their environment, with the intermolecular interactions being only polar and hydrophobic; there is no evidence of covalent bonds in membranes. Biomembranes probably self-assemble in their polar environment (Lehninger, 1972).

Bangham et al. (1965) showed that aqueous dispersions of phospholipids spontaneously form closed bilayer structures. Thus a physical system modeling the phospholipid bilayer aspect of biomembrane structure can be synthesized. These artificial membranes are called liposomes. (Other artificial membranes are also called liposomes, for they are defined as any type of lipid bilayer surrounding an aqueous space (Papahadjopoulos, 1976); i.e., lipids other than phospholipids are allowed.)

Three categories of liposomes have emerged, depending upon size and structure. Historically, the first to be synthesized and studied were multilamellar vesicles, MLV (Bangham et al., 1965). These consist of two or more roughly concentric bilayer spheres with diameters ranging from 1 to 10 μm. Single bilayer vesicles (Huang, 1969), called small unilamellar vesicles, SUV, are usually considered as those with diameters of less than 100 nm (Szoka &

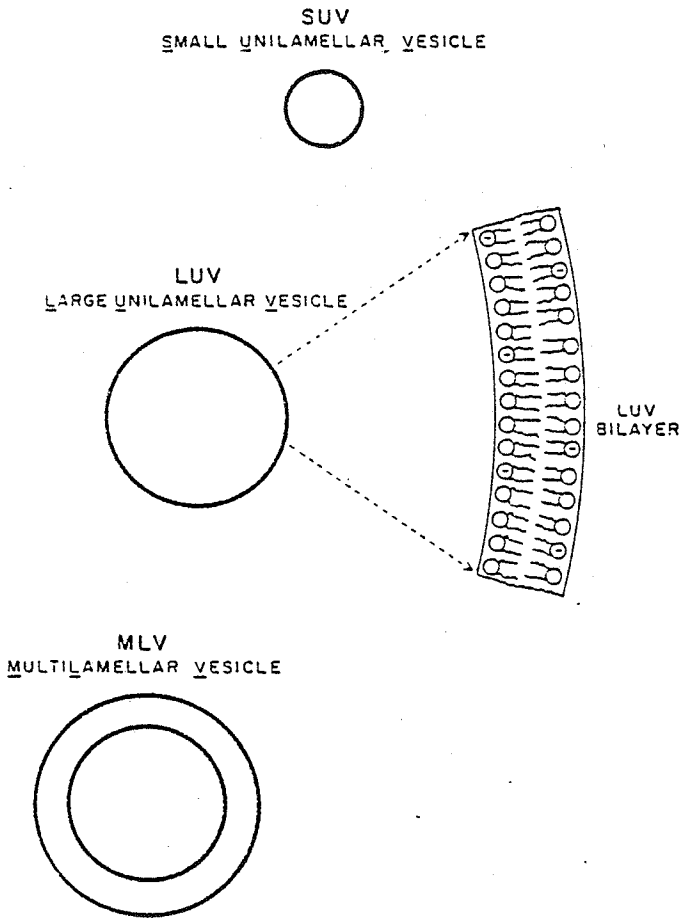

Figure 1.1 The three general categories of liposomes with an enlargement of bilayer portion. The negative head groups indicate the 20% of the molecules which are DPPG (cf. fig. 1.2).

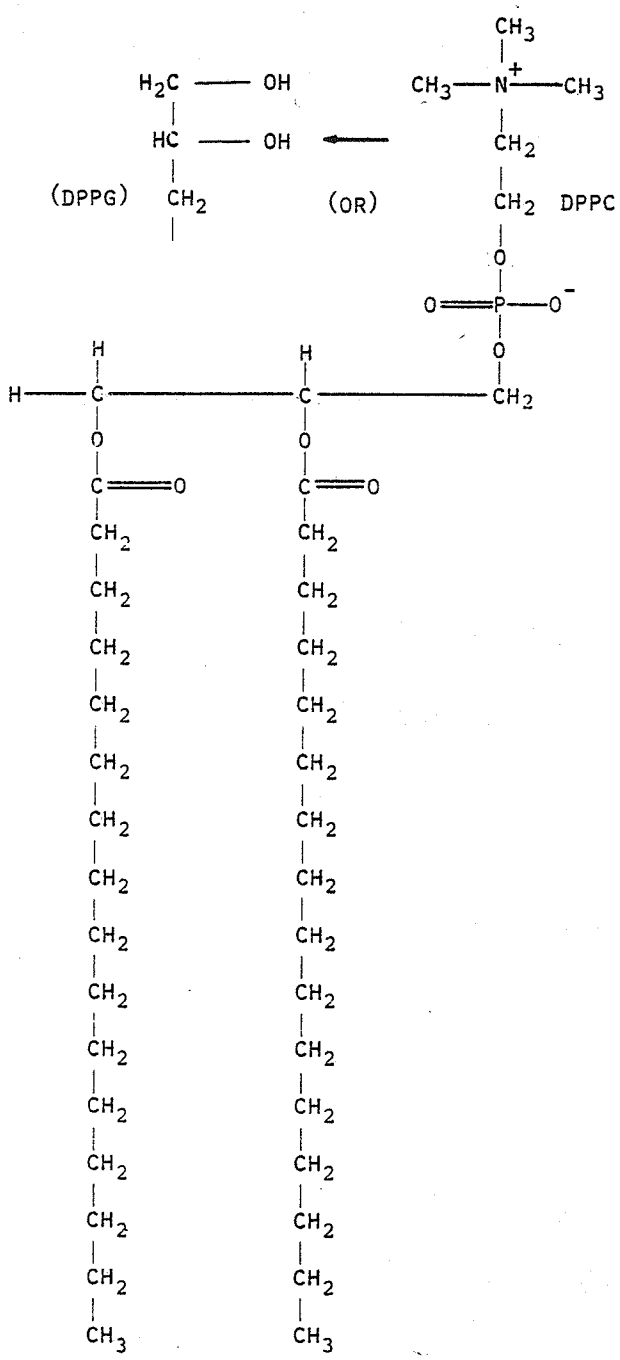

Figure 1.2 Molecular constituents of the liposomes used in this study, viz.,
dipalmitoylphosphatidylcholine (DPPC)
dipalmitoylphosphatidylglycerol (DPPG)
They differ only in the headgroup.

Papahadjopoulos, 1980). Larger single bilayer vesicles (Deamer & Bangham, 1976) are called large unilamellar vesicles, LUV.

The responses of liposomes to a variety of physiologic and pharmacologic agents in terms of ionic and molecular diffusion are qualitatively the same as those of erythrocytes, lysosomes, and mitochondria (Sessa & Weismann, 1968). In addition to their role as model membranes, other uses and potential uses of liposomes suggest the importance of acquiring a better understanding of these vesicles. These uses include a biodegradable package for localized drug delivery, a foreign particle with which to study the recognition of "non-self", and an agent to deliver substances into cells in vitro for the purpose of studying cell growth, division, genetic manipulation, and death (Bangham, 1981).

One of the most interesting physical properties of liposomes is their ability to undergo a reversible thermotropic transition (Chapman & Collin, 1965). The low temperature state is called the solid, gel, crystalline, or ordered phase, and the high temperature state is called the liquid, fluid, liquid-crystalline, or disordered phase (Jain, 1983). Some authors qualify speculation by referring to a phase as, for example, the crystalline-like state, or the quasi-crystalline state (Melchior & Steim, 1976), all symptoms of a system not well understood.

What is known about this transition concerns the intramolecular behavior of the hydrocarbon chain (Jain, 1983). In the ordered phase, the all-trans state is energetically favored. These chains can pack closely. If an activation energy of 3 kcal/mol is supplied, a C—C bond rotation can occur. The new conformation, gauche, is another energetically favorable state,

with a free energy 0.3 to 0.5 kcal/mol greater than that of the trans conformer. The resulting bend in the chain prevents close packing unless more than one trans-gauche transition per chain occurs, forming a kink which minimizes the bend. Even so, kinks cause some disorder compared to a completely close-packed structure. Since the hydrocarbon chain interactions are largely responsible for the bilayer organization, the study of the changing membrane behavior as a function of temperature should yield information of this organization.

A strong dependence of ultrasonic absorption on temperature over a particular temperature range has been observed for all types of liposomes studied (Sano et al., 1982). A number of techniques have shown similarly strong dependences at the same, or nearly the same, temperatures. These include dilatometry, NMR spectrometry, X-ray diffraction, IR and raman spectroscopy, spin and fluorescent labeling, and differential scanning calorimetry (DSC) (Fleischer & Packer, 1974). Spectroscopic techniques and techniques which involve the addition of a label can yield valuable information concerning the molecular events which are part of a transition. However, the overall course of a transition seems to be described best by thermodynamic methods (Melchior & Steim, 1976). The extent to which it has occurred can be revealed by DSC, which measures the change in the heat capacity exhibited by a thermal transition. Heat capacity data define a peak near the transition temperature, "whose shape faithfully reflects the extent of the transition" (Melchior & Steim, 1976). Sound is also a thermodynamic method which reveals an entropy change (cf. Eq. 2.6) upon acoustic perturbation of an equilibrium.

A pertinent question emerges as: To what extent, if any, does the temperature dependence of ultrasonic absorption reflect the extent of a membrane phase transition? The answer, based upon the coincident temperature dependence of DSC and ultrasonic absorption measurements, seems to be: quite well. Harkness and White (1979) obtained an absorption peak for SUV at 39.8°C, and Sano et al., (1982) reported 38.0°C, while Melchior and Steim (1976), using DSC, obtained 39.3°C. Harkness and White obtained a peak for MLV at 41.7°C, while DSC yielded values of 41.5°C (Hinz & Sturtevant, 1972) and 43.5°C (Melchior & Steim, 1976). The broadness of the peaks, quantified as the width at one half of the amplitude, is also similar. For SUV, Harkness and White obtained a value of 7.3°C using ultrasound, and Melchior and Steim obtained 8°C using DSC. All of these results pertain to liposomes synthesized from DPPC (cf. section 3.1.1) and are in general agreement with the other techniques. Thus ultrasound appears to provide a tool which can be used to study membrane phase transitions.

In addition to its role as a thermodynamic method agent, along with DSC and dilatometry, of being sensitive to the overall course of a transition, ultrasound fills an important position in the study of phase transitions due to its dynamic nature. If the transition is due to a single process, the dynamic nature of the method should be irrelevant. However, if there is more than one process having partially compensating contributions to the measured thermodynamic variables, a static method, which reflects only the end points of a process occurring on a time scale of less than about a minute (Adamson, 1973), will yield the net

contribution. Ultrasound, in addition to being a function of thermodynamic variables, is also a function of frequency (cf. Eq. 2.27). Therefore, ultrasound can interact with processes having a time constant on the order of the period of the sound wave, and will do so individually to the extent that these time constants differ (Eggers & Funck, 1976).

The relevance of the study of liposome phase transitions involves more than the elucidation of the determinants of bilayer organization. Practical applications, such as the potential use of liposomes as drug delivery vesicles, exploit the occurrence of such transitions because the membrane permeability increases significantly near the transition temperature (Bangham, 1981). Phase transitions and spatial phase separation also occur in biomembranes. Little is known about the actual role played by these phenomena in physiological well-being, viability, or even survival (Jain, 1983). However, many specific effects have been observed, such as the enhancement of enzymatic activity and specific transport by the experimental induction of the transition (Overath & Träuble, 1973). In one case, a $1^{o}C$ decrease of temperature resulted in the doubling of sugar transport (Linden et al., 1973). At physiological temperatures, evidence of phase transitions is accumulating, e.g., the cytochrome P450-reductase system in liver microsomes (Stier & Sackmann, 1973). The potential for physiological control of function by membrane phase variations is great.

Typical results of phase transition studies of SUV and MLV were given above. They are quantitatively quite different, as are their sizes. The more recently developed LUV have been studied

much less. For some liposome applications, however, LUV would be preferable. For example, as a drug delivery vesicle, their size is advantageous compared to that of SUV, and their more homogeneous structure makes them preferable to MLV. These same two characteristics also make them a better choice for model membranes.

There have been two previous ultrasonic investigations of LUV. Strom-Jensen (1983) studied LUV, of the same composition as those used in this study, with an average diameter of 200 nm and a rather broad distribution of sizes, as a function of the addition of cholesterol or gramicidin to the membrane. The pure phospholipid bilayers exhibit a temperature dependent absorption coefficient similar to that of MLV. Sano et al., (1982) studied LUV with a similar composition to that used here, and with an average diameter of 90 nm and a rather narrow distribution.

Two parameters from these studies can be compared to those same transition characteristics for SUV and MLV in an attempt to understand the reasons for the different characteristics exhibited by the two size extremes. Those parameters are the temperature at which the peak has its maximum value, T_m, and the van't Hoff enthalpy, ΔH_{vH}, which is a function of the sharpness of the peak. LUV have a larger T_m than SUV and about the same as MLV. ΔH_{vH} increases for both size increases. The results are summarized below:

$$\begin{array}{ccccc} \text{SUV} & \longrightarrow & \text{LUV} & \longrightarrow & \text{MLV} \\ T_m\uparrow & & T_m= & & \\ \Delta H_{vH}\uparrow & & \Delta H_{vH}\uparrow & & \end{array}$$

The following describes studies undertaken of all three types of liposomes, including several different size distributions of LUV and MLV.

CHAPTER 2

ACOUSTIC THEORY

2.1 PLANE WAVE PROPAGATION IN FLUIDS

2.1.1 Ideal

A repeated pressure disturbance propagates in a fluid due to the inertial and restoring force properties of the medium. The propagation is described by a wave equation, which involves the temporal and spatial behavior of the disturbance. It is derived from an analysis of the effect of pressure changes on the translational and dimensional changes of a material particle of the medium. The particle is a mass unit of the fluid which is large enough to be characterized thermodynamically yet small enough so that the thermodynamic properties are constant over its volume. In a homogeneous fluid, for any function which describes the cause of a disturbance at each point in space and time, there is a function which describes the effect of the disturbance; e.g., for any function which describes the spatial and temporal behavior of pressure, there is a function which describes the spatial and temporal behavior of the particle velocity. The wave equation is a combination of these two functions. As such, it must be derived from two independent relations involving these variables. These relations are the law of conservation of mass and Newton's second law of motion. In addition, an explicit relationship between the thermodynamic variables which describes the medium independently of the laws of motion, i.e., an equation of state, is required.

2.1.1.1 Continuity Equation

The mass conservation law for fluid motion leads to the equation of continuity. For a particle with mass, m, density, ρ, and volume, V, conservation of mass can be expressed as

$$\frac{dm}{dt} = \frac{d}{dt}(\rho V) = 0 \qquad (2.1)$$

Here, d/dt is the total derivative,

$$\frac{d}{dt} = \frac{\partial}{\partial t} + \frac{\partial x}{\partial t}\frac{\partial}{\partial x} + \frac{\partial y}{\partial t}\frac{\partial}{\partial y} + \frac{\partial z}{\partial t}\frac{\partial}{\partial z} = \frac{\partial}{\partial t} + \vec{v} \cdot \vec{\nabla}$$

which includes the consideration of the particle's translational motion. The dynamic conservation equation essentially states that if a volume element is assigned as the container of a certain amount of mass, any spatial or temporal change in the volume element is accompanied by the corresponding density change which will maintain the constant amount of mass. The total derivative can be applied to V to yield an equivalent expression involving a change in velocity only [Symon, 1971]:

$$\frac{dV}{dt} = V\,\vec{\nabla} \cdot \vec{v}$$

Substituting this equation into Eq. (2.1) and dividing by V yields

$$\rho\,\vec{\nabla} \cdot \vec{v} + \frac{\partial \rho}{\partial t} + \vec{v} \cdot \vec{\nabla}\,\rho = 0 \qquad (2.2)$$

Also since

$$\rho\vec{\nabla} \cdot \vec{v} + \vec{v} \cdot \vec{\nabla}\rho = \vec{\nabla} \cdot (\rho\vec{v})$$

(Symon, 1971), Eq. 2.2 then takes the form referred to as the equation of continuity:

$$\frac{\partial \rho}{\partial t} + \vec{\nabla} \cdot (\rho \vec{v}) = 0 \ . \qquad 2.3$$

The meaning of this equation is more easily realized by considering its volume integral. This expresses the rate of mass change in the constant volume as a density change. Equations 2.1 and 2.3 differ essentially only in the parameter which is chosen to be constant.

Since the density changes and particle velocities dealt with in this study are small, the continuity equation can be simplified by retaining only first order terms involving these variables. (These criteria are satisfied if the intensity is appreciably less than 1 W/cm^2 (Eigen & de Maeyer, 1963).) In particular, if the relative density change, the condensation, is defined as

$$\delta \equiv \frac{\rho - \rho_o}{\rho_o} \ ,$$

where ρ_o is the ambient density, then Eq. 2.3 simplifies to

$$\frac{\partial \rho}{\partial t} = -\vec{\nabla} \cdot \vec{v} \ . \qquad 2.4$$

2.1.1.2 Motion Equation

An ideal fluid experiences no shear viscosity. Therefore, a force exists only when there is a normal (non-tangential) pressure gradient. The force on the particle is

$$\vec{F} = -\vec{\nabla} pV$$

where p is the acoustic, or excess, pressure, i.e., the difference between the instantaneous pressure and the constant ambient pressure. Newton's second law will then be

$$-\vec{\nabla}pV = \rho V\frac{d\vec{v}}{dt}.$$

When this equation is made linear with respect to small terms, in the same way as the continuity equation, the result is

$$-\vec{\nabla}p = \rho_o \frac{\partial\vec{v}}{\partial t} . \qquad 2.5$$

2.1.1.3 State Equation

Next the explicit relationship between pressure and density must be determined. To a first approximation, a sound wave is an adiabatic process both at relatively high and low frequencies. It has long been reasoned that high frequencies have periods which are too short to allow significant dissipation of the rather small temperature gradients which accompany the pressure gradients. However, the irreversible heat transfer by conduction is proportional to the square of the frequency. Thus the adiabatic characteristic of sound actually increases as the frequency decreases (Herzfeld & Litovitz, 1959). Therefore, it is prudent to consider a form of the combined first and second laws of thermodynamics in which pressure and volume are independent, viz.,

$$Tds = \kappa_s dP + dv \qquad 2.6$$

where T is temperature, κ_s is adiabatic compressibility, P is pressure, and s and v are specific entropy and volume,

respectively. ("Specific" denotes the mass independent form of an extensive variable, e.g., v = V/m.) For a reversible adiabatic process, the entropy remains constant, in which case Eq. 2.6 becomes

$$dP = \frac{1}{\rho \kappa_s} d\rho,$$

where ρ has been substituted for 1/v. This is an equation of state since it is a relationship between two independent state variables, pressure and density, with a third state variable, entropy, held constant. The relevant pressure is the acoustic pressure, p, defined as

$$p \equiv P - Po,$$

where Po is the constant equilibrium pressure. Therefore, dP = dp, and the state equation becomes

$$dp = \frac{1}{\kappa_s} d\delta,$$

where the condensation has been substituted for the relative excess density, and small density changes have been assumed. An acoustical equation of state must be dynamic. The partial time derivative, simplified because of small density and pressure changes and the assumption that κ_s is approximately independent of time, is

$$\frac{\partial \delta}{\partial t} = \kappa_s \frac{\partial p}{\partial t} . \qquad 2.7$$

2.1.1.4 Wave Equation

The acoustical equation of state can be used to write the motion equation in terms of density rather than pressure or the continuity equation in terms of pressure rather than density. Substituting Eq. 2.7 into the continuity equation (2.4) yields

$$\kappa_s \frac{\partial p}{\partial t} = - \vec{\nabla} \cdot \vec{v} \ . \qquad 2.8$$

The juxtaposition of the motion equation,

$$\rho_o \frac{\partial \vec{v}}{\partial t} = - \vec{\nabla} p \quad , \qquad 2.5$$

illustrates the two fundamental differential equations (2.8 and 2.5) for sound waves (Symon, 1971). They show that for the pressure and velocity describing the propagation of sound, the time derivative of either is proportional to the space derivatives of the other.

These two equations can be combined, eliminating either of the dependent variables, to yield an equation which completely describes the behavior of the other, the wave equation. Taking the partial time derivative of Eq. 2.8, the divergence of Eq. 2.5, interchanging the order of differentiation in either (since the partial derivatives are continuous (Leithold, 1968)), and combining the resulting equations, eliminates $\vec{v}$:

$$\frac{\partial^2 p}{\partial t^2} = \frac{1}{\rho_o \kappa_s} \vec{\nabla}^2 p \ . \qquad 2.9$$

In general, the constant in a wave equation is denoted as c^2. It is obvious from Eq. 2.9 that $1/\rho_o\kappa_s$ has the same units as has velocity squared. Indeed, it will be shown that c_o is the phase velocity of the wave described by

$$\frac{\partial^2 p}{\partial t^2} = c_o^2 \vec{\nabla}^2 p \ , \qquad 2.10$$

where $c_o \equiv 1/(\rho_o \kappa_s)^{1/2}$. defn. 2.1

The subscript denotes that the phase velocity is constant, a condition which holds only in the ideal case.

The propagation of plane waves in one dimension only is considered. Therefore, Eq. 2.10 can be simplified to a one-dimensional wave equation:

$$\frac{\partial^2 p}{\partial t^2} = c_o^2 \frac{\partial^2 p}{\partial x^2} \ . \qquad 2.11$$

Wave equation

2.1.1.5 Solution

A solution to the wave equation can be obtained by the method of separation of variables:

$$p(x,t) = F(x)G(t) \qquad 2.12$$

Substituting into Eq. 2.11 and dividing by F(x)G(t) yields

$$\frac{1}{G(t)} \frac{\partial^2 G(t)}{\partial t^2} = \frac{c_o^2}{F(x)} \frac{\partial^2 F(x)}{\partial x^2} \ .$$

With the variables so separated, each side must equal the same constant. It is conveniently denoted as $-\omega^2$ to assure that it is negative. A consideration of the physical situation discloses the

necessity of requiring the instantaneous pressure, G(t), to be opposite its acceleration in order to assure a return to equilibrium. The resulting equations are

$$\frac{\partial^2 G(t)}{\partial t^2} + \omega^2 G(t) = 0 \quad \text{and} \quad \frac{\partial^2 F(x)}{\partial x^2} + \frac{\omega^2}{c_o^2} F(x) = 0 \ .$$

Solutions to the first are $G(t) = G(0)e^{\pm i\omega t}$ and to the second are $F(x) = F(0)e^{\pm i(\omega/c_o)x}$. It is thus seen that the square root of the negative of the constant, $-\omega^2$, functions as an angular frequency. The solution to the wave equation is, using Eq. 2.12,

$$p(x,t) = p_o e^{\pm i(\omega/c_o)x \pm i\omega t} = p_o e^{\pm i(\omega/c_o)(ct \pm x)} ,$$

where $p_o \equiv p(0,0)$. From this form of the solution, it can be seen that c_o is indeed the phase velocity. The solution is often written in terms of the wavenumber, k_o, as

$$p = p_o e^{\pm i(\omega t \pm k_o x)} , \qquad 2.13$$

where $k_o \equiv \omega/c_o$.

2.1.2 Absorption

There is, of course, energy involved in the propagation of acoustic waves, both potential, which is an explicit function of acoustic pressure, and kinetic, which is an explicit function of particle velocity. (Equations 2.5 and 2.8 could have been solved for the velocity, as they were for the pressure.) The derivation of the ideal wave equation assumed no net energy transfer from the wave to the medium. This was formally introduced by maintaining constant entropy. In reality, ultrasonic wave propagation is accompanied by attenuation of the wave energy. Attenuation is

conveniently divided into two categories, defined by whether or not boundaries are involved. A system without boundaries will be considered here. The attenuation for this case is referred to as absorption. Absorption is conveniently divided into two categories, depending upon whether or not it is a function of macroscopic properties of the medium or microscopic properties. There are two macroscopic absorption mechanisms. No fluid will propagate a dynamic shear stress without loss because all fluids have the macroscopic property of viscosity (Herzfeld & Litovitz, 1959); i.e., there is a resistance to relative motion which prevents a proportional relationship between pressure and density changes from being instantaneous. The other macroscopic absorption mechanism is heat conduction, which occurs if the medium has a nonzero thermal conductivity, a characteristic of most, if not all fluids (Herzfeld & Litovitz, 1959). Thus all fluids absorb ultrasound via a macroscopic mechanism. In addition, all fluids which are not monatomic absorb ultrasound via one or more microscopic mechanisms (Herzfeld & Litovitz, 1959). These involve molecular energy exchanges, resulting in structural and thermal changes of the medium.

The effect of absorption on the propagation of ultrasound is illustrated formally by a modification of the wave equation. This modification has been developed by a number of different theories; in each case, it is the acoustic equation of state in which absorption is introduced, although this is not always obvious. The approach is based upon the recognition that, in general, acoustic absorption is due to a phase angle difference between the instantaneous values of pressure and condensation. This can be

deduced by considering the combined first and second laws of thermodynamics,

$$TdS = dW + dU,$$

where S is entropy, W is work, and U is internal energy. As discussed below, absorption is always accompanied by an increase in entropy. Since TdS undergoes a net increase over one complete cycle, dW + dU does also. For an acoustic process, the energy initially appears as work being a function of pressure and volume. To obtain an increase in dW over one complete pressure cycle, there must be a phase difference between pressure and volume. This can be represented by separate paths of integration on a pressure vs. volume diagram. Any of this energy which is converted to internal energy will, even if totally reconverted to work, contribute to an increase in dW, since it will contribute to this phase difference. Work done on the medium is, of course, energy lost by the ultrasonic wave and, since the energy density is proportional to the square of the pressure amplitude (Kinsler & Frey, 1962), absorption results in a decrease in pressure amplitude. The explicit dependence of pressure on absorption is given below.

2.1.2.1 Equations of State

Before an equation of state is used to derive this relation and an expression for the absorption coefficient in terms of thermodynamic variables and frequency (section 2.1.2.2), a general discussion of state equations is presented. The choice of the state equation is usually a function of what is already known aaabout a system and what the speculations are concerning what is

not known. Therefore, it is of central importance in the analysis of absorption behavior, and its restrictions, if any, on that analysis should not be forgotten. The theories which have been designed to investigate absorption are divided here into five categiries, viz., kinetic, statistical thermodynamic, irreversible thermodynamic, viscoelastic, and phenomenological. They all yield an equation of state and, consequently, an expression for the absorption coefficient, of the same form. The basic problem in the search for an absorption mechanism then is the assignment of particular parameters to the general form. One special case, heat conduction, is given as as example. The general form of the state equation can also be obtained by the combination of two earlier and simpler approaches. One of these has been proven to be an accurate description of one particular absorption mechanism. These simpler approaches are discussed first. An acoustic equation of state proferred by Maxwell (1867) is

$$p = -\frac{1}{\gamma_s}\frac{\partial p}{\partial t} + \frac{1}{\kappa_s}\frac{\partial \delta}{\partial t} \qquad 2.14$$

where γ_s is a constant of the medium. The different time functions experienced by pressure and condensation result in a phase difference between them. However, the resulting absorption coefficient, (which will be defined later), has a frequency dependence which is unrelated to experience.

The first successful acoustic state equation was introduced by Stokes (1845). Analagous to the static stress-strain relationship for a solid, Stokes added a term, proportional to the rate of strain, to the ideal equation of state:

$$p = \frac{1}{\kappa_s}\delta + \zeta\frac{\partial \delta}{\partial t}, \qquad 2.15$$

where ζ is a constant associated with the viscosity of the medium. In an isotropic medium, two independent constants are necessary to describe completely the stress-strain relationship, even in one dimension (Beyer & Letcher, 1969). For a fluid, they are put into the convenient form:

$$\zeta = \eta' + \frac{4}{3}\eta ,$$

where η is the shear viscosity coefficient, and η' is often referred to as the bulk, or volume, viscosity. Although Stokes recognized the possibility that liquids could experience a viscous reaction to a stress applied uniformly in three dimensions, measuring the effects seemed hopeless. Therefore, he assumed that $\eta' = 0$ (Herzfeld & Litovitz, 1959). The resulting absorption coefficient can be shown to be

$$\alpha = \frac{\omega}{\sqrt{2}c_o}\left\{\frac{\left[1+\left(\frac{4\eta}{3\rho_o c_o^2}\omega\right)^2\right]^{1/2}-1}{1+\left(\frac{4\eta}{3\rho_o c_o^2}\omega\right)^2}\right\}^{1/2} \qquad 2.16$$

(Kinsler & Frey, 1962). In all but very viscous liquids, $4\eta/3\rho_o c_o^2 \ll 1$. For example, its value for water at 20°C is 6×10^{-13} seconds. Thus for all practical frequencies, Eq. 2.16 can be approximated as

$$\alpha \simeq \frac{2\eta}{3\rho_o c_o^3}\omega^2 .$$

In nonmetallic monatomic liquids, this equation quantitatively describes the absorption. The same is true for polyatomic liquids at relatively high frequencies (Herzfeld & Litovitz, 1959).

Experimental results have shown that in order to describe most of the absorption in most liquids at ultrasonic frequencies, a frequency dependence which is qualitatively different from that of Eq. 2.16 is necessary (fig. 2.1) (Markham et al., 1951). A number of theories have been developed in an attempt to account for this absorption. With one exception, they each take one of two basic approaches. The liquid is assumed to be either a very dense gas or a very disordered crystal (Herzfeld & Litovitz, 1959). The first three theories to be discussed, viz., kinetic, statistical thermodynamic, and irreversible thermodynamic, take the former approach, and viscoelastic takes the latter; the phenomenological approach is the exception. They all yield an equation of state of the same form.

One approach considers the motion as described by gas kinetic theory and tries to determine the stresses after introducing dense packing and smaller mean free paths (Herzfeld & Litovitz, 1959). Absorption occurs because particles can exist in different energy states, and there is a phase lag between the change in translational energy due to a collision with another particle and the attainment of a new thermodynamic equilibrium within the particle, which will be a function of the fraction of this translational energy change which is converted to the particle's internal energy. This approach is more applicable to unassociated liquids.

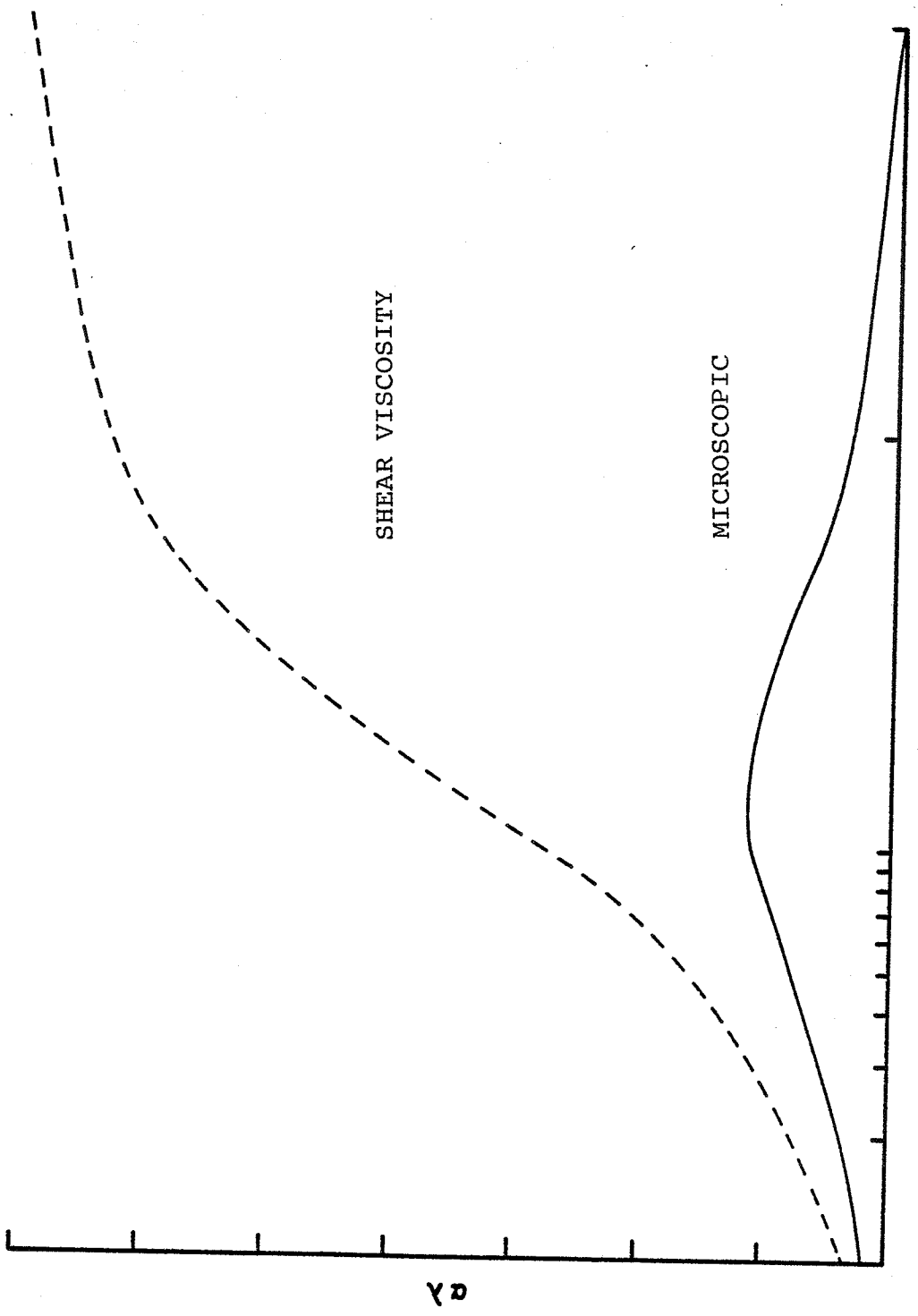

Figure 2.1 Absorption coefficient per wavelength vs. frequency for the shear viscosity mechanism (cf. Eq. 2.16) and for a microscopic mechanism (cf. Eqs. 2.27 & 2.28) (Markham et al., 1951).

The method of statistical thermodynamics also assumes different energy states, but the states are separated by an energy barrier. The energy state is a molecular characteristic rather than a particle characteristic. In an associated liquid, it is a function of the intermolecular bonding, such as hydrogen bonding (Markham et al., 1951). A perturbation, such as a pressure disturbance changes the energy states, thus biasing the probability of transition from one state to another for each molecule. Since this net probability is an exponentially decreasing function of time, the effect of the perturbation outlasts the perturbation, resulting in absorption.

A third approach utilizes irreversible thermodynamics. Any process which experiences absorption is thermodynamically irreversible. Therefore, although the acoustic process is still adiabatic, the entropy change is no longer zero (cf. Eq. 2.6). The problem thus becomes one of finding an expression for the rate of entropy increase. One of the more advanced approaches contains a variable which may be related to an internal temperature (cf. kinetic theory) or to a population of states (cf. statistical thermodynamics) (Markham et al., 1951).

A particular application of irreversible thermodynamics describes the absorption mechanism of heat conduction. This is the second macroscopic mechanism, shear viscosity being the first. As mentioned above, sound propagation is not isothermal. Therefore, temperature gradients occur. The general adiabatic behavior of sound was discussed in section 2.1.1.3. However, under certain circumstances, mentioned at the end of this paragraph, heat conduction can occur. It is discussed here both

because the expession for the absorption coefficient has the form common to the other theories and because, unlike the others, the mechanism is understood well enough to assign specific expressions involving thermodynamic variables to the general variables, thus acting as an example of this assignment. The temperature gradients cause a flow of heat, dissipating these gradients and the pressure gradients to which they return their energy. A form of the combined first and second laws, analagous to Eq. 2.6, with p and T rather than p and v as the independent variables, is used. In this case, the entropy increase is given simply by $K(\partial^2 T/\partial x^2)$, where K is the thermal conductivity. Note that in this special case, the state equation contains a spatial derivative; generally, the equation of state contains only temporal derivatives. It will be seen, however, that the frequency dependence is qualitatively the same. The resulting absorption coefficient for small absorption is

$$\alpha = \frac{c_r}{2c_o^2} \frac{\kappa_s^\infty - \kappa_s^o}{\kappa_s^o} \frac{\omega^2 \tau}{1 + \omega^2 \tau^2}, \qquad 2.17$$

where c_r is the phase velocity when there is absorption (which will be discussed later), κ_s^∞ is the infinite frequency (instantaneous) adiabatic compressibility, κ_s^o is the zero frequency (static) adiabatic compressibility, and τ is a relaxation time (Markham et al., 1951). Eqn. 2.17 is in a general form to facilitate a subsequent comparison with other mechanisms. For heat conduction, $\kappa_s^\infty = \kappa_T$, the isothermal

compressibility, $\kappa_s^o = (c_v/c_p)\kappa_T$ where c_v and c_p are the specific heats at constant volume and pressure, respectively, and $\tau = K/c_p \rho_o c_o^2$. For all liquids except metals, at practical frequencies, $\omega\tau << 1$. Therefore,

$$\alpha \simeq \frac{1}{2c_o} \frac{\kappa_s^\infty - \kappa_s^o}{\kappa_s^o} \omega^2 \tau \ .$$

For water, the contribution of heat conduction to the macroscopic absorption is < 0.1%. Therefore, it can be ignored.

The viscoelastic approach uses the analogy of the stress-strain relationships for an isotropic crystal to write stress-strain and time dependent stress-strain relationships for a liquid (Beyer & Letcher, 1969). It is basically an expansion of the approach used by Stokes, retaining the entire viscosity coefficient. The Stokes equation (2.15) is combined with the Maxwell equation (2.14).

All of the theory categories which attempt to explain microscopic absorption, viz., kinetic, statistical thermodynamic, irreversible thermodynamic, and viscoelastic, assume a model. The qualitative dependence of absorption upon frequency is known from experiments. Therefore, the form of the equation of state which will yield this dependence is known. Indeed, the state equation obtained in all of these theories except for the case of heat conduction, can be put in this form:

$$p = \frac{1}{\rho_o \kappa_s^o} \rho - \tau \frac{\kappa_s^\infty}{\kappa_s^o} \frac{\partial p}{\partial t} + \frac{\tau}{\rho_o \kappa_s^o} \frac{\partial p}{\partial t} \ . \qquad 2.18$$

The coefficients have been defined generally in the paragraph describing heat conduction. The specific parameters upon which

these coefficients depend are a function of the model. These functions for heat conduction appear in that paragraph as examples.

The final approach to the development of an absorption theory is qualitatively different from the others in that it is completely a posteriori. Since the form of the state equation is known, no model need be assumed and, therefore, the coefficients of Eq. 2.18 can be arbitrary, e.g.,

$$p = A\rho + B\frac{\partial p}{\partial t} + C\frac{\partial \rho}{\partial t} . \qquad 2.19$$

An advantage of this approach is that equations of state can be investigated without constructing complicated models. A disadvantage is that the final equations are complicated (Markham et al., 1951).

2.1.2.2 Absorption Coefficient

This approach will be used here to illustrate the origin and, therefore, the meaning of the absorption coefficient and dispersion, i.e., a frequency dependent phase velocity. However, this can be accomplished by avoiding the rigor and complexities mentioned regarding Eq. 2.19 by simply eliminating one of the derivatives. Dropping the pressure derivative leaves the form of the state equation used by Stokes, and substituting condensation for density increases the comparability with the ideal derivation. Thus the new equation of state is

$$p = A\delta + B\frac{\partial \delta}{\partial t} , \qquad 2.20$$

where, at this point, A and B are arbitrary. Following the same procedure as for the derivation of the ideal wave equation, a wave equation which includes the effect of absorption is

$$\frac{\partial^2 p}{\partial t^2} = \frac{A}{\rho_o}\frac{\partial^2 p}{\partial x^2} + \frac{B}{\rho_o}\frac{\partial^3 p}{\partial x^2\, t} .$$

The application of defn. 2.1 results in

$$\frac{\partial^2 p}{\partial t^2} = c_o^2\frac{\partial^2 p}{\partial x^2} + \frac{B}{\rho o}\frac{\partial^3 p}{\partial x^2 \delta t} ,$$

and $$A = \rho_o c_o^2. \qquad 2.21$$

Since for ultrasound, pressure and, therefore, condensation are periodic, the latter can be represented as $\delta = \delta_o e^{i\omega t}$ where δ is the amplitude. Substitution into Eq. 2.20 and using Eq. 2.21 yields

$$\delta = \frac{p}{\rho_o c_o^2 + i\omega B} = \frac{p(\rho_o c_o^2 - i\omega B)}{\rho_o{}^2 c_o{}^4 + \omega^2 B^2} ,$$

which shows that the condensation lags the pressure by a phase angle, ϕ, where $\tan \phi = \omega B/\rho_o c_o^2$.

The periodic aspect of the solution to the wave equation can also be applied to its derivation to result in a more manageable and useful form of the equation. Again substituting $\delta = \delta_o e^{i\omega t}$ into Eq. 2.20 and using Eq. 2.21, this time without the rearrangement used above to solve for δ, the result is

$$p = \rho_o c_o^2 \delta + i\omega B\delta = \rho_o c_o^2(1 + i\omega B/\rho_o c_o^2)\delta. \qquad 2.22$$

If a complex velocity, c, is defined as

$$c \equiv c_o(1 + i\omega B/\rho_o c_o^2)^{\frac{1}{2}}, \qquad \text{defn. 2}$$

Eq. 2.22 becomes

$$p = \rho_o c^2 \delta.$$

The partial time derivative of this equation is an acoustic equation of state which considers absorption. The resulting wave equation is

$$\frac{\partial^2 p}{\partial t^2} = c^2 \frac{\partial^2 p}{\partial x^2} .$$

The solution, expressed in the form of Eq. 2.13, is

$$p = p_o e^{\pm i(\omega t \pm kx)}, \qquad 2.23$$

where the wavenumber is now complex:

$$k = \omega/c. \qquad 2.24$$

It will be useful to separate real and imaginary parts. Therefore, if

$$k_r \equiv \text{Re } k \quad \text{and} \quad \alpha \equiv \text{Im } k, \qquad \text{defn. 3}$$

Eq. 2.23 becomes

$$p = p_o e^{-\alpha x} e^{\pm i(\omega t \pm k_r x)},$$

from which it can be seen that the wave amplitude is damped by the factor, 1/e, upon traveling the distance, $1/\alpha$. Thus, α is referred to as the absorption coefficient.

Referring to Eq. 2.24, it can be seen that by using defns. 2 and 3, α and k_r can be expressed in terms of ω, c_o, ρ_o, and B. Eqn. 2.24, written explicitly in terms of its complex components is

$$\omega = (k_r + i\alpha) c_o (1 + i\omega B/\rho_o c_o^2)^{\frac{1}{2}}.$$

If this is squared and separated into real and imaginary parts, the resulting equations can be solved for α and for k_r. The result for α^2 is

$$\alpha^2 = \frac{-\omega^2}{2c_o^2} \frac{1 \pm [1 + (\omega \frac{B}{\rho_o c_o^2})^2]^{\frac{1}{2}}}{1 + (\omega \frac{B}{\rho_o c_o})^2}, \quad (\pm \rightarrow -) \qquad 2.25$$

Only the solution with the negative sign will result in α being real. Thus

$$\alpha = \frac{\omega}{\sqrt{2} c_o} \left\{ \frac{[1 + (\omega \frac{B}{\rho_o c_o^2})^2]^{\frac{1}{2}} - 1}{1 + (\omega \frac{B}{\rho_o c_o})^2} \right\}^{\frac{1}{2}}.$$

It can be seen that when B = 0, i.e., when there is no loss, $\alpha = 0$.

Equation 2.25 can be simplified for the two cases when ($\omega \sim \rho_o c_o^2/B$) is not true. Consider first $\omega B/\rho_o c_o^2 << 1$. To avoid the trivial result of $\alpha = 0$, use of the Maclaurin series for

$\exp(\omega B/\rho_o c_o^2)^2$ results in the following approximation of Eq. 2.25:

$$\alpha^2 \simeq \frac{-\omega^2}{2c_o^2}\left(-\frac{1}{2}\right)\left(\frac{\omega B}{\rho_o c_o^2}\right)^2, \text{ or } \alpha \simeq \frac{B}{2\rho_o c_o^3}\,\omega^2.$$

When $\omega B/\rho_o c_o^2 >> 1$, $\alpha \simeq (\omega\rho_o/2B)^{\frac{1}{2}}$

The result for k_r is

$$k_r^2 = \frac{\omega^2}{2c_o^2}\,\frac{1 + \left[1 + \left(\omega\frac{B}{\rho_o c_o^2}\right)^2\right]^{\frac{1}{2}}}{1 + \left(\omega\frac{B}{\rho_o c_o^2}\right)^2} \qquad 2.26$$

It can be seen that when $B = 0$, $k_r = \omega/c_o = k_o$. Since the phase velocity is ω/k_r, c_o is no longer the phase velocity. Rather, from Eq. 2.26,

$$c_r = \frac{\omega}{k_r} = \sqrt{2}\; c_o \left\{\frac{1 + \left(\omega\frac{B}{\rho_o c_o^2}\right)^2}{1 + \left[1 + \left(\omega\frac{B}{\rho_o c_o^2}\right)^2\right]^{\frac{1}{2}}}\right\}^{\frac{1}{2}}$$

When $\omega B/\rho_o c_o^2 << 1$, $c_r \simeq c_o\left[1 + \frac{3}{8}\left(\omega\frac{B}{\rho_o c_o^2}\right)^2\right]$.

When $\omega B/\rho_o c_o^2 >> 1$, $c_r \simeq (2\omega B/\rho_o)^{\frac{1}{2}}$.

These approximations show that for the general Stokes form of the equation of state, both the absorption coefficient and the velocity have the same frequency dependencies; viz., at low frequencies, they are proportional to ω^2, and at high frequencies, they are proportional to $\omega^{\frac{1}{2}}$.

An analagous derivation using the equation of state for the model based theories (Eq. 2.18) yields the following general form for the absorption coefficient

$$\alpha = \frac{c_r \tau}{2c_o^2} \frac{\kappa_s^\circ - \kappa_s^\infty}{\kappa_s^\circ} \frac{\omega^2}{1 + \omega^2\tau^2} \qquad 2.27$$

The parameters are defined in the paragraph on heat conduction. This derivation made use of the inequality, $k_r >> \alpha$ (cf. defn. 3). This inequality is valid since the data for this study yield the following order of magnitude values: $k_r \sim 10^2$, $\alpha(\max) \sim 10^{-2}$. Again making use of the inequality,

$$c_r = \left(\frac{1}{\rho_o} \frac{1 + \omega^2\tau^2}{\kappa_s^\circ + \kappa_s^\infty \omega^2\tau^2}\right)^{\frac{1}{2}} . \qquad 2.28$$

When $\omega\tau << 1$, $c_r \simeq (\rho_o \kappa_s^\circ)^{-\frac{1}{2}} = c_o$.

When $\omega\tau >> 1$, $c_r \simeq (\rho_o \kappa_s^\infty)^{-\frac{1}{2}} \equiv c_\infty$.

Using these approximations,

when $\omega\tau << 1$, $\quad \alpha \simeq \frac{\tau}{2c_o} \frac{\kappa_s^\circ - \kappa_s^\infty}{\kappa_s^\circ} \omega^2$,

When $\omega\tau >> 1$, $\quad \alpha \simeq \frac{c_\infty}{2c_o^2\tau} \frac{\kappa_s^\circ - \kappa_s^\infty}{\kappa_s^\circ}$.

2.2 ACOUSTIC INTERFEROMETRY

2.2.1 Introduction

An interferometric method for measuring acoustic attenuation and velocity in fluids was introduced by Pierce (1925). A piezoelectric plate transducer is positioned at one end of a liquid column, and an acoustic reflector is positioned parallel to the vibrator and at the opposite end of the column. The

electrical input impedance of the transducer is a function of the mechanical load provided by the liquid. Since there are reflected waves, this load impedance is not a constant with separation distance of the transducer and reflector. As this distance changes, the load impedance will be be minimal at half wavelength intervals, as will the electrical input impedance. If the transducer is driven by a constant voltage source, the resulting current maxima reflect these impedance changes. When the source is operating at a fixed frequency, the velocity of sound in the intervening medium can be determined from the distance changes which correspond to these maxima. The absorption can be obtained from the ratio of current maxima to minima. The frequencies which can be used are limited to the resonant frequencies of the transducer so that its contribution to the total impedance is real and constant. Even with this simplification, an absorption coefficient is obtained only after much analytical and graphical analysis. In addition, the necessity to move the reflector makes the maintenance of parallelism difficult.

The theory of Pierce considered only a single reflection, which was a good assumption since the fluids being studied were gases. Hubbard (1931) extended the theory by including an infinite number of reflections, thus relaxing the restriction on the magnitude of the absorption coefficients for which the theory is applicable and permitting the inclusion of the effect of imperfect reflections.

An improvement of this method was achieved by Hunter and Fox (1950) by orienting the column vertically with the transducer at the bottom and the upper liquid surface in contact with air. The

reflector is the liquid-air interface, which is a more nearly perfect reflector, resulting in sharper impedance minima.

The two transducer interferometer, introduced by Fry (1949), has the reflector replaced by a transducer identical to the original transducer. One transducer functions as the transmitter and the other as the receiver. This system allows frequencies slightly different from the transducer resonant frequencies to be used and permits a wider range of transducer loading due to fluid absorption. Rather than monitoring current minima, the voltage maxima of the receiving transducer are detected, while again maintaining the transmitting transducer at a constant voltage.

A significant advancement in ultrasonic interferometry was introduced by Eggers (1968). Instead of a fixed frequency, variable pathlength device, the Eggers interferometer is a fixed path length, variable frequency system. In addition to the basic instrumentation change, an analytical change allows a much easier determination of relative absorption coefficients to a very good approximation.

2.2.2 Fixed Path - Two Transducer Interferometer

2.2.2.1 Absorption Coefficient

In many investigations of ultrasonic absorption and velocity in liquids, a solute or suspended body is the object of the study, rather than the solution or suspension as a whole. Therefore, it is unnecessary to obtain absolute values. For example, an attenuation coefficient may be obtained for an interferometer containing a solution and for the same interferometer containing the solvent only, which functions as a reference. The absorption

coefficient for the solute is then found simply by subtraction if all other losses can be made constant between the measurement procedures. More specifically, the total energy loss of a resonant system is inversely proportional to the quality factor, Q, of that system. Contributions to this energy loss in the acoustic interferometer include, in addition to absorption in the liquid, diffraction of the sound beam, imperfect reflection, transducer losses due to clamping and motional destructive interference while being driven at an off resonant frequency, electrical circuit losses, and coupling losses. Assuming that these losses are additive, the overall quality factor may be expressed as (Eggers & Funck, 1973)

$$1/Q_{total} = 1/Q_{unknown} + 1/Q_{extra}. \quad 2.29$$

If $1/Q_{total}$ and $1/Q_{extra}$ are measured, an expression relating the absorption coefficient only to $1/Q_{unknown}$, hereafter referred to as 1/Q, is needed.

The derivation of this relationship is based upon part of Hubbard's theory (1931) which describes the particle velocity everywhere in a fluid between two infinite plane parallel boundaries when one of the boundaries is forced to vibrate with a periodic velocity normal to its surface. Boyd (1971) applied this theory in a derivation of an expression for the pressure amplitude at a boundary of such a system at resonance, and at a frequency shifted off resonance by an amount equal to half of the bandwidth which defines the Q. Errors in the derivation prevented the correct expression relating the absorption coefficient to the Q from being obtained. The correct derivation is given here.

The derivation makes use of the definition of the quality factor as

$$Q \equiv \frac{f_o}{f_+ - f_-} \equiv \frac{f_o}{\Delta f} \qquad 2.30$$

where f_o is the resonant frequency, and f_+ and f_- are, respectively, the frequencies greater than and less than the resonance frequency at which the average power has decreased to half its value at resonance (Kinsler & Frey, 1962). The power at resonance is obtained in terms of the pressure amplitude, which is a function of the absorption coefficient. Half of this power is then set equal to the power at f_+ or f_-.

A wave emitted from the source and traveling in the positive x direction may be described by $p(+) = p_o e^{-\alpha x} e^{i(\omega t - kx)}$. Upon being reflected after traveling a distance, L, it is described by $p(-) = p_o e^{-\alpha(2L-x)} e^{i[\omega t + k(x-2L)]}$. (The total distance traveled is 2L - x; for a wave traveling in the negative x direction, x and t must have the same sign.) No reflection factor need be included since a reference liquid can be chosen to have the same impedance as the liquid containing the unknown. Therefore, the reflection losses will be the same, and included in $1/Q_{extra}$. After a second reflection, the wave, again traveling in the positive x direction, is described by $p(+) = p_o e^{-\alpha(2L+x)} e^{i[\omega t - k(2L+x)]}$. After another reflection, $p(-) = p_o e^{-\alpha(4L-x)} e^{i[\omega t + k(x-4L)]}$. All of the waves traveling in the positive x direction are described by

$$p(+) = p_{oe}^{-\alpha x} e^{i(\omega t - kx)} \left(1 + \sum_{n=1} e^{-\alpha 2nL} e^{-ik2nL}\right), \qquad 2.31$$

and all traveling in the negative x direction by

$$p(-) = p_o e^{\alpha x} e^{i(\omega t + kx)} \left(\sum_{n=1} e^{-\alpha 2nL} e^{-ik2nL}\right). \qquad 2.32$$

The pressure of the standing wave for any x is the sum of Eqs. 2.31 and 2.32:

$$p = p_o e^{i\omega t}\left[e^{-(\alpha + ik)x}\left(1 + \sum_{n=1} e^{-\alpha 2nL} e^{-ik2nL}\right) + e^{(\alpha + ik)x}\left(\sum_{n=1} e^{-\alpha 2nL} e^{-ik2nL}\right)\right]. \qquad 2.33$$

Acoustic power is related to the pressure amplitude by

$$\left(\text{power} = SI = SP^2/2\rho_o c\right) = \frac{\text{Area}\,(\text{Press})^2}{2\rho_o c_{\text{rel.}}} \qquad 2.34$$

where I is intensity, S is area, and P is pressure amplitude (Kinsler & Frey, 1962). Since Q is independent of x, the power ratio obtained by changing the frequency is independent of x. and S are constants, and c is independent of x. Therefore, the pressure amplitude at any x can be used to determine Q. For simplicity, x = 0 is chosen. At x = 0, Eq. 2.33 becomes

$$\begin{aligned} p(o) &= p_o e^{i\omega t}\left(1 + 2\sum_{n=1} e^{-\alpha 2nL} e^{-ik2nL}\right) \\ &= p_o e^{i\omega t}\left[1 + 2\sum_{n=1} e^{-\alpha 2nL}(\cos k2nL - i \sin k2nL)\right]. \end{aligned} \qquad 2.35$$

From Gradshteyn and Ryzhik (1965),

$$1 + 2 \sum_{n=1} e^{-\alpha 2nL} \cos k2nL = \frac{\sinh \alpha 2L}{\cosh \alpha 2L - \cos k2L}$$

and

$$\sum_{n=1} e^{-\alpha 2nL} \sin k2nL = \frac{1}{2} \frac{\sin k2L}{\cosh \alpha 2L - \cos k2L}.$$

Therefore, Eq. 2.35 becomes

$$p(o) = p_o e^{i\omega t} \frac{\sinh \alpha 2L}{\cosh \alpha 2L - \cos k2L} - i \frac{\sin k2L}{\cosh \alpha 2L - \cos k2L} \qquad 2.36$$

At resonance, the wavelength satisfies $n\lambda_r/2 = L$. (This will be shown to be the case in the next section.) Therefore, the wavenumber satisfies

$$k_r 2L = 2\pi n. \qquad 2.37$$

Equation 2.36 then becomes

$$p_r(0) = p_o e^{i\omega t} \frac{\sinh \alpha 2L}{\cosh \alpha 2L - 1}.$$

The power at resonance is obtained by substituting the amplitude of this pressure into Eq. 2.34:

$$\text{power}_r(0) = \frac{S p_o^2}{2\rho_o c} \frac{\sinh^2 \alpha 2L}{(\cosh \alpha 2L - 1)^2} \qquad 2.38$$

The power will be reduced to half of this value when the frequency is changed by $\Delta f/2$ (cf. Eq. 2.30). If the corresponding wavenumber change is defined as Δk, half power will occur when $k = k_r \pm \Delta k$. Substituting this into Eq. 2.36 yields

$$p(0) = p_o e^{i\omega t} \left[\frac{\sinh \alpha 2L}{\cosh \alpha 2L - \cos (k_r 2L \pm \Delta k 2L)} - i \frac{\sin (k_r 2L \pm \Delta k 2L)}{\cosh \alpha 2L - \cos (k_r 2L \pm \Delta k 2L)} \right] \qquad 2.39$$

Use of the following trigonometric identities simplifies this expression:

$$\cos(k_r 2L \pm \Delta k 2L) = \cos(k_r 2L)\cos(\Delta k 2L) \mp \sin(k_r 2L)\sin(\Delta k 2L)$$
$$\sin(k_r 2L \pm \Delta k 2L) = \sin(k_r 2L)\cos(\Delta k 2L) \pm \cos(k_r 2L)\sin(\Delta k 2L).$$

Using Eq. 2.37, the right sides of these equations become, respectively, cos $\Delta k2L$ and sin $\Delta k2L$. Substituting these into Eq. 2.39, and the amplitude of the resulting pressure into Eq. 2.34 yields

$$\text{power } (0) = \frac{Sp_o^2}{2\rho_o c} \frac{\sinh^2 \alpha 2L + \sin^2 \Delta k 2L}{(\cosh \alpha 2L - \cos \Delta k 2L)^2} \qquad 2.40$$

Recalling the definition of Δk, the right side of Eq. 2.40 is set equal to one-half the right side of Eq. 2.38:

$$\frac{\sinh^2 \alpha 2L + \sin^2 \Delta k 2L}{(\cosh \alpha 2L - \cos \Delta k 2L)^2} = \frac{1}{2} \frac{\sinh^2 \alpha 2L}{(\cosh \alpha 2L - 1)^2} \qquad 2.41$$

Although c is a function of frequency (cf. defn. 2), its change over the relatively small shift of $\Delta f/2$ is negligible. To that extent, this equation expresses an exact relationship between the absorption coefficient and the quality factor, via Δk.

However, Eq. 2.41 can be greatly simplified with a negligible loss of accuracy because the maximum values for both $\alpha 2L$ and $\Delta k2L$ in this study are on the order of 0.01. The Maclaurin series are used, truncating the sin and sinh series after the first term, and the cos and cosh series after the first two terms. Equation 2.41 becomes

$$\frac{(\alpha 2L)^2 + (\Delta k 2L)^2}{[1 + \frac{(\alpha 2L)^2}{2} - 1 + \frac{(\Delta k 2L)^2}{2}]^2} = \frac{1}{2} \frac{(\alpha 2L)^2}{[1 + \frac{(\alpha 2L)^2}{2} - 1]^2},$$

which simplifies to

$$\alpha = \Delta k. \qquad 2.42$$

Recalling the definitions of Δk and Δf, the following relationship is obtained:

$$\Delta k = 2\pi\Delta f/2c = \pi\Delta f/\lambda_r f_o.$$

Equation 2.42 then becomes $\alpha = \pi\Delta f/\lambda_r f_o$. This gives the absorption occurring over a distance, x. The absorption normalized to the distance of one wavelength is

$$\alpha\lambda_r = \pi\Delta f/f_o = \pi/Q. \qquad 2.43$$

2.2.2.2 Resonant Frequencies

In deriving the expression for the absorption coefficient, the interferometer could be considered as an ideal single stage device, viz., a fluid column and two perfect reflectors, because all nonidealities contributing to attenuation were accounted for by the reference measurement. To determine an expression identifying the frequencies at which the fluid column resonates, however, the fact that the device is a coupled interferometer must be considered. A description of the resonant frequencies is necessary to the calculation of velocity and helps to illustrate the basic operation of the resonator.

For the case of two perfect reflectors, the resonant frequencies are only a function of the phase velocity in the fluid

and the length of the fluid column. In the real case, they also depend upon the fluid density and all three of these properties of the reflectors. The equation identifying the resonant frequencies is obtained by developing expressions for the acoustic impedance at the transducer-liquid interface in terms of acoustic variables first in the transducer and then in the liquid. Since the impedance must be continuous across the interface, the expressions are set equal.

Acoustic impedance is defined as the ratio of pressure and volume velocity:

$$\vec{Z} \equiv p/\vec{U}.$$

For a medium in a pipe of cross sectional area, S, the impedance can be written in terms of the particle velocity (Kinsler & Frey, 1962):

$$\vec{Z} = p/S\vec{v}.$$

An impedance change at some point along the pipe will cause an incident wave to be at least partially reflected. The impedance will then be

$$\vec{Z} = \frac{1}{S} \frac{p_i + p_r}{v_i + v_r} \qquad 2.44$$

where the subscripts, i and r, denote the incident and reflected waves, respectively. To obtain the acoustic impedance as a function of pressure only, the definition of the characteristic acoustic impedance is used (Kinsler & Frey, 1962):

$$\vec{Z}_c = p/\vec{v}$$

This applies only to waves having a constant phase relationship between pressure and velocity. Therefore, it must be applied individually to incident and reflected waves. p and v can each be expressed as a function of particle displacement, from which it can be seen that

$$p_i/v_i = \rho_o c \quad \text{and} \quad p_r/v_r = -\rho_o c.$$

Equation 2.44 becomes

$$Z = \frac{\rho_o c}{S} \frac{p_i + p_r}{p_i - p_r},$$

where the explicit vector notation for Z is dropped. In order to express the impedance as a function of distance, x, along the pipe, one-dimensional plane waves are assumed, yielding

$$Z = \frac{\rho_o c}{S} \frac{Ae^{i(\omega t - kx)} + Be^{i(\omega t + kx)}}{Ae^{i(\omega t - kx)} - Be^{i(\omega t + kx)}}$$

where A and B are complex pressure amplitudes of the wave traveling in the positive and negative x directions, respectively. The time dependence cancels leaving

$$Z = \frac{\rho_o c}{S} \frac{Ae^{-ikx} + Be^{ikx}}{Ae^{-ikx} - Be^{ikx}} \qquad 2.45$$

If this equation is evaluated twice, each time in terms of a specific value for x, A and B can be eliminated.

Since the electrodes have a negligible effect on the impedance, the subscript, q, will denote the parameters pertaining only to the quartz crystal. The subscripts, a and l, refer to air

and liquid, respectively. d is the length (thickness) of the crystal, and L is the length of the liquid column (fig. 2.2). The origin of the distance parameter is arbitrary.

Considering the quartz first, let x = 0 be at the air-quartz interface. Then x = d is at the quartz-liquid interface (fig. 2.3). The acoustic impedance at the left face of the quartz is, from Eq. 2.45,

$$Z_{qo} = \frac{\rho_q c_q}{S} \frac{A + B}{A - B}$$

and at the right face of the quartz is

$$Z_{qd} = \frac{\rho_q c_q}{S} \frac{Ae^{-ik_q d} + Be^{ik_q d}}{Ae^{-ik_q d} - Be^{ik_q d}} .$$

If each of these equations is solved for A/B, the resulting expressions equated, and solved for Z_{qd}, the result is

$$Z_{qd} = \frac{\frac{\rho_q c_q}{S} Z_{qo} - i\frac{\rho_q c_q}{S} \tan k_q d}{\frac{\rho_q c_q}{S} - iZ_{qo} \tan k_q d} \qquad 2.46$$

The fact that the left face of the crystal is in contact with air allows this equation to be simplified. Since the impedance must be continuous across the air-quartz interface,

$$Z_{ao} = Z_{qo}.$$

Because the characteristic acoustic impedance of air is negligible compared to that of quartz, (the sound power transmission coefficient is $\sim 10^{-4}$),

$$Z_{qo} = 0.$$

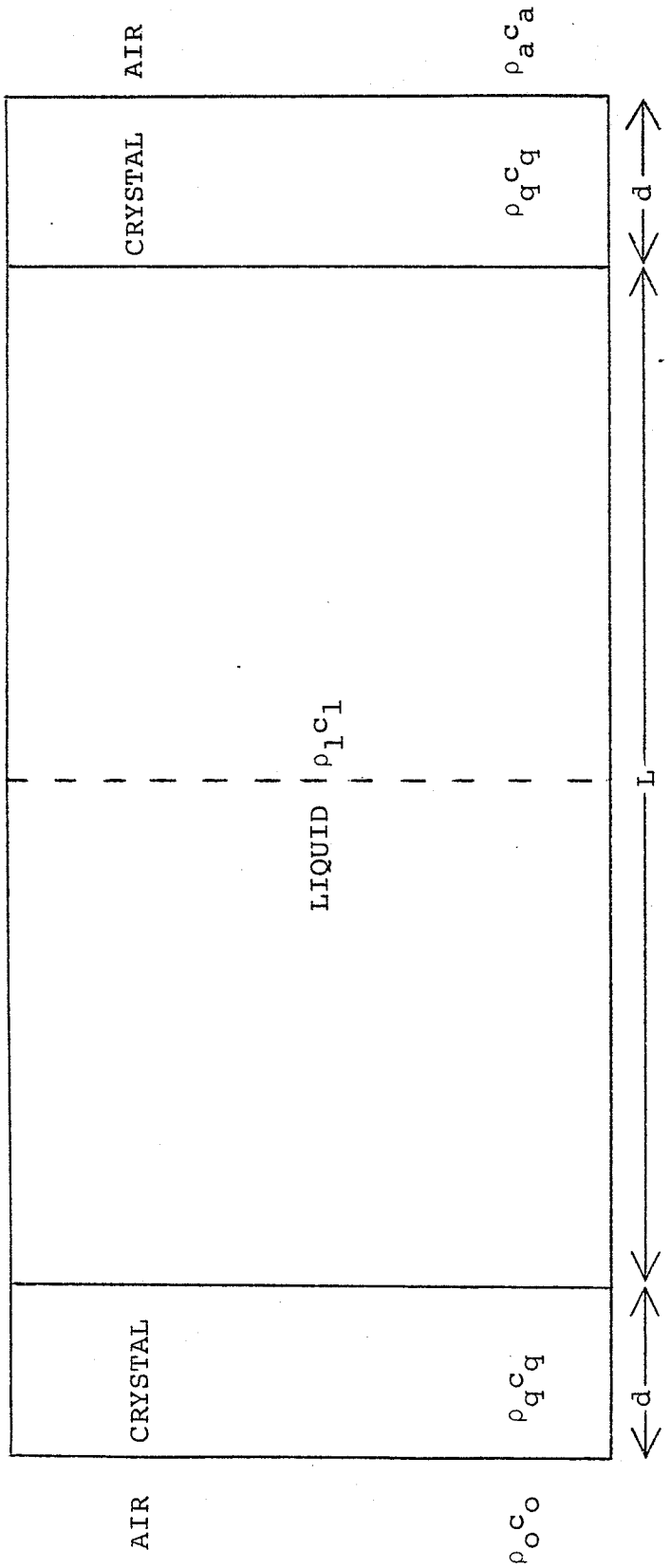

Figure 2.2 Schematic drawing of the acoustic interferometer.

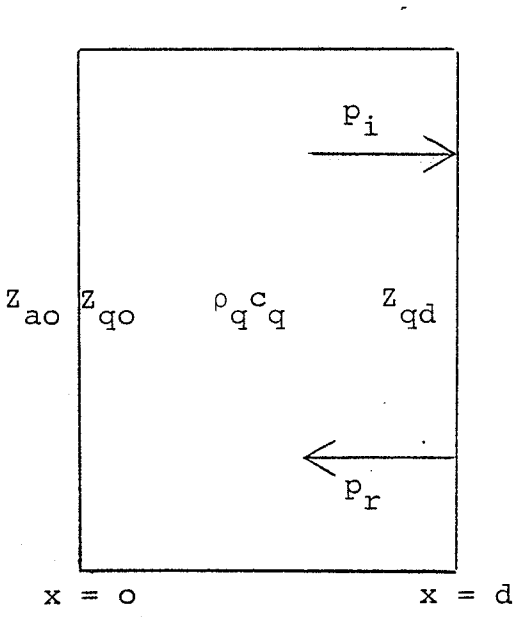

Figure 2.3 Schematic diagram of the air-backed quartz transducer showing acoustic terminating impedances.

Therefore, Eq. 2.46 becomes

$$Z_{qd} = -i(\rho_q c_q/S)\tan k_q d. \qquad 2.47$$

The acoustic impedances in the liquid are found in a similar way. For convenience, x = 0 is assigned to the quartz-liquid interface (fig. 2.4). The impedance at the origin is, from Eq. 2.45,

$$Z_{lo} = \frac{\rho_l c_l}{S}\frac{A + B}{A - B} \qquad 2.48$$

where A and B do not necessarily have the same values as above. Since the interferometer is symmetrical with respect to the liquid, only half of the column need be considered. In addition, knowledge of the impedance at the center of the column yields a more complete description of the interferometer. From Eq. 2.45,

$$Z_{lL/2} = \frac{\rho_l c_l}{S}\frac{Ae^{-ik_l L/2} + Be^{ik_l L/2}}{Ae^{-ik_l L/2} - Be^{ik_l L/2}} \qquad 2.49$$

Eliminating A and B from Eqs. 2.48 and 2.49 and solving for Z_{lo} yields

$$Z_{lo} = \frac{\rho_l c_l}{S}\frac{Z_{lL/2} + i\frac{\rho_l c_l}{S}\tan k_l L/2}{\frac{\rho_l c_l}{S} + iZ_{lL/2}\tan k_l L/2} \qquad 2.50$$

Since $Z_{qd} = Z_{lo}$,

Eqs. 2.47 and 2.50 yield

$$-i\rho_q c_q \tan k_q d = \rho_l c_l \frac{Z_{lL/2} + i\frac{\rho_l c_l}{S}\tan k_l L/2}{\frac{\rho_l c_l}{S} + iZ_{lL/2}\tan k_l L/2}$$

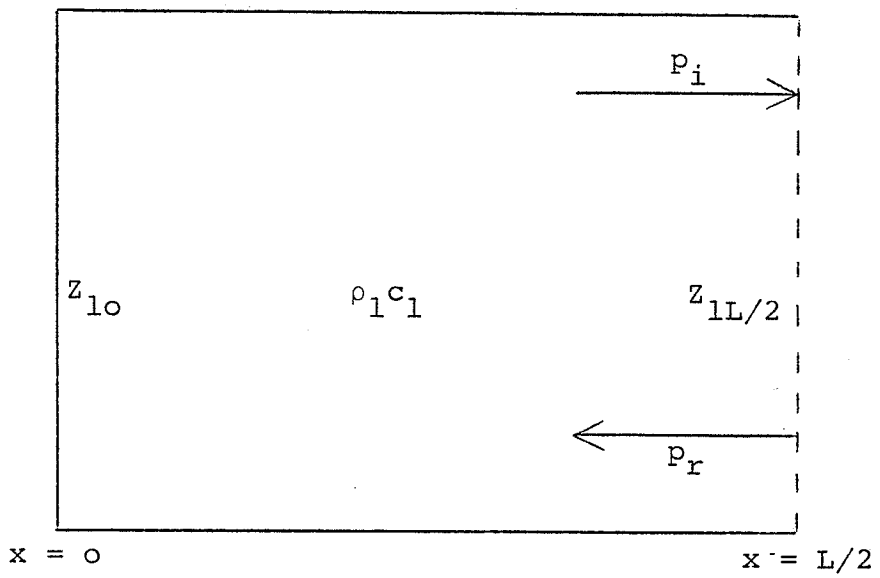

Figure 2.4 Schematic diagram of one-half the interferometer column showing acoustic terminating impedances.

To make this equation more useful, the frequency at which the interferometer is driven is included explicitly:

$$-i\rho_q c_q \tan\frac{2\pi f}{c_q}d = \rho_1 c_1 \frac{Z_{1L/2} + i\frac{\rho_1 c_1}{S}\tan\frac{2\,f\pi L}{c_1\,2}}{\frac{\rho_1 c_1}{S} + iZ_1 L/2\,\tan\frac{2\pi f}{c_1}\frac{L}{2}} \qquad 2.51$$

For a given interferometer, this expresses the relationship between the acoustic impedance at the center and the driving frequency.

The condition of resonance can now be applied to this equation by first applying it to Eq. 2.49. In addition, reflection is assumed to occur in an identical manner at each crystal. When there are many reflections, the fact that the initial, unreflected wave does not have the coefficient, A, can be ignored. Therefore, A is set equal to B. By definition, the reactive component of the acoustic impedance is zero at resonance (Kinsler & Frey, 1962). Applying this criterion and using Euler's identity shows that $k_1 L/2$ must equal multiples of $\pi/2$. Therefore, the magnitude of $Z_{1L/2}$ at resonance must be zero or infinity. Equation 2.51 at resonance takes the form

$$\rho_q c_q \tan\frac{2\pi f_n}{c_q}d = -\rho_1 c_1 \tan\frac{2\pi f_n}{c_1}\frac{L}{2} \qquad 2.52$$

for $Z_{1L/2} = 0$ and

$$\rho_q c_q \tan\frac{2\pi f_n}{c_q}d = \rho_1 c_1 \cot\frac{2\pi f_n}{c_1}\frac{L}{2} \qquad 2.53$$

for $Z_{1L/2} = \infty$, where the subscript, n, denotes the n^{th} resonance. The arguments of the tangents may be written in terms of the

fundamental frequencies of the quartz and liquid, f_Q and f_L, respectively, rather than the velocities and dimensions. The fundamental frequencies are defined in terms of the lowest ideal vibrational mode:

$$f_Q = c_q/2d \quad \text{and} \quad f_L = c_l/2L$$

Therefore, $(2\pi f_n/c_q)d = \pi f_n/f_Q$ and $(2\pi f_n/c_l)L/2 = (\pi/2)f_n/f_L$.

Substituting these expressions into Eqs. 2.52 and 2.53 and combining them into a single form yields

$$\rho_q c_q \tan \pi f_n/f_Q = \rho_l c_l \begin{bmatrix} -\tan \\ \cot \end{bmatrix} \pi f_n/2f_L, \qquad \begin{matrix} a \\ b \end{matrix} \; 2.54$$

the expression for the resonant frequencies for a two crystal coupled interferometer.

In order to illustrate further the basic operation of the resonator, the four different cases of ideal resonance are considered. The perfect reflection of the ideal case requires that the left side of this equation, which is the acoustic impedance of the quartz at d, must be zero or infinity. For each of these two cases, the acoustic impedance at the center of the liquid column must be either zero or infinity. In all four of the ideal situations, Eqs. 2.54 yield the expected result that the liquid column contains an integral number of half wavelengths. For example, for the case, $Z_{qd} = 0$ and $Z_{lL/2} = 0$, $-\tan \pi f_n/2f_L$ must $= 0$.

Since $f_n = c_l/\lambda_n$
and $f_L = c_l/2L$, 2.55

the argument of tan must satisfy $\pi L/\lambda_n = n\pi$, or $L = n\lambda_n$. The other three cases may be found in a similar manner. A summary of the results is

$$Z_{qd} = 0 \quad Z_{1L/2} = 0 \quad L = n\lambda_n$$

$$Z_{1L/2} = \infty \quad L = (2n - 1)\lambda_n/2$$

$$Z_{qd} = \infty \quad Z_{1L/2} = 0 \quad L = (2n - 1)\lambda_n/2$$

$$Z_{1L/2} = \infty \quad L = n\lambda_n$$

In all four cases, substitution of L for λ_n in Eq. 2.55 shows that f_n is a multiple of f_L. The results are

$$f_n = c_1 n/L \quad \text{and} \quad f_n = c_1(2n - 1)/2L$$

which can be combined into

$$f_n = c_1 n/2L. \qquad 2.56$$

2.2.3 Application to Real Case

The latter case for the quartz, $Z_{qd} = \infty$ (fig. 2.5), approximates the situation present in this study. The characteristic acoustic impedance of the quartz is greater than that of the liquid, and the quartz is driven away from its harmonic frequencies. Applying the same analysis to the quartz as for the liquid shows that $Z_{qd} = \infty$ when $d = (2n - 1)/4\lambda$, i.e., at the anti-resonances of the quartz. Therefore, the ideal case of perfect reflection is achieved in reality at these anti-resonant frequencies.

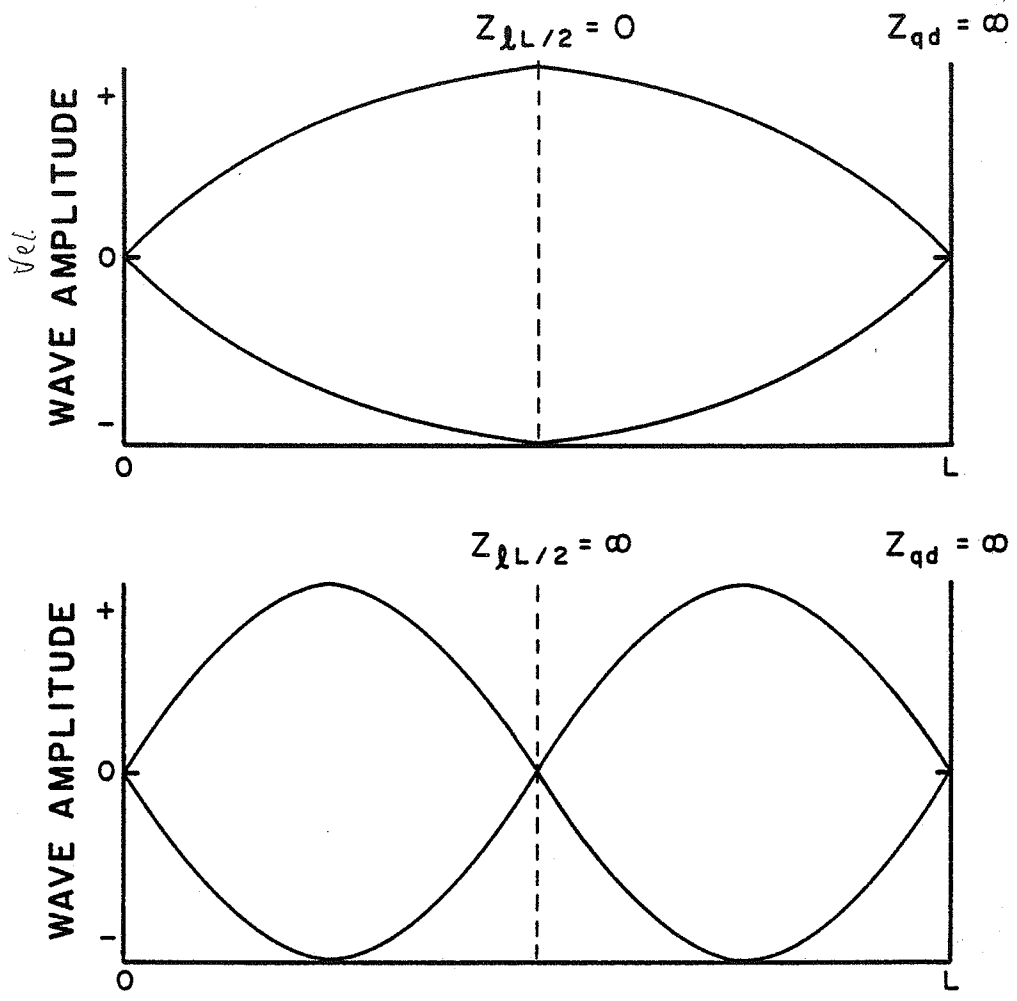

Figure 2.5 Wave amplitude as a function of position along the liquid column for the first two resonant modes, for ideal one-dimensional plane wave behavior, with the column terminated with infinite impedances.

The velocity can easily be obtained at the anti-resonant frequencies of the quartz using Eq. 2.56, if a reference liquid with a known and similar velocity can be used to determine n and L. To determine the velocity at any other frequencies, a simplified approximation of Eqs. 2.54 a,b should be used.

The infinite impedance exhibited by the transducers at their anti-resonant frequencies is also relevant to absorption measurements. In the derivation of the absorption coefficient as a function of the quality factor, perfect reflection was assumed because reference measurements would account for the imperfect behavior. At the anti-resonant frequencies, however, this source of energy loss is eliminated physically, making the measured attenuation coefficient a better approximation to the true liquid absorption coefficient.

CHAPTER 3

MATERIALS & METHODS

3.1 SUSPENSIONS

3.1.1 Chemicals

Dipalmitoylphosphatidylcholine (DPPC), and dipalmitoylphosphatidylglycerol (DPPG) were obtained from Avanti Polar Lipids (Birmingham, AL). Samples of DPPC and DPPG (100 gm) gave single spots on thin layer chromatograms (silica gel G developed with $CHCl_3$:CH_3OH:H_2O 64:24:4, visualized with I_2 vapor). Crystalline cytosine 1- β -D-arabinofuranoside (Ara-C) and N-2-hydroxyethylpiperazine-N'-2 ethanesulfonic acid (HEPES) were obtained from Sigma Chemical Company (St. Louis, MO). Tritiated cytosine arabinoside, [^{3}H]-Ara-C (64 mCi/mg, 98% pure by thin layer chromatography) and [^{14}C]-DPPC (156 μCi/mg, 98% pure by thin layer chromatography) were obtained from Amersham Corp.

3.1.2 Liposome Preparation

3.1.2.1 Synthesis

All liposomes were made from a 4:1 (by weight) mixture of DPPC:DPPG. They were mixed in an organic solvent (125 mg lipid/6.5 ml), which was then removed by a rotary evaporator. The procedure diverges at this point, being a function of the type of liposome desired (Szoka and Papahadjopoulos, 1978, modified by Magin and Weinstein, 1984).

To make MLV, the dried lipids are hydrated at a temperature well above T_m in a solution of HEPES buffer (10 mM HEPES, 139 mM NaCl, 6 mM KCl), distilled water, Ara-C, and 0.1 N HCl. The

solution concentration to 300 mM, and HCl adjusts the pH to 7.4 (physiologic). The suspension was vortically mixed, at which time the liposomes formed. They were kept at this temperature for about 30 minutes to assure liposome stability, and then were cooled with an ice bath to a temperature several degrees below T_m. The suspension was dialyzed at low temperature against the buffer.

SUV are made from MLV by breaking them up in a bath-type sonicator (80 kHz, cavitating intensity). The MLV suspension was sealed under nitrogen gas to prevent oxidation of the lipids and sonicated at a temperature well above T_m until the suspension became transparent. After decreasing the temperature to a value several degrees below T_m, the suspension was placed in an ultracentrifuge to eliminate any large vesicles.

LUV were made by the reverse phase evaporation process. After the initial mixing and drying, the lipids were redissolved in an organic solution of 8 ml isopropyl ether and 4 ml chloroform. At a temperature well above T_m, 4 ml of the buffer dilution described above were added. The mixture was sealed under nitrogen gas and sonicated for five minutes, forming an emulsion. This was then transferred to a rotary evaporator, where reverse evaporation, i.e., preferential removal of the organic phase, took place. The buffer dilution which evaporated was replaced. The suspension was dialyzed at low temperature.

Szoka and Papahadjopoulos (1978) have speculated that the sonication produces a dispersion of reverse micelles, viz., the phospholipid head groups are inside, encapsulating the aqueous solution. When the micelles are concentrated to a gel-like state by evaporation of the organic phase, they further speculate that

some of the micelles disintegrate, and the free phospholipids form the complementary monolayer around the remaining micelles, thus forming liposomes. Two experiments support this. About half of the aqueous phase evaporates along with the organic phase (Magin & Weinstein, 1984). When [^{14}C]-sucrose was added to the gel state, only 5% was encapsulated, implying that there is little formation of new vesicles at this stage (Szoka and Papahadjopoulos, 1978).

3.1.2.2 Extrusion DO NOT NEED THIS.

Different size distributions were obtained by extrusion through one or more filters of successively smaller pore sizes (Szoka et al., 1980). The suspension was diluted to 8-10 mg lipid/ml in order to decrease the pressure needed for extrusion, thereby decreasing the possibility of leaks. The temperature was maintained several degrees above T_m because extrusion is much more difficult below T_m, often clogging or breaking the filter (Olson et al., 1979). The filter consisted of a polycarbonate membrane, containing pores of a well defined diameter, held by a leur-lock polycarbonate filter holder. The suspension was forced by a syringe through the filter and into another syringe. MLV were successively extruded through filters with pore sizes of 0.8, 0.6, 0.4, 0.2, and 0.1 μm. LUV were successively extruded through filters with pore sizes of 0.4, 0.2, 0.08, 0.05, and 0.03 μm. Finally, the suspensions were dialyzed at low temperature. Radioactive labels were used to monitor the extrusions. [^{14}C]-DPPC indicated that no lipid was lost. The capture by the liposomes of [^{3}H]-Ara-C decreased with each extrusion.

Although the mechanism by which extrusion results in smaller vesicles is unknown, there is evidence which suggests that the integrity of some of the bilayers is destroyed, but only temporarily. If a solute marker is removed by dialysis from the external environment of the liposome prior to extrusion, it has been found that extrusion results in the loss of captured solute (Olson et al., 1979) thus indicating some type of lysis. Thin-layer chromatography after five sequential extrusions revealed no detectable permanent liposome breakdown (Papahadjopoulos and Miller, 1967). If a solute marker is removed from the external environment after extrusion, the captured solute can be obtained. Olson et al. (1979) found an increase in this captured solute, supporting the proposal that single bilayer vesicles, with their larger fraction of volume available to the solution, are formed at the expense of the outer bilayers of other vesicles. Olson et al. (1979) have proposed that the pressure difference across the pore results in deformation of the liposome and eventually "pinching-off" part of it. The polar environment makes it likely that this separated part would immediately form a new liposome. However, MLV made for this ultrasonic study have yielded a decrease in capture following extrusion. This could be either due to a significant decrease in pinching-off, which would occur if these liposomes were more deformable and, therefore, would simply be squeezed through the pores, or due to a significant increase in pinching-off, the newly formed liposomes being so small that the volume to surface ratio is significantly decreased. There is a significant difference in the composition

of the liposomes between the two studies in that Olson et al. (1979) used 50 mole % cholesterol.

3.1.2.3 Size Estimation

Need this + my CM data

Indications of the actual sizes of some of the liposomes have been obtained from the literature, from low angle light scattering (LALS), and from transmission electron microscopy (TEM). A TEM study for this lab of unfiltered MLV yielded a mean diameter of 0.5 μm but a wide range of sizes, extending from less than 0.2 μm up to about 2 μm (Niesman, personal communication). About half of the liposomes had diameters between 0.3 and 0.8 μm. Olson et al. (1979) have obtained MLV size data following extrusion which show that the mean diameter of the vesicles is slightly less than the pore diameter for both 0.8 and 0.6 μm pores, about the same for the 0.4 μm pore, and slightly greater than the 0.2 μm pore diameter. The different lipid composition and capture behavior mentioned above make it clear that the application of these results to the present study results only in the best estimate of size available, not as an accurate indication of size. The techniques used in each study were the same, which removes some of the tentativeness from the comparison. Olson et al. (1979) have also shown that extrusion results in a more homogeneous distribution of sizes; viz., there is an increase in the number of smaller vesicles and an elimination of the largest vesicles. There is a general agreement from many studies that SUV have a narrow size distribution compared to that for MLV, and the average diameter is about 20 nm (Bergelson, 1978). The ultracentrifugation step in the preparation of SUV for this study

helps to assure this. The LUV size estimates are taken from the literature (Sano et al., 1982) either directly or by extrapolation and from LALS done in this lab. The estimated average diameter for each liposome population is given in Table 4.1.

3.1.2.4 Measurement Preparation

Just prior to putting the suspension into the ultrasound cell, degassed buffer dilution is added to reduce the lipid concentration to 2 mg/ml. Degassing is done for two reasons. The possibility of bubbles in suspension contributing to attenuation is minimized. The likelihood of bubbles adhering to the transducers is diminished.

3.2 APPARATUS

3.2.1 Materials

Figure 3.1 is a cross-sectional view of the interferometer. The body (diagonal lines) consists of two identical stainless steel halves. A previous version was made of brass, which is easier to machine. Though the performance of the two interferometers was the same, the brass one was much more susceptible to corrosion caused by the ionic solvent employed for the liposome suspensions. The two halves are held together by four stainless steel bolts and nuts. A lucite spacer, which forms the side walls of the cylindrically shaped cell, is situated between the steel halves. Lucite was chosen because its transparency makes it possible to see bubbles adhering to the end walls of the cell, during the filling procedure, and because its characteristic acoustic impedance is closer to that of the liquid

INTERFEROMETER

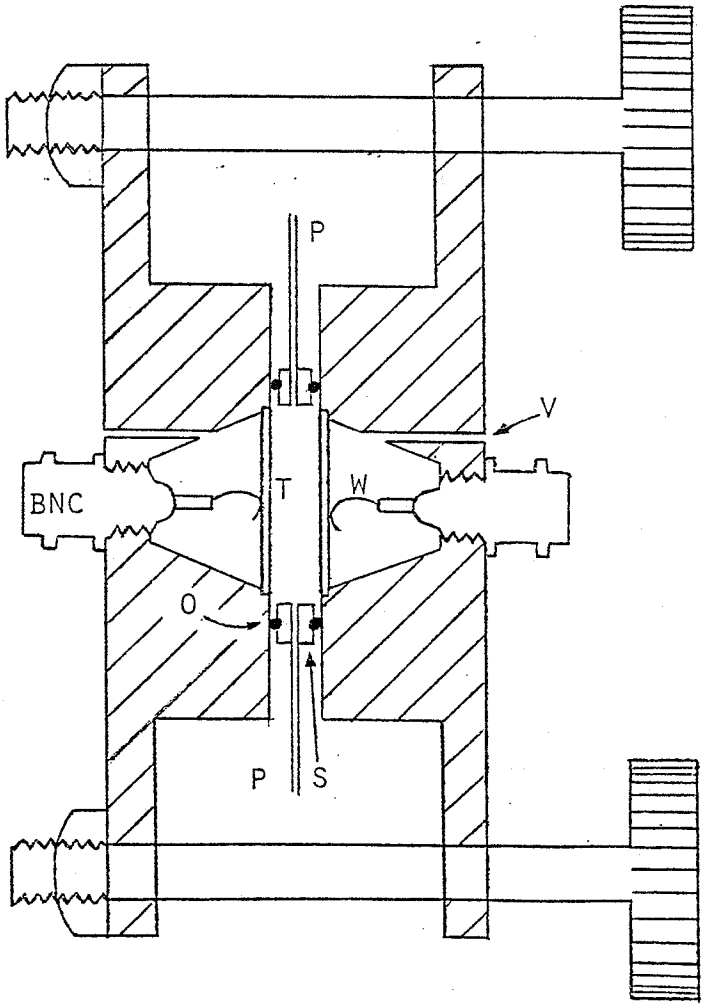

P FILLING AND EMPTYING PORTS
S PLEXIGLASS SPACER
T QUARTZ TRANSDUCER
V AIR VENT
W PLATINUM WIRE SPRING CONTACT

Figure 3.1 Cross-sectional view of the acoustic interferometer.

than are the impedances of other materials that could be chosen for this purpose, viz.,

Table 3.1

material	$\rho_o c$[1] (MKS rayl x10^{-6})
water	1.5
lucite	3.2
glass (pyrex)	13
steel (stainless)	46

[1]The characteristic acoustic impedance is $\rho_o c$. (cf., e.g., Kinsler & Frey, 1962)

This approximate impedance matching minimizes the reflection of the acoustic energy which escapes the rectilinear boundaries of the ideal plane wave. A hole, with an inserted tube, at the bottom of the spacer functions as a port for filling and emptying the cell. An identical port at the top of the spacer allows for maintaining atmospheric pressure over the liquid, which is desirable for the filling procedure. Rubber O-rings between the spacer and the steel halves provide the liquid-tight seal while allowing the slight angular movements of one interferometer half with respect to the other when paralleling the two transducer faces. The end walls of the cell are piezoelectric transducers, which are held in polished recesses of the steel body by the adhesive properties of high vacuum grease (Dow Corning Corp., Midland, MI). The transducers are X-cut quartz with overtone polish (flatness 1-10 λ light) (Valpey-Fisher Div., Hopkinton, MA), one inch in diameter and with a fundamental frequency, f_Q, of 4 MHz. The ground potential electrode (gold over chrome) of each transducer covers the entire face which is in contact with the liquid specimen. The electrode on the opposite face is coaxial,

with a diameter of 7/8", so chosen such that no contact with the (grounded) steel occurs. Electrical contact is made to these electrodes via 34 gauge platinum wires soldered to female BNC connectors and bent into a slight spring shape. The pressure applied by the wires to the transducers is minimal in order not to affect the vacuum grease adhesion retaining the transducers. Holes are drilled through the steel body to assure that the pressure on the back sides of the transducers does not exceed the ambient pressure.

3.2.2 Dimensions

3.2.2.1 Volume

The inside diameter of the spacer is 2.9 cm and that of the O-rings is 3.1 cm. The distance, D, between the inside faces of the transducers is calculated from the frequency separation of two adjacent resonances, $f_n - f_{n-1}$, near $f_Q/2$ for a liquid with an accurately known acoustic velocity, $c_{w,T}$, viz., distilled water at a known temperature. D will then be one-half of an acoustic wavelength:

$$D = \frac{c_{w,T}}{2(f_n - f_{n-1})}$$

Although D is slightly different each time the interferometer is assembled, it is always within 0.515 ± 0.003 cm. The spacer is 0.3 cm wide. Thus, each O-ring contributes approximately 0.1 cm to D. The cell volume is then

$$\pi\left(\frac{2.9\text{cm}}{2}\right)^2 \; 0.3\text{cm} + \pi\left(\frac{3.1\text{cm}}{2}\right)^2 \; 0.2\text{cm} = 3.5\text{cm}^3 \quad .$$

3.2.2.2 Parallelism Criterion

The diameter of the steel body, more specifically, the distance of the assembly bolts from the center of the interferometer, was made large enough to satisfy stringent requirements for control of the parallelism of the transducer faces. The requirement can be described in terms of the angular displacement of one transducer surface relative to the other and is inversely proportional to the number of reflections of sound, which occurs before the amplitude decreases to 1/e of its original value. Specifically, the planarity of one transducer with respect to the other must be able to be controlled to $\sim\lambda/m$ (Eggers et al., 1978), where m is the number of such reflections occurring. m is determined by D, the distance between reflections, and α, the attenuation coefficient, since the stated amplitude decrease occurs when the total distance traveled, mD, is $1/\alpha$, i.e., $m = 1/\alpha D$. Since water has the lowest absorption of any liquid specimen used in this study, it determines the requirement on m. The worst case (low) frequency can be taken as 1 MHz for this study. The absorption coefficient at 1MHz in water at 39°C is approximately $2\times10^{-4}cm^{-1}$. Thus m is 10^4 reflections. The acoustic wavelength for these conditions is about 0.15 cm, giving approximately 1.5×10^{-5} cm for λ/m. This is the precision with which it is necessary to control the angular deviation from perfect parallelism of the transducers. The actual dimensions involved are illustrated in fig. 3.2. The distance between either pair of diagonally opposed bolts is 10.75 cm, and the diameter of the electrode on each transducer is 2.22 cm. (The transducer is shown schematically to be off-center, with one edge

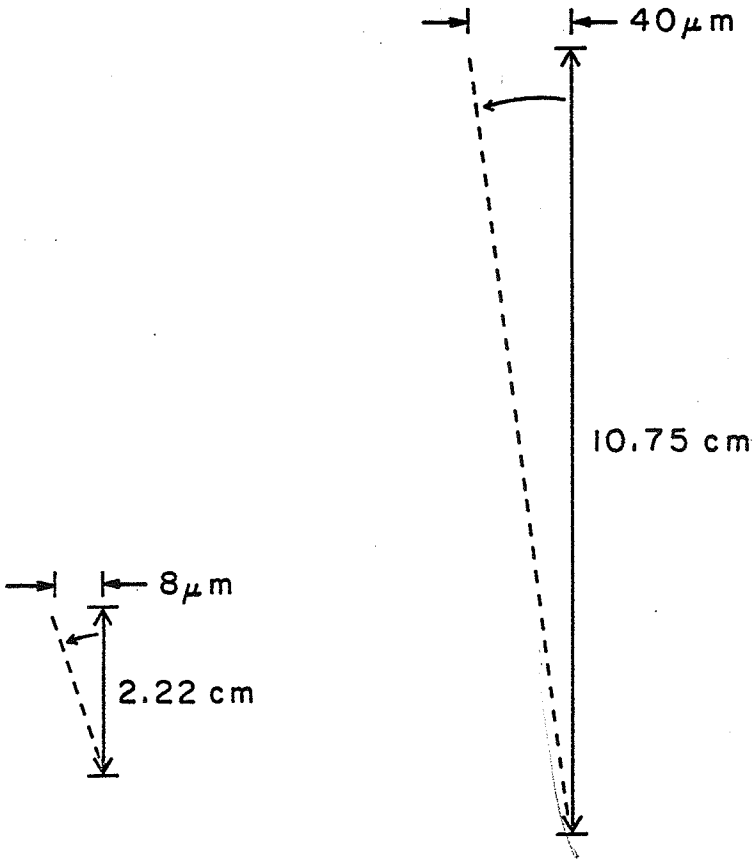

Figure 3.2 Illustration of the precision with which the angular position of the steel cell support can be controlled and the resulting precision of control over the transducer orientation (the angles greatly exaggerated).

fixed, as it is only the net displacement of one edge with respect to the other that is of concern.) It is estimated that the precision with which the bolt can be adjusted is about 1/1000 turn, or about 20' of arc. As the bolts have 64 threads per inch, this translates to an adjustment of about 40 μm for the steel body and, most importantly, 8 μm for the transducer. Thus the criterion of 15 μm determined from λ/m can be satisfied.

3.2.3 Cleaning

After each measurement use, if the interferometer did not need to be disassembled, the cell was rinsed six times with distilled water, and then dried using a stream of nitrogen gas.

Disassembly of the interferometer was necessary when a leak occurred. Disassembly was always accompanied by a thorough cleansing as follows. With the axis of the interferometer oriented vertically, the bolts were removed, followed by removal of the top half of the steel and the spacer. The O-rings, spacer, and connected tubing were rinsed thoroughly with distilled water. The adhesion of the transducers to the grease was broken by pushing the back of the transducers with a small wooden rod inserted through the air vent. The BNC connectors were removed to avoid damaging the platinum wires.

A special cleansing procedure was used to avoid contamination of liposomes by detergent material. First the grease, silver paint (discussed later), and any suspension residue were removed by wiping the steel with a silicone remover (Cee-Bee C-105HF, McGean Chemical Co., Cleveland, OH) followed by wiping with acetone and then ethanol. The transducers were wrapped in lens

paper and soaked in the silicone remover to dissolve the grease near the edge, then rinsed with acetone, wrapped in lens paper, and soaked in stirred acetone, then rinsed with ethanol, wrapped, and soaked in stirred ethanol, and finally rinsed with distilled water.

3.2.4 Assembly

The BNC connectors were mounted into the threaded bores at the center of each half of the steel body. The high vacuum grease was applied to the nonelectroded area of a transducer crystal. The crystal was then set on the recessed ring in the steel body and rung-on by simultaneously pushing down and rotating the crystal with aid of a lucite cylinder having a diameter equal to that of the crystal. The end surface of the cylinder in contact with the crystal was coated with rubber, and a piece of lens paper was placed between this rubber and the crystal to protect the electrode. Breakdown of the grease seal occurred during the early experiments but was inhibited by the additional application of grease to the recessed steel ring prior to ringing-on the crystal. Any unseen dirt should have had a much less debilitating effect on the seal with this practice.

The ground connection between the gold electrode on the crystal face and the stainless steel body is made with silver conducting paint (SC 12, Micro-Circuits Co., New Buffalo, MI). During the earlier experiments, several spots of paint, approximately 3 cm in diameter, were used to bridge the small gap between the gold on the crystal and the steel body. About 10 hours is required for complete drying, which is necessary for

minimum resistance, usually about 1 ohm, to be established. In later experiments application of the paint around the entire gap was found to produce a superior seal, with regard to leakage during the measurement procedure. This usually required touching up several times, as holes developed during the drying process.

The interferometer was assembled by the concentric stacking of the members, a simple reversal of the process described above. Flake graphite was sprinkled onto the threads of the bolts to minimize binding during the fine adjustment procedure. The bolts were turned down just to the point where they were beginning to compress the O-rings. The interferometer was then oriented to its normal horizontal position and placed on a wooden holder. Each bolt was then tightened one complete turn. An initial, and very course, parallelism adjustment was made by further tightening the bolts, if needed, until the two steel halves were equally spaced to ± 0.01 cm around the entire circumference of the body, as determined with calipers.

The wooden holder was set on the base of an L-shaped lucite support (fig. 3.3). Attached to the vertical side of the lucite support was a stainless steel piston tightly fitted into a cylinder with O-rings and machined such that a positive or negative pressure could be carefully controlled. Access to the cylinder was via a bleeder valve or a tube identical to those of the cell ports. Polyethylene tubing (1.19 mm i.d., 1.70 mm o.d.) connected the top port to this tube. Tubing also connected the bottom port to a reservoir suspended above the interferometer.

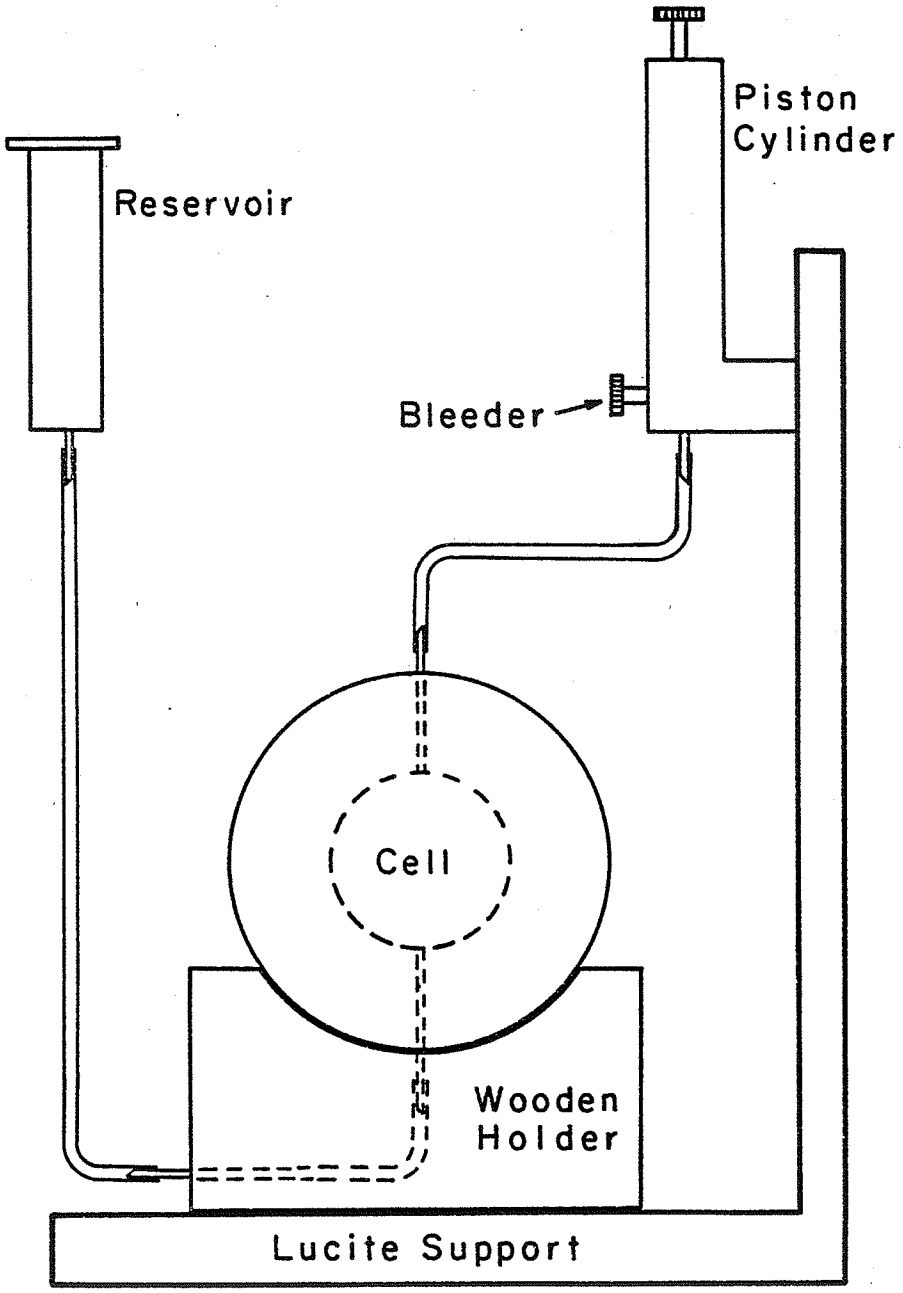

Figure 3.3 The support structures for the interferometer and the filling and emptying apparatus.

3.2.5 Filling

The cell was filled by first putting the liquid specimen into the reservoir. For early experiments, the piston was moved up slowly to create a negative pressure inside the cell, and thereby drawing the liquid into it. Once the cell was filled, the bleeder was opened to expose both ports to atmospheric pressure, which was important as the cell was extremely sensitive to any pressure difference. For later experiments, the bleeder valve was slightly opened, allowing atmospheric pressure to force the liquid into the cell. It was found that the bleeder valve could be used while still maintaining a sufficiently smooth liquid flow to preclude bubble formation. This positive pressure method is believed preferable considering the way in which the transducers are mounted; a negative pressure in the cell could tend to break the grease seal. The amount of liquid left in the tubing was minimized for three reasons. First, although not critical for these experiments, in general it is desirable to minimize the amount of liquid needed. Secondly, the contribution of the two opposing liquid columns to the pressure difference mentioned above is minimized. The third reason is related to temperature control and will be discussed later.

3.2.6 Temperature Control

The temperature must be controlled very precisely because the resonant frequency of the cell and its contents is a very strong function of temperature. The interferometer and wooden holder were placed in plastic bags and set on the lucite support, and the entire ensemble suspended in a temperature controlled bath (Exacal

500 with Endocal 350 refrigeration unit, Neslab, Portsmouth, NH). The temperature was stable to within 0.1°C for however long it was necessary to obtain data at a particular temperature, and to within 0.01°C while a particular bandwidth measurement was being made.

The interferometer is extremely sensitive to external pressure variations, the major source of which are the vibrations of the bath liquid produced by the circulation pump. In order to minimize this problem, the isolation of the pump from the bath walls was improved, from what the manufacturer had provided, by increasing their separation with packing material. This technique was used also between the interferometer and holders. Another precaution undertaken was the third reason, alluded to in sec. 3.2.5, for minimizing the amount of liquid in the tubing. To the extent that the tubing contained liquid, it comprised an extremely sensitive coupler of pressure variations to the cell.

3.2.7 Electronics

A synthesized signal generator (8660B with 86601A RF section, Hewlett-Packard) druves one crystal transducer (the transmitter) via a length of RG 58A/U coaxial cable and a BNC connector. The receiving transducer is connected via cable and a BNC to a spectrum analyzer (8553B RF section, 8552A IF section, 140B oscilloscope, Hewlett-Packard).

The signal generator drives one of the transducers at a frequency which can be controlled and read to the nearest hertz. The frequency is adjusted until an acoustic resonance occurs, as evidenced by a peak on the screen of the spectrum analyzer.

3.2.8 Parallelism Adjustment

The cell was filled with distilled water, and a resonant frequency near 1 MHz was found. The bolts were adjusted in an attempt to increase the amplitude of the peak exhibited on the spectrum analyzer screen. An amplitude increase verified that the adjustment had made the transducers more nearly parallel. Since any such adjustment slightly changes the distance between the transducers, each adjustment was followed by a retuning of the driving frequency to return the interferometer to a resonant condition.

At the shorter wavelengths, a particular transducer movement is a larger fraction of a wavelength, thus increasing the destructive interference effects of nonparallelism. Therefore, the procedure becomes more sensitive at higher frequencies. It was repeated at several such frequencies. No improvement could be obtained by going above 7 MHz. This may have been partly because for any shorter wavelengths, the bolts could not be adusted precisely enough to induce such an improvement.

Each resonance which has been referred to here is actually only the first mode of a spectrum of resonant modes, which result in satellite peaks at neighboring frequencies. This spectrum is due to nonideal plane wave behavior, resulting in image sources, imposed by the cylindrical cavity (Labhardt & Schwarz, 1976). The amplitude of the first mode was compared to that of the largest satellite peak, as this relative amplitude of wanted to unwanted resonances increases as the transducers become more nearly parallel. Once the largest achievable relative amplitude was determined from experience, this amplitude was used as a criterion

for the overall success of the procedure. A typical example of the relative amplitudes of the main resonance (amplitude = 1) to the largest satellite is given in Table 3.2:

Table 3.2

Amplitude of the second mode peak normalized to that of the first mode

f_o (MHz)	relative satellite amplitude
2	0.11
3	0.24
5	0.36
6	0.48
7	0.58

It has been shown that this alignment, done at room temperature, is maintained down to 4°C and up to 51°C at least within the uncertainty with which the system can measure absorption, viz., approximately ±5%. (Strom-Jensen, 1983).

3.3 DATA ACQUISITION

3.3.1 Method

The expression used to calculate the absorption coefficient per wavelength directly from the data is obtained from the discussion of the relationship between the absorption coefficient and the quality factor in sec. 2.2.2.1. From Eqs. 2.29 and 2.42,

$$\alpha\lambda = \pi(\Delta f_{tot} - \Delta f_{ref})/f_o,$$

where f_o is any resonant frequency, Δf_{tot} is the half power bandwidth at that frequency due to all losses of the interferometer containing the liquid with the unknown component,

Δf_{ref} is the corresponding bandwidth for a system with the same acoustical properties except for the absence of the unknown absorption, and α is the absorption coefficient for this component. (The bandwidth related to Q_{extra}, Δf_{ref}, is called the reference bandwidth and is explained further in the next paragraph.) The subscript for λ, which denoted it as the wavelength at resonance, is dropped because from now on, resonance always is assumed.

The liquid used to obtain Δf_{ref}, i.e., the reference liquid, should not necessarily be the solvent, if a solute is being studied, or the solution part of a suspension, if the suspended particles are being studied. In practice, however, they often are used as references because they satisfy the two important criteria for reference liquids. The first is that the absorption coefficient of the reference should have the same value as that of the solvent or solution component of a suspension. The second is that the acoustic impedance of the two liquids should be the same. This impedance influences other sources of attenuation in the interferometer, such as imperfect reflection. Only when both of these criteria are met will the reference measurement account for all of the attenuation contributing to the bandwidth obtained for the system containing the unknown, except for that due to absorption by the unknown. In the present study, the liposomes in suspension are responsible for the unknown absorption. Therefore, the bandwidths and resonant frequencies are recorded for the interferometer containing such a suspension, i.e., Δf_{tot} and f_o are obtained. This is accomplished by adjusting the synthesizer frequency until a standing wave is produced at a characteristic

frequency, f_o. At each of these frequencies, the output transducer delivers a voltage peak to the spectrum analyzer. To obtain Δf, the synthesizer frequency is adjusted to a value above and below f_o for which the voltage of the output transducer has decreased to 0.707 of its value at f_o. The procedure is then repeated for the buffer in which the liposomes were suspended, yielding Δf_{ref} at the same resonant frequencies. $\alpha\lambda$ is obtained by subtraction, according to Eq. 3.1. Figure 3.4 illustrates a set of raw data.

3.3.2 Nonideal Behavior

Most of the data for this study are bandwidth measurements as a function of temperature at a particular resonant frequency. The first resonance above 3 MHz was chosen after considering the quality of data as a function of frequency for this interferometer. If the reference measurement perfectly fulfilled its function of accounting for all attenuation other than the absorption by the liposomes, any frequency could be chosen. However, such is not the case. In secs. 2.2.2.2 and 2.2.3 it was shown that the behavior of the interferometer is closest to ideal at the anti-resonant frequencies of the crystals, which, for the interferometer used in this study, includes 2 and 6 MHz. Choosing any frequency between about 1½ and 3½ MHz, or between about 5½ and 6½ MHz would have yielded fairly good data. However, there was a little more imprecision for the bandwidths at the lower and higher frequencies due to diffraction and asymmetric resonant peaks, respectively.

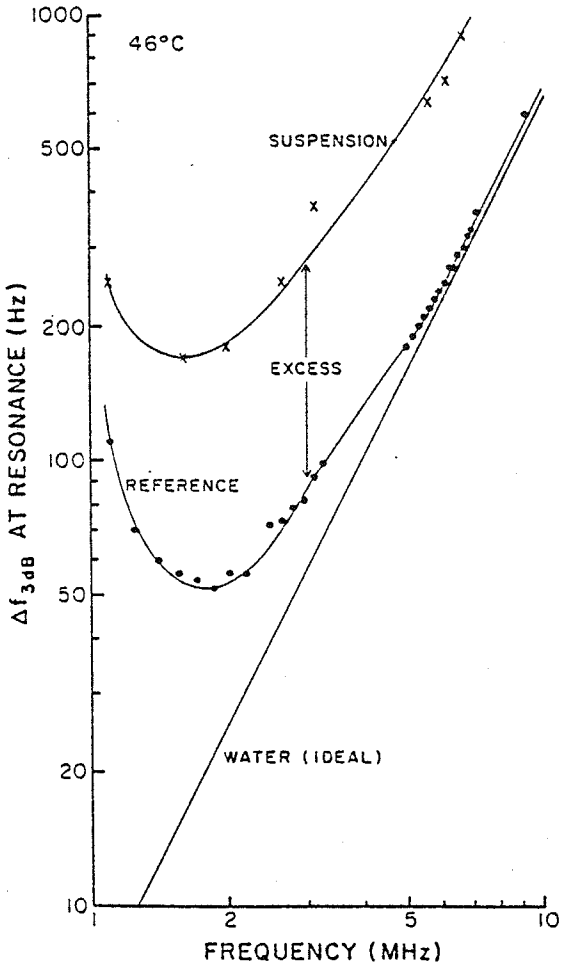

Figure 3.4 Half-power width of resonant peaks vs. frequency.

Diffraction is by far the largest nonabsorption contribution to attenuation at low frequencies and, in fact, is responsible for the low frequency limit at which this interferometer can be used. Diffraction of the sound field in an interferometer has its origin in the imperfect plane wave character of the waves their orignin, and has a result, beam spreading out of the rectilinear volume defined by the transducers. The effect increases as the ratio of wavelength to transducer diameter increases. Figure 3.4 shows that this effect is not just a function of frequency, but also of absorption. For the more highly absorbing liquid, the bandwidth minimum occurs at a lower frequency, and the diffraction-caused increase in bandwidth at the lowest frequencies is not as steep.

The asymmetry of resonant peaks is usually the first significant effect of nonideal behavior to manifest itself as the frequency increases, and it sometimes determines the high frequency limit for this interferometer. It mainly affects every other resonance. When it became significant, these data were discarded and, hence, are not illustrated in fig. 3.4. As for diffraction, the effect is not just a function of freqency, but also of absorption, being larger at lower frequencies for more highly absorbing liquids.

Thus, both the low and high frequency data imply that the increased absorption due to the presence of the liposomes influences one or more of the other sources of attenuation. This shows that the assumption of additivity for Eq. 2.29 is not always true.

3.3.3 Reporting Data

An example of bandwidths due to the total loss at 3 MHz as a function of temperature are shown in fig. 3.5, along with the reference contribution and the bandwidth which would be obtained if the only loss were due to water absorption.

Most of the absorption data presented here are in terms of specific absorption per wavelength, specific referring to the fact that any variation in the concentration of phospholipids between suspensions is accounted for by dividing the absorption per wavelength by the concentration. It is emphasized that it is the absorption per phospholipid molecule which is reported, the absorption for the larger liposomes, for example, being due to a smaller number of liposomes.

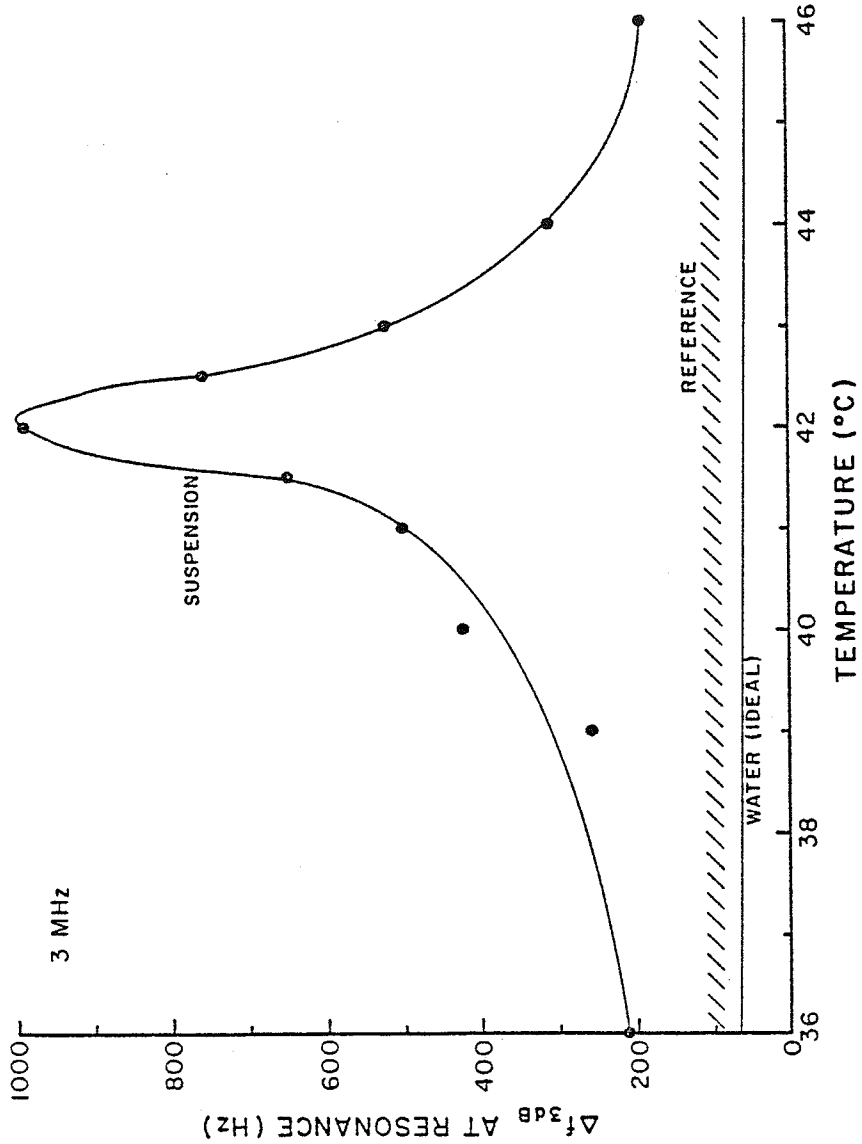

Figure 3.5 Half-power bandwidth vs. temperature. Reference data vary slightly with each cell reassembly, but always fall within the area indicated.

CHAPTER 4

RESULTS

The analysis of the data of this study is concerned with the implications of the temperature dependence of ultrasonic absorption. However, part of this analysis involves calculations which require velocity values. Figure 4.1 illustrates one set of such values for the buffer, obtained as described in section 2.2.3, along with values for distilled water, taken from the literature (Del Grosso & Smura, 1953 and Greenspan & Tschiegg, 1957). The chosen frequency of 2 MHz was a function of the characteristics of the interferometer, as described in section 2.2.3. Velocity data need be obtained at only a single frequency since the frequency dependence of velocity is insignificant, except in the case of a large absorption (cf. Eq. 2.28). As can be seen in fig. 3.5, nowhere in the temperature range of this study is this the case for the buffer. (The fact that the velocity of the buffer is less, in this case, than that for water is not significant. Another set of data parallels these, but the values are greater than those for water.) The velocity in the suspension differed from that in the buffer by no more than 0.2%, which is also the approximate uncertainty inherent in these measurements. Considering this uncertainty and the requirements on velocity values for computational purposes, as described in the DISCUSSION, the velocity in the suspension need not be considered further.

All the liposome suspensions studied exhibit a peak in the absorption coefficient versus temperature. This peak will be

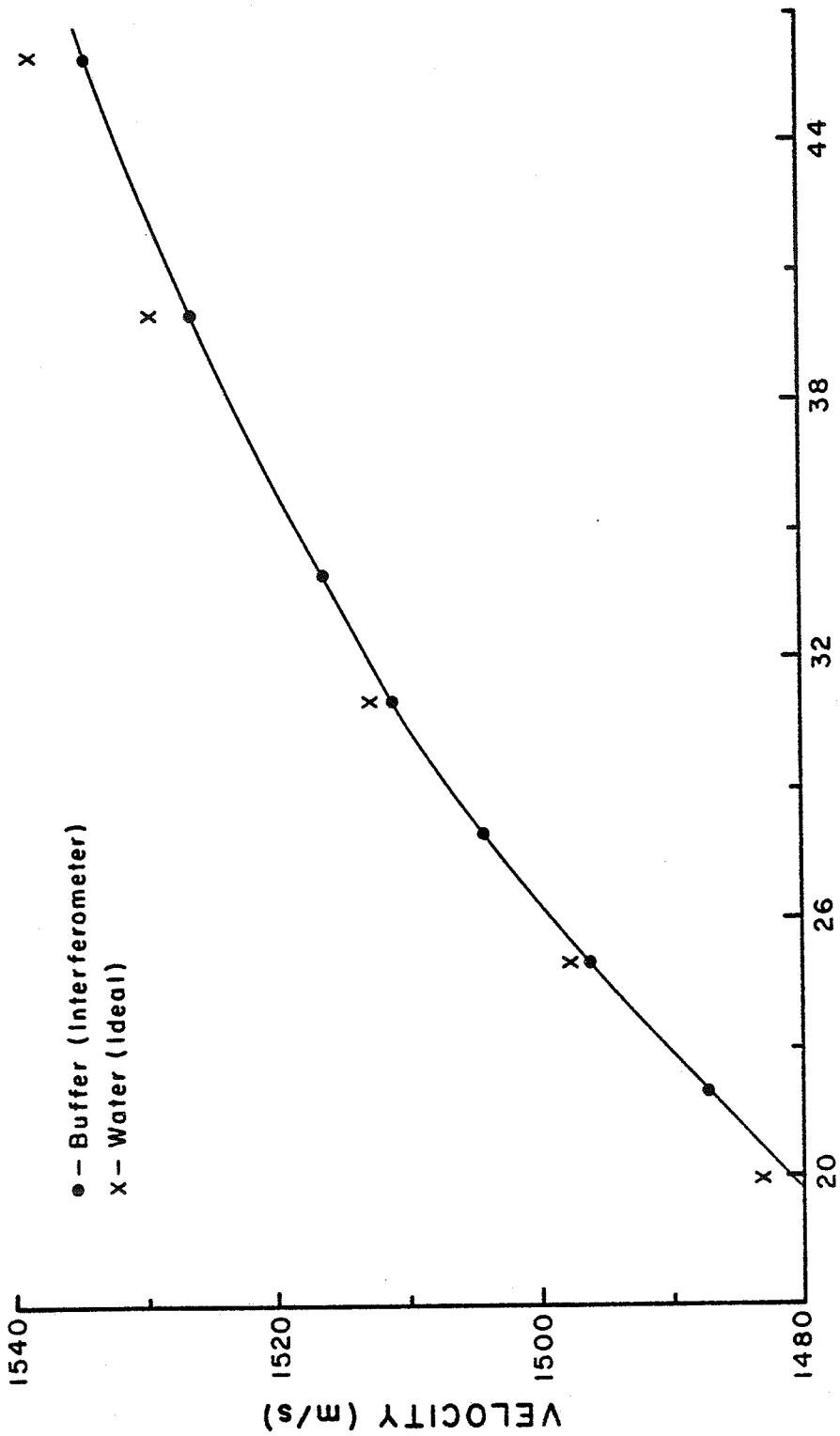

Figure 4.1 Temperature dependence of velocity for buffer, as measured with the interferometer, and selected values for water from the literature.

treated as representing the phase transition of the liposome membrane, which was justified in the INTRODUCTION. Four characteristics of this peak are considered quantitatively, viz., amplitude, width, area, and the temperature at which the maximum amplitude occurs, T_m (fig. 4.2). The amplitude used in the calculations is the amplitude of the peak, per se, obtained by subtracting the baseline amplitude. This was obtained by collecting a set of data over a wider temperature range than that usually obtained near the transition temperature. The measured width is defined at one-half of the peak height and is denoted by $T_{\frac{1}{2}}$.

The area under the curves is used to estimate the enthalpy of the transition, ΔH. The near coincidence of the ultrasonic absorption vs. temperature curves and the heat capacity vs. temperature curves, discussed in the INTRODUCTION, justifies the use of absorption curves as estimates of heat capacity provided there is at least one absorption curve which corresponds to a known heat capacity and can, therefore, be used as a reference. The enthalpy of the transition is the integral of the heat capacity, with respect to temperature, in excess of that not due to the transition:

$$\Delta H = \int_{T_1}^{T_2} C_{ex} dT$$

(fig. 4.2) (Mabrey-Gaud, 1981). Thus C_{ex} corresponds to the net absorption coefficient mentioned in the previous paragraph. Note that C_{ex} is the (extensive) heat capacity, as opposed to the specific heat used in the ACOUSTIC THEORY. The area was determined simply by plotting the curves on a grid and counting

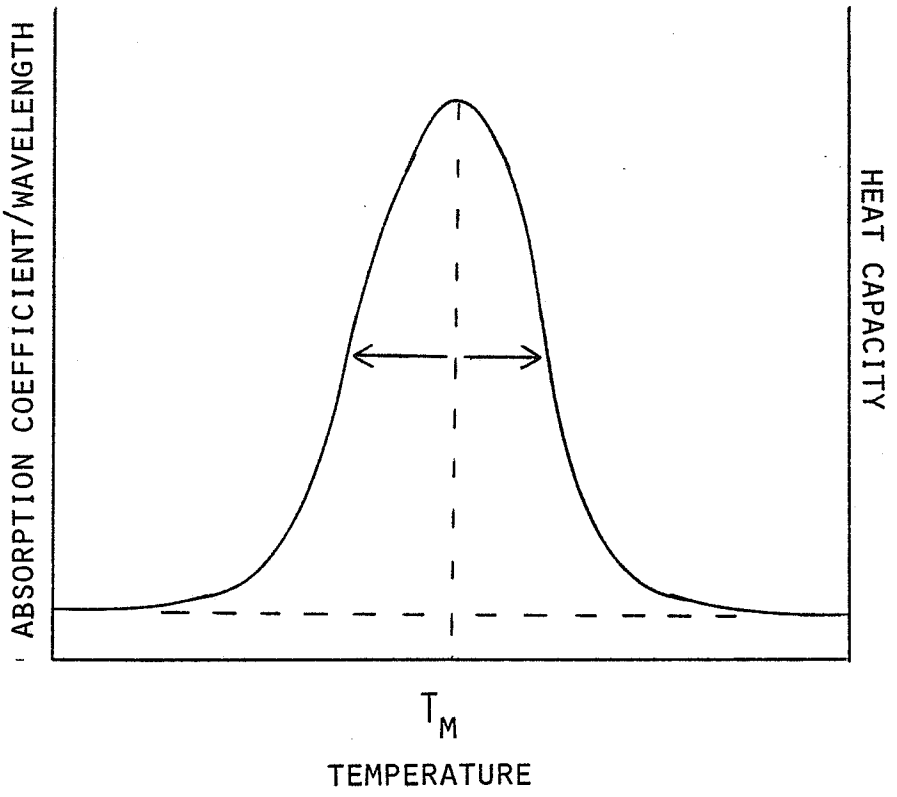

Figure 4.2 General dependence of ultrasonic absorption coefficient and of heat capacity on temperature in the vicinity of a liposome phase transition, the heat capacity behavior indicating an endothermic reaction.

the squares. A single exception to this procedure was the determination from the SUV data. Due to the large asymmetry (cf. fig. 4.3), the area to the right of T_m was found and doubled. Thus the transition enthalpy value more accurately reflects the behavior between the middle of the transition and the liquid crystalline state than between the middle of the transition and the solid state.

The use of the subscript, m, with T to denote the temperature of maximum amplitude has its origin in the interpretation of the ultrasonic absorption according to the analogy with DSC. Since the DSC data reflect the extent of the phase transition, the temperature at which these data reach a maximum was termed the melting temperature, T_m. The definition of T_m, however, involves enthalpy and entropy (Kanehisa & Tsong, 1978).

The ordinates of all of the graphs illustrating absorption results are in terms of the absorption coefficient per wavelength normalized with respect to concentration. Temperature is always in degrees centigrade. The ultrasonic frequency was always 3 MHz. The composition of the phospholipids was a 4:1 weight ratio of DPPC:DPPG.

The temperature dependence of the absorption coefficient for the small unilamellar vesicles, SUV, is shown in fig. 4.3. T_m is 38°C. This peak is rather broad, compared to others which will be presented, having a $T_{1/2}$ of 8°C. This broad temperature effect is not due to a broad size distribution because, as mentioned in section 3.1.2.3, the size distribution of SUV should be at least as narrow as that for any of the other vesicle types. The asymmetry is considered later in the context of a model for

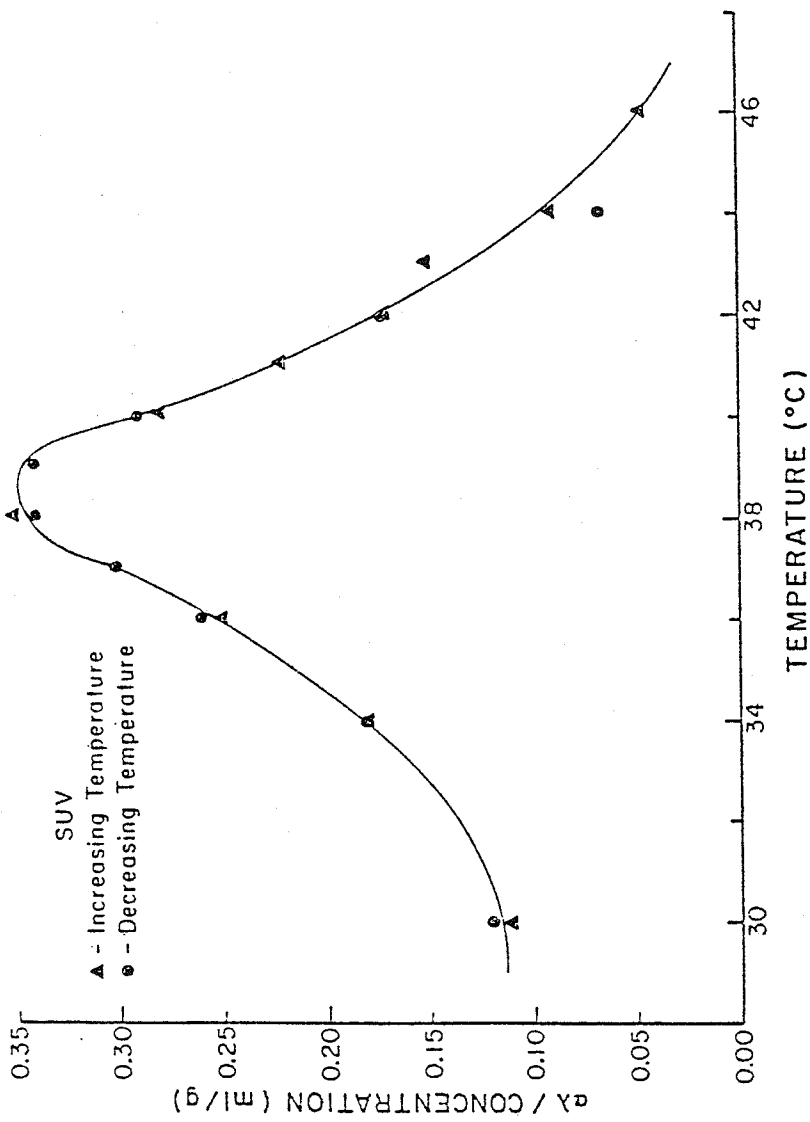

Figure 4.3 Temperature dependence of the specific ultrasonic absorption coefficient per wavelength for a suspension of small unilamellar vesicles showing lack of effect of the direction of temperature change.

absorption. All of the characteristics of the peak are independent of the direction of the temperature change, indicating that, at least for those liposome characteristics to which ultrasound is sensitive, passing through the absorption peak does not cause a permanent change. If there is hysteresis associated with the temperature change, it is completed in a time shorter than that in which the data are obtained. This finding is in contrast with some results from the literature, which show different values upon reversing temperature. One such study (Harkness & White, 1979) also found that the average diameter of the vesicles doubled upon cycling through the transition. The observed change was an increase in absorption only on the high temperature side of the peak. In another study, the temperature was cycled up to 25 times (Van Dijck et al., 1978), yielding a second peak at a higher temperature, specifically, that which is characteristic of MLV. The amplitude was found to grow linearly with the number of cycles at the expense of the SUV peak. Thus the nonrepeatability of the data indicates vesicle aggregation at least, and possibly fusion. The absence of any such effect in this study suggests that the presence of the negatively charged DPPG has the desired effect of preventing such aggregation. This satisfactory behavior of SUV implies that the same is true for the larger vesicles, because even for those studies in which aggregation of SUV occurred, aggregation did not occur in larger liposomes.

The absorption vs. temperature results for the populations of the largest and smallest sized multilamellar vesicles, MLV, are shown in fig. 4.4. The smallest vesicles exhibit the smallest

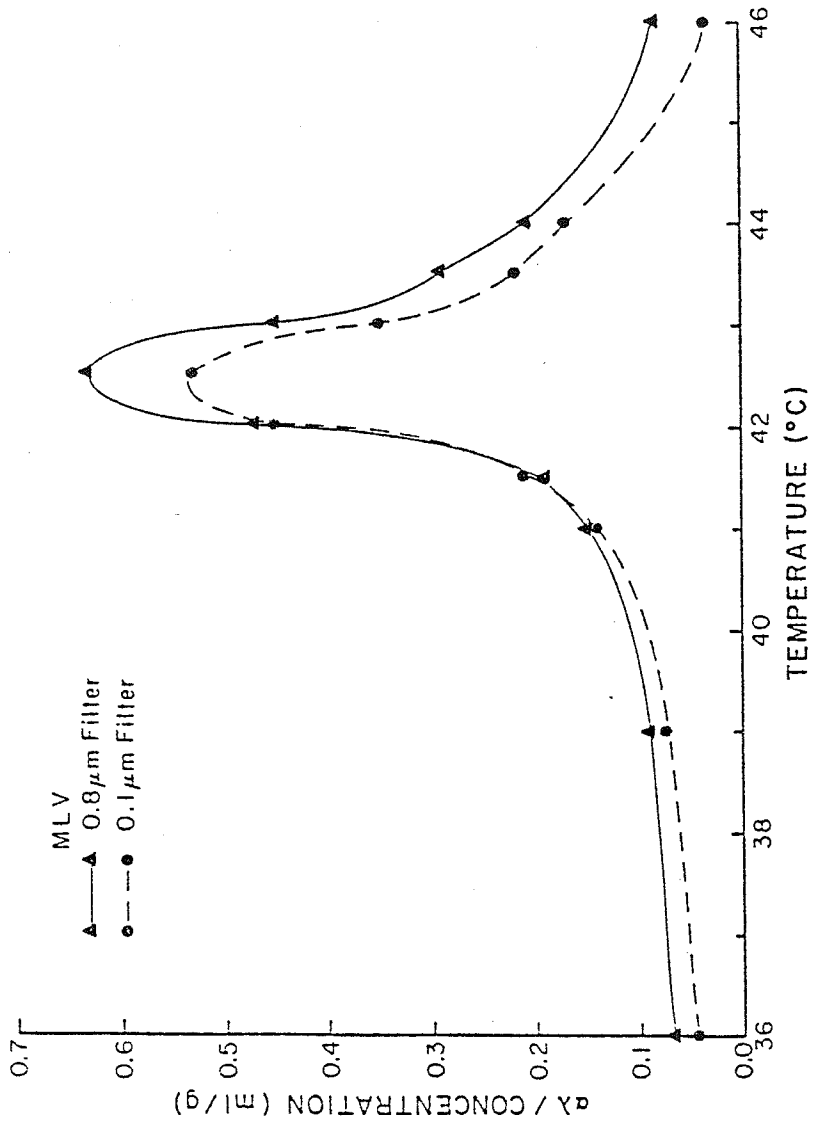

Figure 4.4 Temperature dependence of the specific ultrasonic absorption coefficient per wavelength for suspensions of largest and smallest multilamellar vesicles.

peak amplitude. The intermediate sized vesicles have peak amplitudes between the two illustrated. $T_{\frac{1}{2}}$ and T_m are affected only slightly, if at all, by the size change. $T_{\frac{1}{2}}$ is 1.4°C for the largest MLV and 1.3°C for the smallest. T_m was found to be 42.5°C. Successive elimination of the larger vesicles by extrusion may have been responsible for the slight decrease in amplitude in the higher temperature region of the transition. It will be seen below, when comparisons are made to more extreme size changes, that this is the expected behavior. However, these changes within the MLV category are too small to be considered further. The largest MLV are used as the reference for the calculation of the transition enthalpy, as discussed previously in this section. These were chosen because the transition enthalpy value used was obtained, directly by DSC, for unfiltered MLV (Hinz & Sturtevant, 1972). Extrusion through the 0.8 μm filter does not have a significant effect on the liposome population, as it only eliminates the largest members of the size distribution. Therefore, the area under the absorption curve for these liposomes should represent a transition with the enthalpy found by Hinz and Sturtevant, viz., 9.7 kcal/mol. The areas for all of the liposome types studied, relative to that of the largest MLV, are listed in Table 4.1, as are the transition enthalpies, based upon these fractions.

The absorption per wavelength vs. temperature results for the largest and smallest sized large unilamellar vesicles, LUV, are shown in fig. 4.5. The absorption amplitude exhibits the same trend with size as does that of the MLV, viz., a decreasing amplitude with decreasing size. The intermediate sized vesicles

Table 4.1

Properties of liposomes of different diameters as obtained from ultrasonic absorption measurements

	pore diam (nm)	lip. diam (nm)	$\alpha\lambda/n_o$ [i,j] (ml/g)	T_m [i] (^oC)	$T_{1/2}$ [i] (^oC)	relat area [i,k]	ΔH [l] (kcal/mol)	ΔH_{VH}[m] (kcal/mol)
SUV		20[c]	0.32	39	8	1.62	15.7	190
LUV	30	40[d]	0.28	42.5	2.7	0.72	7.0	670
	50	60[d]	0.31	42.5	2.6	0.77	7.5	690
	80	90[c]	0.44	42.0	2.4	0.88	8.5	740
	200	130[e]	0.40	42.0	1.6	0.86	8.3	1100
	400	160[f]	0.44	42.0	1.4	0.80	7.8	1300
	X[a]	190[f]						
MLV	100	100[g]	0.50	42.5	1.4	0.79	7.7	1300
	400	400[g]	0.53	42.5	1.3	0.89	8.6	1400
	800	500[h]	0.60	42.5	1.3	1	9.7	1400
	X[b]	500[h]					9.7	

[a] - no filter used
[b] - no filtration reported
[c] - Sano et al. (1982)
[d] - extrapolated from Sano et al. (1982)
[e] - extrapolated from Sano et al. (1982), and LALS done in this lab
[f] - from LALS done in this lab
[g] - estimate based on filter size and Olson et al. (1979)
[h] - TEM by Michael Niesman of this lab
[i] - from this study
[j] - net value: baseline due to absorption away from transition has been subtracted
[k] - area under curves and above baseline (see [j] above) divided by area for 800 nm pore MLV
[l] - from "relative area" from this study, except for last value, which is from Hinz and Sturtevant (1972)
[m] - from $\Delta H \sim 6.9\ T_m^2/T_{1/2}$

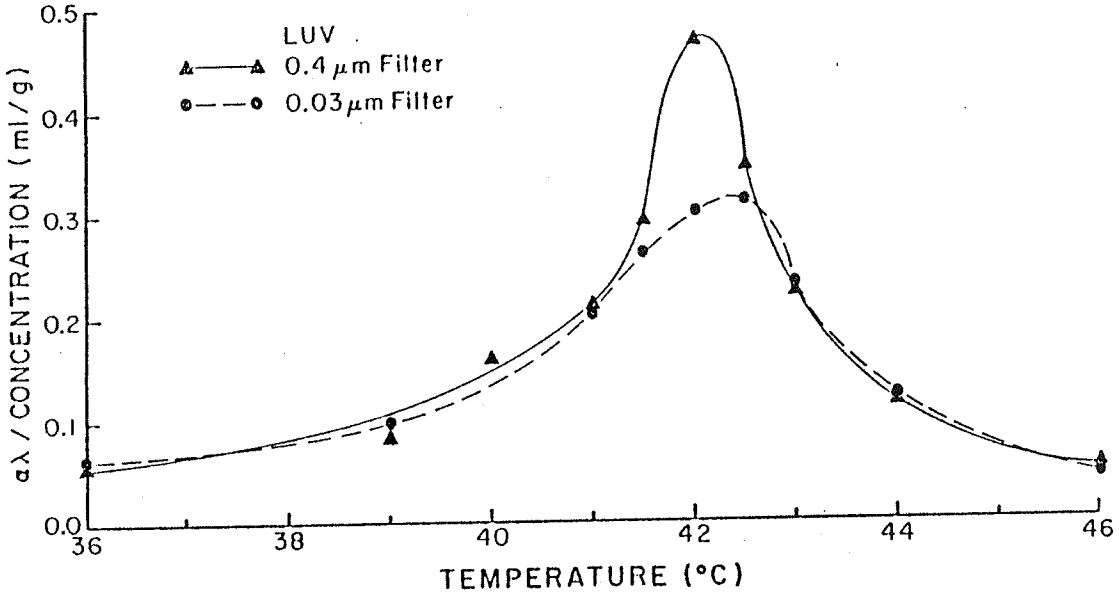

Figure 4.5 Temperature dependence of the specific ultrasonic absorption coefficient per wavelength for suspensions of the largest and smallest large unilamellar vesicles.

have peak amplitudes between the two illustrated. T_m is 42.0°C for the three larger sizes and 42.5°C for the two smaller sizes. This last result is unexpected since T_m has moved back to the value it has for MLV. $T_{\frac{1}{2}}$ undergoes a significant change from 1.4°C for the largest LUV to 2.7°C for the smallest. The area under the curves, and thus the transition enthalpy, decreases slightly for the smallest sizes.

Figure 4.6 is a composite of portions of figs. 4.3, 4.4, and 4.5. Results for the largest MLV and LUV have been reproduced. The salient features of the data are illustrated, viz., large LUV and MLV exhibit similar temperature dependent absorption characteristics in terms of both position and shape of the peaks. SUV behavior differs in every way.

Although the large LUV behave quite differently from the SUV, fig. 4.5 illustrates that the LUV undergo significant changes over their size range, except for T_m, and that these changes are increasing the similarity to SUV behavior. Figure 4.7 illustrates, however, that qualitatively different behavior is maintained. Data for the smallest LUV are plotted along with those for the SUV.

A more quantitative comparison is made in the next three graphs. Figure 4.8 is a plot of the specific absorption coefficient per wavelength vs. vesicle diameter. The greater size dependence of LUV than MLV can be seen. The anomalous behavior of the middle sized LUV appears to be real because similar behavior was obtained in three separate experiments. Figure 4.9 is a log-log plot of the LUV and MLV data from fig. 4.8 with the exception of the two datum points nearest 100 nm.

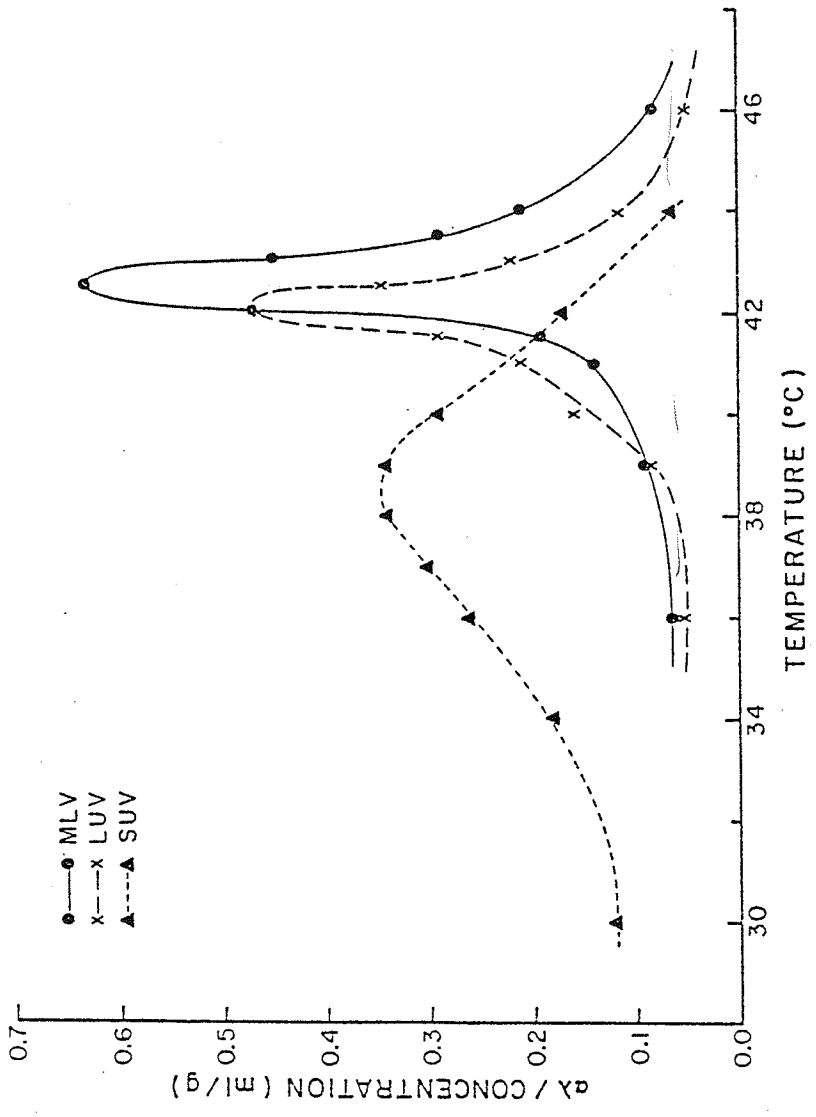

Figure 4.6 Composite from figs. 4.3, 4.4, and 4.5 showing the specific ultrasonic absorption coefficient per wavelength for suspensions of small unilamellar vesicles, the largest large unilamellar vesicles, and the largest multilamellar vesicles.

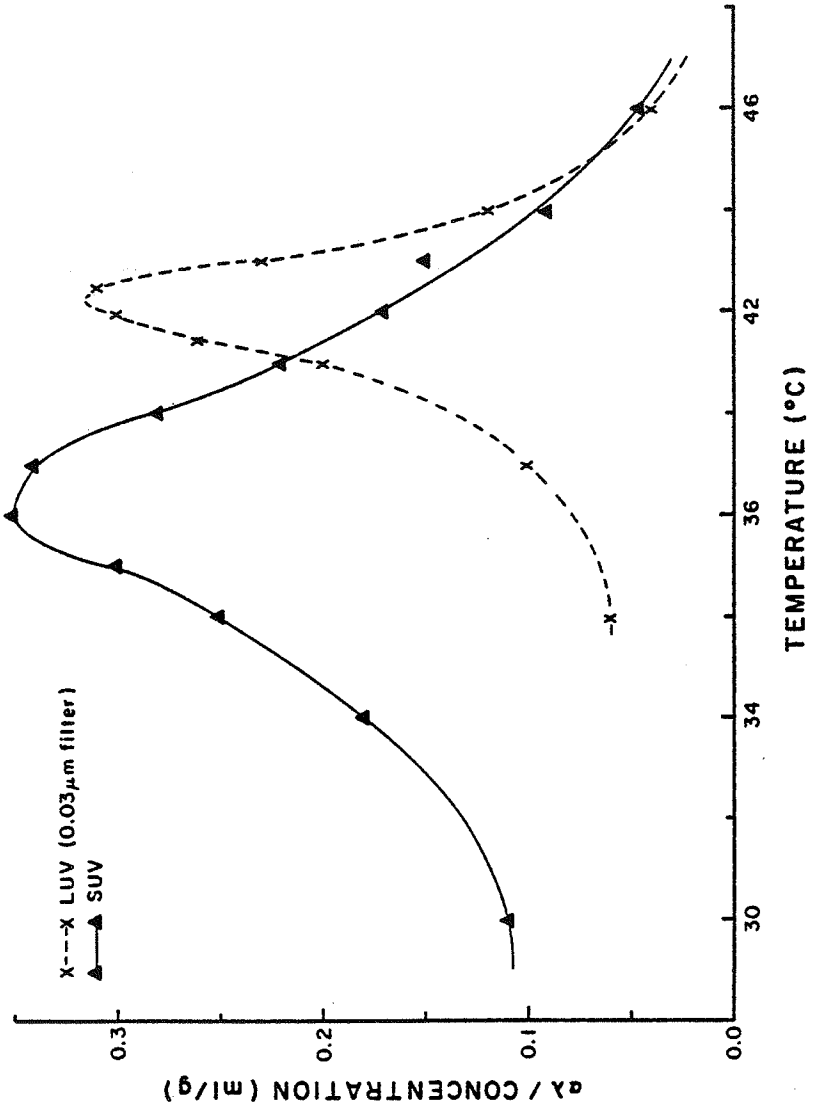

Figure 4.7 Composite from figs. 4.3 and 4.5 showing the specific ultrasonic absorption coefficient per wavelength for suspensions of small unilamellar vesicles and the smallest large unilamellar vesicles.

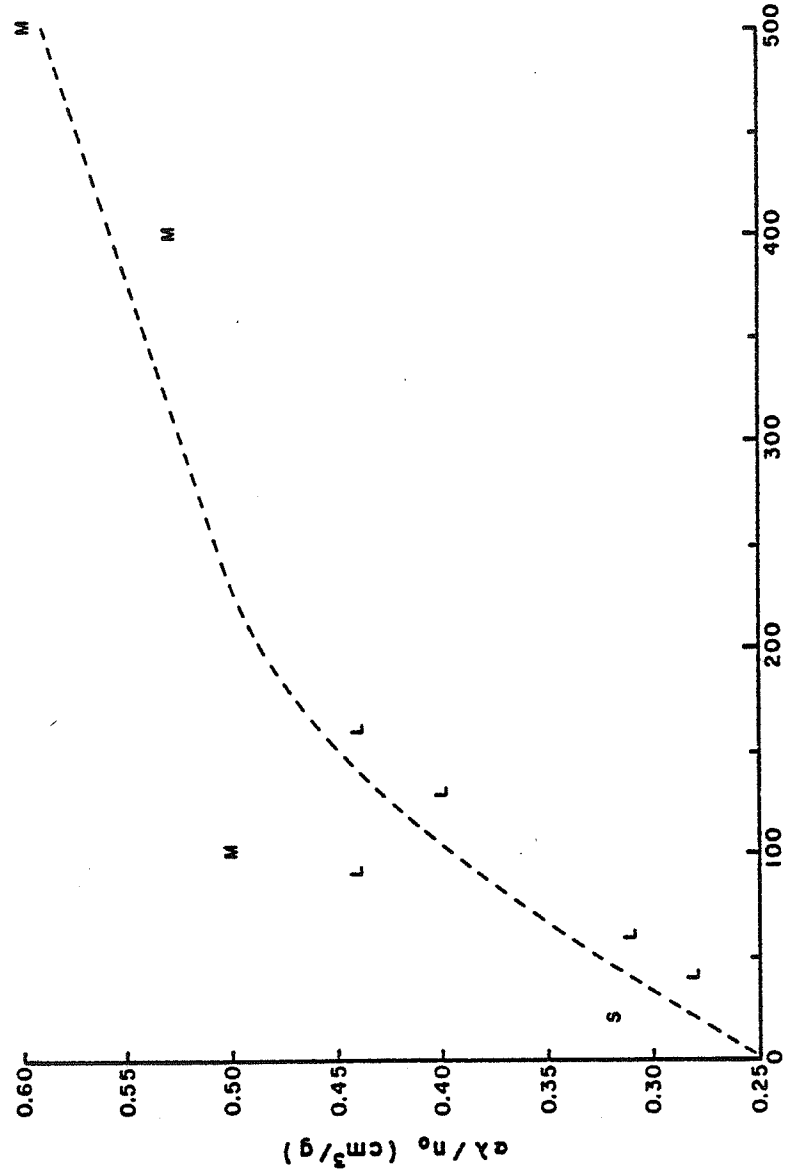

Figure 4.8 Dependence of the specific ultrasonic absorption coefficient per wavelength for liposome suspensions on size. Data are labeled as:
S for small unilamellar vesicles
L for large unilamellar vesicles
M for multilamellar vesicles

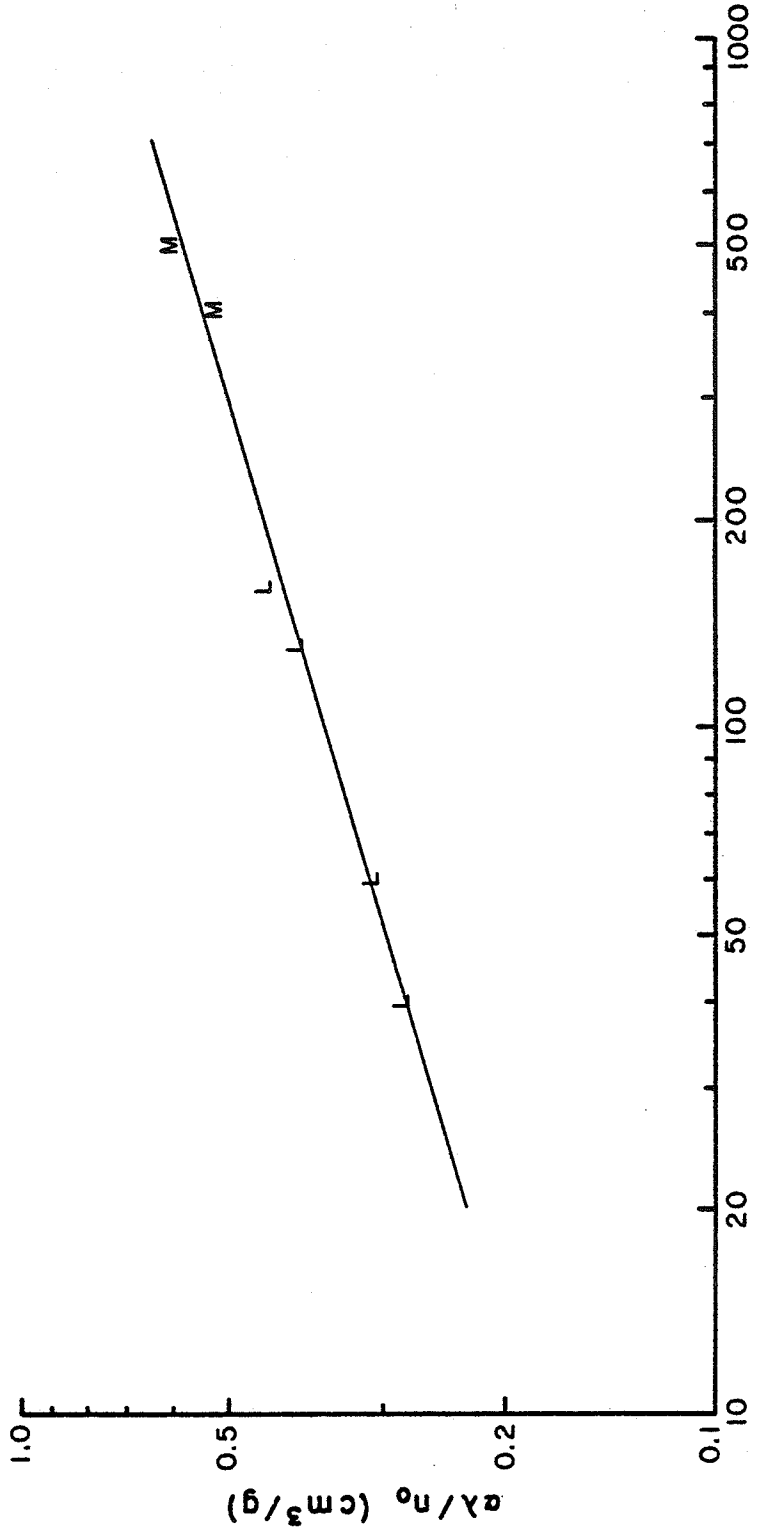

Figure 4.9 Log-log dependence of LUV and MLV on size, from fig.4.8 with exceptions (cf. text). The slope is 0.3.

Calculations from this plot yield: The slope is 0.3. The straight line formula can be applied, using this slope and any particular point on the line, to calculate $\log \alpha\lambda/n_o$ when log d is equal to zero. This results in a value for $\alpha\lambda/n_o$ of 0.1 cm^3/g when d is 1 nm. The straight line formula is then

$$\log \alpha\lambda/n_o = 0.3 \log d + \log 0.1$$

which becomes

$$\alpha\lambda/n_o = 0.1d^{0.3} cm^3/g$$

where the units of d are nanometers.

Figure 4.10 is a plot of the transition enthalpy, calculated from the areas under the absorption vs. temperature curves as described above, vs. diameter. An interesting feature is a peak for the LUV at 100 nm, which is the same diameter at which anomalous absorption behavior occurs (cf. fig. 4.8). The enthalpy for the SUV is quite large, indicating that they experience either a much larger volume change or internal energy increase than do any of the other vesicles. The MLV data show that vesicles whose diameters exceed about 100 nm all experience about the same enthalpy change.

Fig. 4.11 illustrates the van't Hoff enthalpy, ΔH_{vH}, as a function of vesicle diameter. Unlike the transition enthalpy, the van't Hoff enthalpy is a function of the shape of the absorption parameter vs. temperature curve and thus provides more information about the transition. Also unlike the transition enthalpy, the van't Hoff enthalpy exhibits a monotonic increase with vesicle diameter for the LUV.

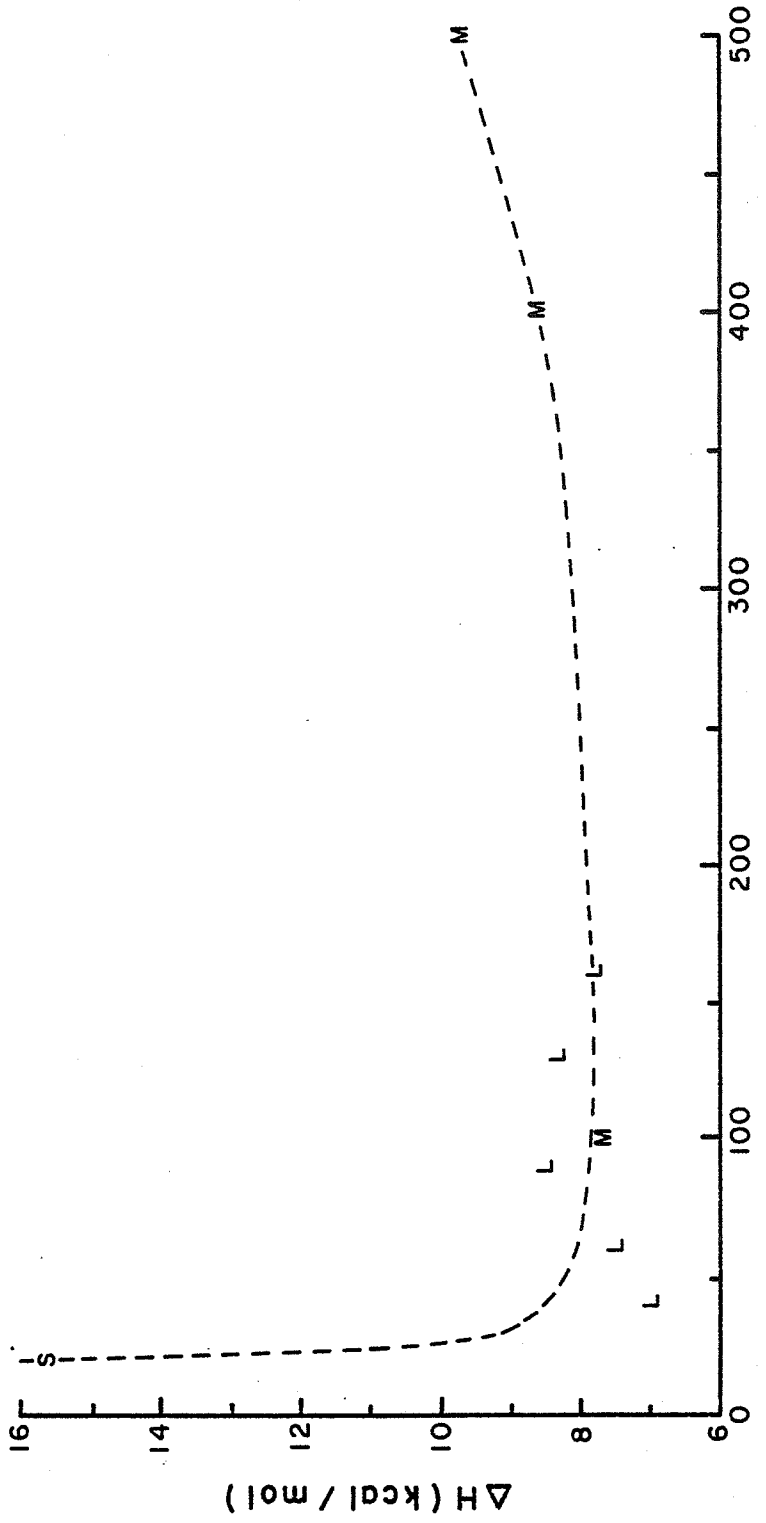

Figure 4.10 The dependence of the phase transition enthalpy for liposome suspensions on size. Data labeled as in 4.8.

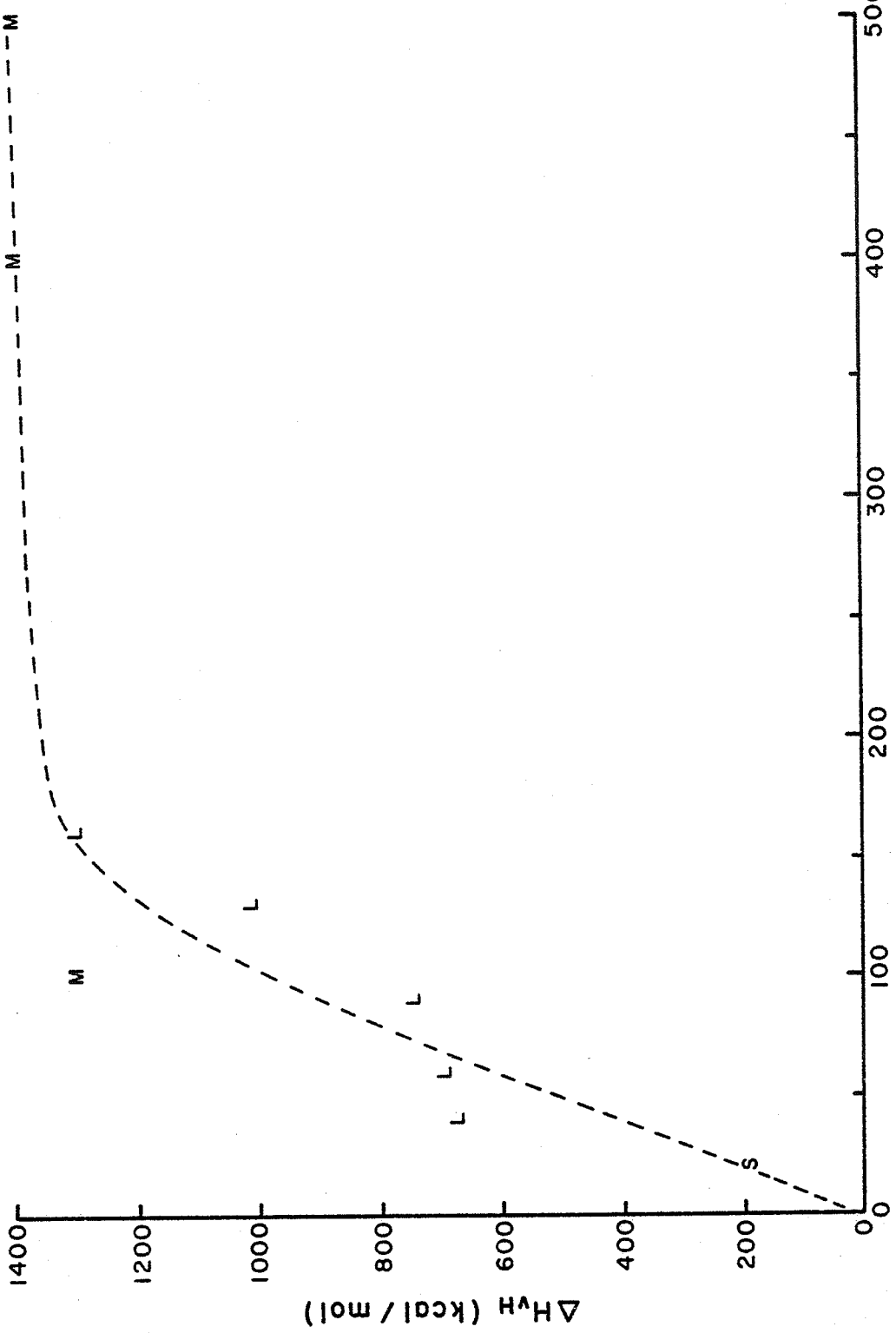

Figure 4.11 The dependence of the van't Hoff enthalpy for the phase transition of liposome suspensions on size. Data labeled as in fig. 4.8.

The ratio, $\Delta H_{vH}/\Delta H$, is proportional to the size of the groups of molecules which simultaneously undergo the transition, i.e., the cooperative unit (Mabrey-Gaud, 1981). Fig. 4.12 shows this ratio as a function of vesicle diameter. It is dominated by the van't Hoff enthalpy and exhibits a general increase with diameter up to 100-150 nm. The data may even indicate three discrete regions of cooperativity, viz., one for the smallest vesicles, one for vesicles with diameters from about 40 to 90 nm, and one for larger vesicles.

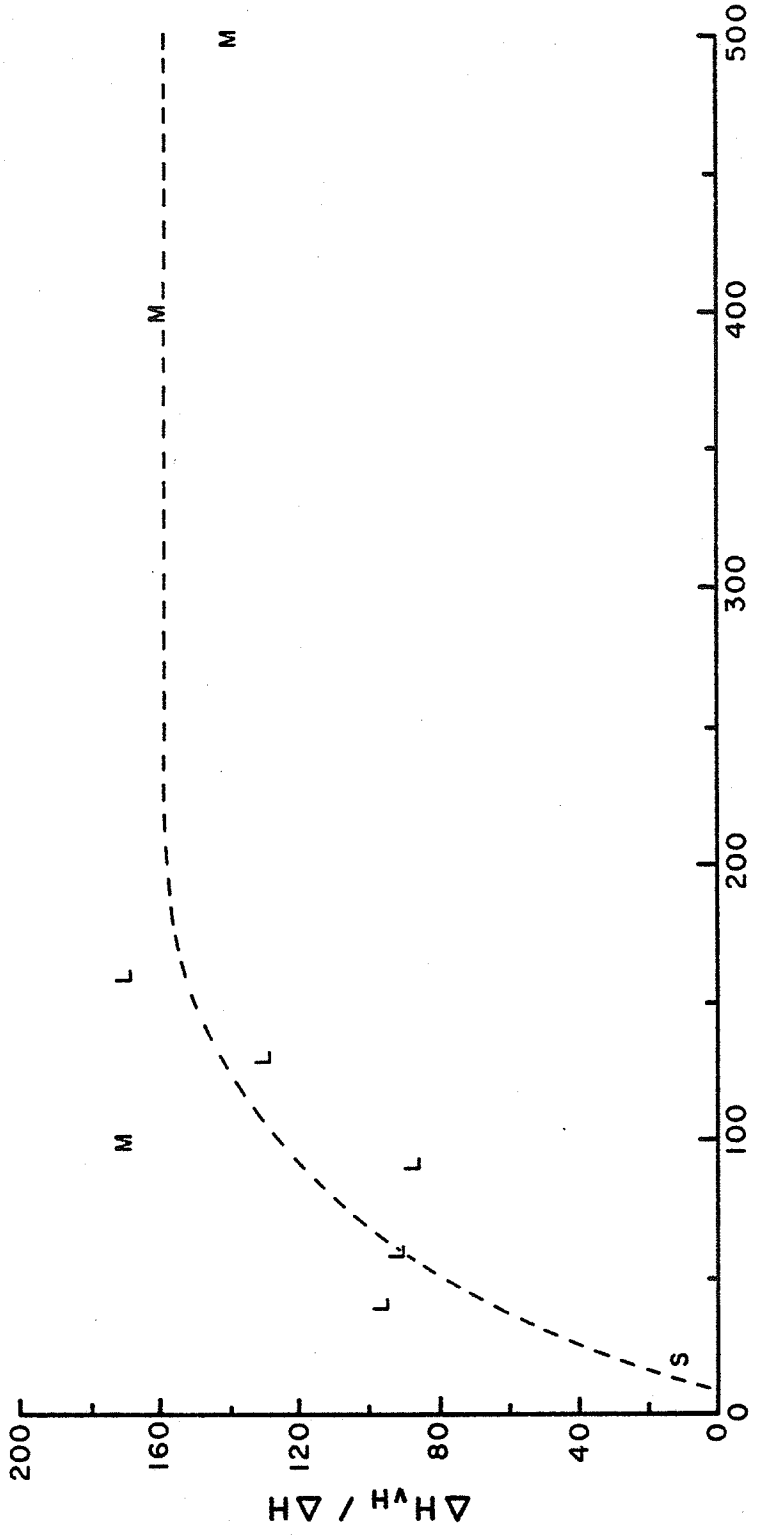

Figure 4.12 The dependence of the ratio of the van't Hoff enthalpy to the transition enthalpy on liposome size. The ratio is proportional to the cooperative unit size (cf. text).

CHAPTER 5

DISCUSSION

5.1 VOLUME CHANGE

5.1.1 Relation to Pressure Perturbation

Irreversible thermodynamics, discussed in section 2.1.2.1, provides a basic approach to a model for ultrasonic absorption. Eigen and De Maeyer (1963) used this approach to obtain an expression for ultrasonic absorption, as a function of the enthalpy change and the volume change experienced by a system which contains equilibria which have been perturbed by a driving force, such as ultrasound. They accomplish this by deriving relationships between three categories of parameters which thermodynamically describe a system in which equilibria are perturbed. The first category is that of the perturbing functions, which are functions of any intensive variable, such as pressure. The second category consists of concentration functions, the concentrations being those of particles in different states. The perturbation of the equilibrium conditions by the changes of the intensive variables causes relative changes in the populations of different states. The third category is that of extensive variables, such as volume. Eigen and De Maeyer (1963) show that the change of the concentration of particles in one state results in a change of extensive parameters.

They begin with Planck's function, $Y = -G/T$, where G is the Gibbs function, $G = H - TS$, the thermodynamic function most suitable when the state of a system is to be specified by

pressure, temperature, and composition variables. The differential of Planck's function is

$$dY = (H/T^2)dT - (V/T)dp - (dU + pdV)/T + dS.$$

The use of Planck's function yields the desired result of a term, $(dU + pdV)/T + dS$, which satisfies two criteria. First, it contains the entropy portion of the function. A nonzero entropy change as the thermodynamic consequence of absorption was discussed in section 2.1.2. Secondly, it contains all of the differentials of the extensive variables and only those differentials. The need for this separation is implied by the summary of the theoretical development in the previous paragraph. Recalling the relationship between these extensive variables and the concentration functions mentioned above, the differentials of the extensive term of Planck's function can be replaced by dn, where n is a concentration term which is a function of the extent of the reaction. This reaction refers to the overall change experienced by a system as the conditions which determine the equilibria are changed, and thus can pertain to a phase transition. Eigen and De Maeyer then consider the coefficient of dn, taking the total differential, i.e., using the operator, d, where $d = \partial/\partial p + \partial/\partial T + \partial/\partial n$. The equilibrium situation with respect to external conditions is expressed by setting the left side of the equation equal to zero. Any change in p or T will shift n to a value which will satisfy a new equilibrium. The function describing the pressure or temperature change is called the forcing function. In this study, p is described by a forcing function, while each chosen value for T determines the particular

equilibrium perturbed by p. The total differential at equilibrium is then solved for $\partial n/\partial p$. The result can be put into the form:

$$\left.\frac{\partial n}{\partial p}\right|_T = \Gamma \left.\frac{\partial \ln K_o}{\partial p}\right|_T \qquad 5.1$$

where K_o is called an equilibrium constant and is defined as the exponential of the coefficient of dn, and Γ is called a function of the equilibrium constant and is

$$\Gamma = \left.\frac{\partial n}{\partial \ln K_o}\right|_{p,T} \qquad 5.2$$

(In the derivation of these equations, the assumptions were made that the perturbations are small and that activity coefficients could be set equal to unity, i.e., only concentrations, not activities, need be considered.) Note that Γ is independent of the forcing function, (p), and simply relates the concentration change, via the change in the extent of the reaction, to a change of the equilibrium constant. Equation 5.1 is an expression of the first relationship which was desired, viz., that between the forcing function and the concentration changes.

This can then be used, along with basic thermodynamic relationships, to obtain dynamic functions relating intensive to extensive variables. The role of adiabatic compressibility in the determination of the ultrasonic absorption amplitude (cf. Eq. 2.27) suggests finding such a relationship between volume and pressure since

$$\kappa_s = -\frac{1}{V}\left.\frac{\partial V}{\partial p}\right|_s$$

In particular, Eq. 2.27 shows that it is the difference, $\kappa_s^o - \kappa_s^\infty$, which contributes to the absorption, and it is this difference which can be determined from the functions developed by Eigen and De Maeyer (1963):

$$\kappa_s^o - \kappa_s^\infty = -\frac{1}{V}\left.\frac{\partial V}{\partial n}\right|_{s,p}\left.\frac{\partial n}{\partial p}\right|_s \qquad 5.3$$

Applying thermodynamic relations and defining Δ as the operator, $\partial/\partial n$, results in the following expression for the first partial derivative:

$$\left.\frac{\partial V}{\partial n}\right|_{s,p} = \Delta V - \Delta H \frac{\beta_p^\infty}{\rho_o c_p^\infty}$$

where β_p^∞ is the coefficient of thermal expansion at infinite frequency. Using thermodynamic relations, the operator, Δ, and Eq. 5.2, the second partial derivative becomes

$$\left.\frac{\partial n}{\partial p}\right|_s = -(\Delta V - \Delta H \frac{\beta_p^\infty}{\rho_o c_p^\infty})\frac{\Gamma}{RT}\frac{c_p^\infty}{c_p^o}$$

where R is the gas constant. Thus Eq. 5.3 becomes

$$\kappa_s^o - \kappa_s^\infty = \frac{\Gamma}{RTV}\frac{c_p^\infty}{c_p^o}(\Delta V - \Delta H \frac{\beta_p^\infty}{\rho_o c_p^\infty})^2 . \qquad 5.4$$

5.1.2 A Model of the Transition

For this study, the phase transition can be considered as a total reaction consisting of the change of state of the molecules in the liposome bilayer. Therefore, at any particular temperature

in the range over which this transition occurs, there will be a particular equilibrium concentration of molecules in each state. The model will be applied to the two state reaction, $A \rightleftharpoons B$, where A and B refer to the (low temperature) solid state and the (high temperature) liquid state, respectively. Experimental evidence is available justifying, at least as a first approximation, the consideration of this simplest of models. First, several studies have shown that, when liposomal aggregation and fusion are eliminated, specific ultrasonic absorption is independent of concentration (Watts et al., 1978). Contrary to the conclusion of these authors, this does not imply the absence of an intermolecular effect, but rather, in a suspension of liposomes, it implies the absence of an interliposomal effect on the transition. Secondly, there is increasing evidence that a homogeneous liposome population exhibits only one relaxation in the frequency range amenable to ultrasonic interrogation (e.g., Sano, et al., 1982). This is plausible even though many molecules must undergo the transition because a two state reaction is characterized by a single relaxation, even if the reaction is effected by a number of parallel reactions; the single relaxation time contains the sum of the rate constants of the parallel reactions (Eigen & De Maeyer, 1963).

The choice of the type of reaction determines the expression for Γ which is obtained by evaluating the derivative of Eq. 5.2. Applying the model to this equation yields the following expressions:

$$\Gamma = \frac{n_A n_B}{n_o} \quad \text{and} \quad \Gamma = \frac{K_o n_o}{(1+K_o)^2} \qquad \text{a and b 5.5}$$

where $n_o = n_A + n_B$; i.e., n_o is the phospholipid concentration. If X is defined as the extent of the reaction, then

$$X = n_B/n_o \quad \text{and} \quad 1-X = n_A/n_o.$$

From Eq. 5.5 a,

$$\Gamma = X(1-X)n_o \equiv \Gamma_X n_o \qquad \text{defn. 5.1}$$

Figure 5.1 shows a plot of Γ_x vs. X.

5.1.3 Relating Volume Change and Ultrasonic Absorption

Finally, the equation relating the absorption per wavelength to volume change is obtained by multiplying the left side of Eq. 2.27 by λ and the right side by $c_r 2\pi/\omega$, substituting the right side of Eq. 5.4 into Eq. 2.27, expressing $\kappa_s^o c_o^2$ in terms of density, according to defn. 2.1, and obtaining the absorption per wavelength normalized with respect to concentration by using defn. 5.1. After solving for terms involving volume, the result is

$$\frac{\left(\Delta V - \Delta H \frac{\beta_p^\infty}{\rho_o c_p^\infty}\right)^2}{V} = \frac{RT}{\pi \Gamma_x} \frac{c_p^o}{c_p^\infty} \frac{1}{\rho_o c_r^2} \frac{1+\omega^2\tau^2}{\omega\tau} \frac{\alpha\lambda}{n_o} \qquad 5.6$$

It can be seen from this equation that Γ_x is a proportionality function between volume change and absorption.

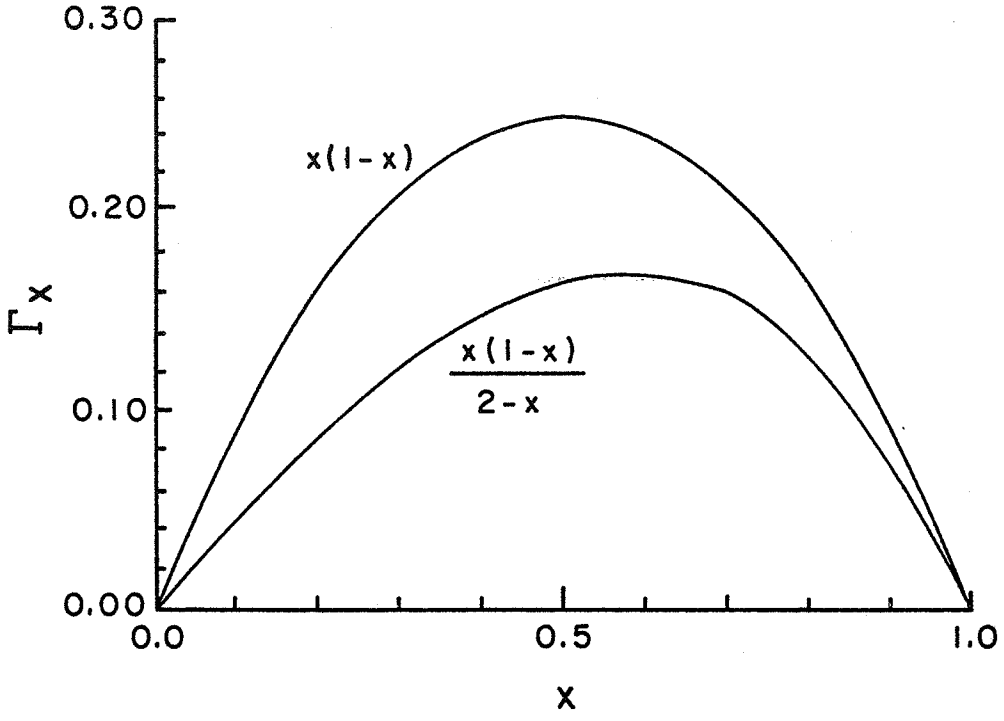

Figure 5.1 The dependence of the specific Γ on the extent of the reaction for different types of one-step reactions.
The upper curve applies to $A \rightleftharpoons B$.
The lower curve applies to $AA \rightleftharpoons B + B$.

To simplify the algebra involved in solving for ΔV, the constants and the variables which can be treated as constants for this study are first introduced:

$$\beta_p^\infty \simeq 10^{-4}/^oC$$

$$\rho_o = 1.0\ g/cm^3$$

$$c_p^\infty = c_p^o = 1\ cal/g^oC$$

$$R = 8.3 \times 10^7\ erg/mol^oC$$

At the midpoint of the reaction, $\Gamma_x = 0.25$, (cf. fig. 5.1). Equation 5.6 may be solved for the absolute value of the volume change:

$$|\Delta V| = 10^{-4}\Delta H + 1.03 \times 10^4 \left(\frac{T}{c_r^2} \frac{1+\omega^2\tau^2}{\omega\tau} \frac{\alpha\lambda}{n_o} V\right)^{1/2} . \qquad 5.7$$

The choice of the value for R determines that the units of ΔH should be cal/mol. The units of volume will be cm^3/mol of phospholipid.

The remaining variables are a function of either the experimental conditions or the type of liposome. There is a paucity of reliable data for ΔH for specific types of liposomes. However, this does not detract appreciably from the use of this equation since $\Delta H\beta_p^\infty/\rho_o c_p^\infty << \Delta V$. A value for ΔH of 9.7 $\pm$ 0.2 kcal/mol for DPPC MLV (Hinz & Sturtevant, 1972) is used for the largest MLV of this study, and values are estimated for the smaller liposomes by comparing the area under the absorption per wavelength vs. temperature curves for these liposomes to that of the large MLV. The relative change in area is also the relative change in ΔH, as described in Chapter 4.

T is T_m, which is described in Chapter 4. Values for both ΔH and T_m are given in Table 4.1.

There are also very few data pertaining to ultrasonic velocity in suspensions of liposomes. Mitaku et al., (1978) report the difference between the velocity in a suspension of DPPC MLV and in the buffer without the liposomes. At the phase transition, this difference is about 50 cm/s. Data obtained during this study using the same type of suspension yielded a difference of about 300 cm/s. Since even this is only 0.2% of the velocity in the buffer, the buffer velocities are used without introducing significant error. Thus c_r will depend only upon T. From results obtained in this study, for T = 39°C, c = 1530 m/s, and for T = 42.0°C or 42.5°C, c = 1535 m/s.

ω is 2π times 3 MHz, the ultrasonic frequency, which was discussed in in section 3.3.2.

The relaxation time, τ, is another parameter whose value is not well established for liposome suspensions. Several studies have found multiple relaxation times for some types of liposomes used in this study, (e.g., Harkness & White, 1979). However, often insufficient attention is given to structural (unilamellar or multilamellar) or size characteristics. Sano et al., (1982), have shown that a homogeneous population of unilamellar liposomes exhibits a single relaxation in the frequency range of 1 to 100 MHz and that the relaxation time is a function of size, thus accounting for the multiple relaxation behavior for a distribution of sizes. The values for τ used in the calculations here, either directly or for interpolation, are shown in Table 5.1, along with the resulting values for the function with ω. It can be seen that

Table 5.1

Some parameters used to calculate the fractional volume change of the liposomes and the results of those calculations

	lip diam (nm) [a]	τ (ns)	$(1+\omega^2\tau^2)/\omega\tau$ [h]	V_e[i] (nm^3)	V[j] (nm^3)	molec x10^3	ΔV (cm^3/mol)	$\Delta V/V$ (%)
SUV	20	18[b]	3.3	0.0042	0.003	2.9	13	1.9
LUV	40	20[c]	3.0	0.034	0.016	13	12	1.6
	60	20[c]	3.0	0.11	0.039	29	13	1.6
	90	23[b]	2.8	0.38	0.093	67	15	1.8
	130	44[d]	2.0	1.2	0.20	150	12	1.5
	160	60[d]	2.0	2.1	0.31	220	13	1.5
	190	76[e]						
MLV	100	24[c]	2.7	0.52	0.21	140	16	1.8
	400	65[f]	2.0	34	3.8	2600	14	1.6
	500	79[g]	2.2	65	6.0	4200	16	1.9
	500	79[g]						

[a] - diameters obtained as described for Table 4.1
[b] - Sano et al. (1982)
[c] - extrapolation from Sano et al. (1982)
[d] - extrapolation from Sano et al. (1982), and Strom-Jensen et al. (1984)
[e] - Strom-Jensen et al. (1984)
[f] - extrapolation from Sano et al. (1982), and White (personal communicaton)
[g] - White (personal communication)
[h] - $\omega=2\pi*3$ Mhz
[i] - volume/liposome, calculated from the external diameter given in the table
[j] - bilayer volume/liposome

the total change in this function over the size range is roughly 50%. Thus the value used for the relaxation time will influence the accuracy of the result, and is, therefore, a source of uncertainty.

$\alpha\lambda/n_o$, the specific absorption per wavelength, is the maximum value for this parameter as determined by the temperature dependence graphs in Chapter 4, and is given in Table 4.1.

The only parameter remaining to be determined is V. It is not the volume change of the entire liposome which is of interest here, but rather, that of the bilayer itself. The buffer can be considered incompressible with respect to the bilayer, and any change in liposome size can be considered the result of an expansion or contraction of the bilayer. The buffer density would remain constant by some of its mass being drawn into or forced out of the liposome, a process which should readily occur given the bilayer's high permeability in the vicinity of the phase transition (Bangham 1981). The thermodynamic development of Eq. 5.7 carries with it the condition that the equation applies to a thermodynamic system. The bilayer and the buffer each constitutes such a system and, therefore, should be considered separately. In this study, only the bilayer is considered.

V must be calculated from the diameters of the liposomes. The thickness of the bilayer is obtained from the literature so that the internal volume can be calculated and subtracted from the total volume. The total volume is

$$V_e = (4/3)\pi(d/2)^3 = (\pi/6)d^3,$$

where d is the diameter describing the external dimensions of the liposomes. The internal volume is

$$V_i = (\pi/6)(d - 2t)^3,$$

where t is the bilayer thickness. The multiple bilayers of the MLV must also be taken into account. Chong & Colbow (1976) used light scattering data and the Rayleigh-Gans scattering theory to estimate the number of bilayers in DPPC MLV. The results range from two to four. Collins (personal communication) used a TNBS fluorescence assay on unfiltered DPPC:DPPG (4:1) MLV synthesized in the same way as were those for this study, and obtained an average of two bilayers per liposome, the number assumed for the following calculations. The volume defined by the external diameter of this internal bilayer is

$$V_{2e} = (\pi/6)[d - 2(t + t_b)]^3,$$

where t_b is the thickness of the buffer layer between the bilayers. The internal volume is

$$V_{2i} = (\pi/6)[d - 2(2t + t_b)]^3.$$

The phospholipid volume per unilamellar and multilamellar vesicle, respectively, is

$$V_e - V_i \quad \text{and} \quad V_e - V_i + V_{2e} - V_{2i}.$$

The value used for t is 40 Å, and that for t_b is 30 Å (Chong & Colbow, 1976). The values for the total volume per liposome and for the bilayer itself are given in Table 5.1.

In the derivation of Eq. 5.7, the definition of the operator, Δ, makes ΔV a specific volume, and the other parameters in the equation determine that ΔV is a per mole volume change. To convert the volume from a per liposome basis to a per mole basis, the number of phospholipid molecules per liposome must be determined. The total outside and inside surface area per liposome can be found by using the diameter and bilayer and buffer layer thicknesses as given in the previous paragraph. The surface area per phospholipid is obtained from the literature as 72 $\mathring{A}$ (Papahadjopoulos & Kimelberg, 1973). The number of phospholipid molecules per liposome is given in Table 5.1. The volume change can then be calculated and divided by the volume to give the fractional change in volume due to the phase transition.

The results shown in Table 5.1 are less than those obtained by Sheetz & Chan (1973), who reported $V = 22$ cm^3/mol, obtained by dilatometry measurements. Dilatometry is a static technique in which the volume change of the suspension is observed directly on a macroscopic scale (Adamson, 1973). Therefore, as discussed in the INTRODUCTION, it is sensitive to only the overall volume change. Because of the periodic nature of ultrasound, it is sensitive to only those processes with a time constant on the order of the period of the sound wave which, for this study, was approximately 50 ns. The smaller volume change obtained in this study suggests, therefore, that the one or more equilibria whose recovery from ultrasonic perturbation occurs approximately during this amount of time are responsible for about half of the total volume change due to the phase transition. Gamble & Schimmel (1978) obtained a value of 25 cm^3/mol using ultrasound. However,

their use of a smaller relaxation time can account for the entire discrepancy. This time is from their own data, and a graph shows that their relaxation time corresponds to a frequency near the lower limit of their measurement capabilities. Thus a more extensive frequency range may indicate a larger relaxation time. Träuble & Haynes (1971) obtained a relative change of 1.4%. However, their T_m was 44°C, which casts doubt on the reliability of their data.

The volume changes can be due to either or both of the two basic components of the system, viz., the phospholipid portion and the associated buffer. For any particular system, the separate effects cannot be detected directly. Because the bilayer structure is better understood, offering more opportunities for speculations concerning models, consideration of the contribution from the associated buffer, referred to as the hydration layer because, in general, it is an aqueous solution, is often ignored. The possibility of this contribution should not be discarded, however, because the amount of bound water is significantly larger above the phase transition. (Watts et al., 1978).

5.1.5 Implications for the Model

In considering the approach to be used in relating these volume changes to the phospholipid portion of the system, per se, the particular suitability of the ultrasonic technique to the study of the thermodynamic state of a system, as discussed in the INTRODUCTION, is recalled. Mechanisms of interaction between ultrasound and the bilayers are considered, therefore, according to their direct contribution to parameters which are functions of

the overall dynamic state of the system, viz., volume and enthalpy (cf. Eq. 5.7). Hammes & Roberts (1970) propose that the volume change obtained by the application of Eq. 5.7 is due to a loosening or tightening of the liposome structure. They are not concerned with temperature changes, but rather with the addition of cholesterol to the bilayer or of positive ions to the buffer of a suspension of liposomes containing negatively charged head groups. A change in such structure is known to occur under these circumstances and also is known to occur as a result of temperature changes (cf. INTRODUCTION). In assuming the simple two state model,

$$A \rightleftharpoons B \quad = \quad \text{tight} \rightleftharpoons \text{loose},$$

the implicit assumption being made is that the phospholipid molecules do not interact in either state, and thus the individual molecules undergo the phase transition independently.

There is evidence, discussed in the INTRODUCTION, which suggests that this may not be the case, but rather, that a more accurate model would be

$$\text{tight} \rightleftharpoons \text{loose} \quad = \quad AA \rightleftharpoons B + B \ ;$$

i.e., there is molecular interaction in the tight (low temperature) state which is absent in the loose (high temperature) state. Note that this still satisfies the one step criterion indicated by a single relaxation time. Γ_X (cf. defn. 5.1) for such a reaction is

$$\Gamma_X = X(1 - X)/(2 - X)$$

(Eigen & DeMaeyer, 1963), which is illustrated in fig. 5.1. In the comments following Eq. 5.6, it was pointed out that Γ_x determines the extent of the reaction at which the volume change will yield the largest absorption. Therefore it can be seen from fig. 5.1 that if the second model more accurately describes the situation, a value of 0.17 should have been used for Γ_x rather than 0.25. The new value of $\Delta V/V$ will be larger than that calculated assuming the first model (cf. Eq. 5.6) by a factor of 1.2. This does not increase the volume change to the values obtained in most other studies, such as Gamble and Schimmel (1978), mentioned in the previous paragraph, but it is a change in the right direction.

It can be seen in fig. 5.1 that, in addition to an amplitude difference, the curves exhibit different shapes. That pertaining to the first model is symmetrical, while that pertaining to the second has a slope with a greater amplitude in the region where the reaction is approaching completion (the high temperature region for this study if, as was usually the case, the dependence upon an increasing temperature was obtained). This is consistent with the shapes of the absorption coefficient per wavelength vs. temperature curves obtained in this study.

CHAPTER 6

SUMMARY AND CONCLUSIONS

The specific ultrasonic absorption coefficient per wavelength as a function of temperature in the vicinity of the phase transition of pure phospholipid liposomes of different sizes was determined using an acoustic interferometer. An absorption peak occurs at the membrane phase transition temperature. The amplitude of the peak exhibits a general increase with size with two exceptions, viz., the SUV and the vesicles with average diameters of 90 to 100 nm. Excluding these exceptions, the absorption coefficient is proportional to the diameter to the 0.3 power. Thus ultrasonic absorption may be used as a general indicator of size, and may be particularly useful in the range where the change from SUV to LUV occurs. All liposome sizes, except the SUV, i.e., even those with diameters as small as approximately 40 nm, exhibit nearly the same transition temperature as do the largest MLV. The enthalpy change due to the transition is found to be independent of size except for the SUV, whose value is approximately twice that of the other sizes. The van't Hoff enthalpy exhibits a general increase with size, with a strong dependence for the smallest vesicles and an approach to independence for the largest vesicles. The ratio of the van't Hoff enthalpy to the transition enthalpy indicates that cooperativity increases with size to a diameter of 100 to 150 nm, above which it is independent of vesicle size.

The absorption coefficient and the transition enthalpy are used to calculate the relative volume change of the membrane. This change is approximately the same for all sizes of liposomes

studied, indicating that the large enthalpy change difference between the smallest vesicles and all of the larger vesicles is due to a larger change in the internal energy of the former, and not to more work performed on them.

The contributions to the increase in knowledge regarding the physical properties of the more useful, intermediate size liposomes shows more precisely the diameters at which these characteristics apparently undergo change. More accurate dimensional data on liposomes having diameters less than 200 nm, together with ultrasonic measurements, should aid in the determination of the critical dimensions, which in turn could be used to test theories describing lateral membrane organization. More accurate data of the diameters for all sizes of liposomes, but especially for the smaller ones, would confirm or refine the empirically derived power relation between the ultrasonic absorption coefficient and liposome diameter, which may prove useful in predicting energy deposition in liposomes at greater ultrasonic intensities. A potential application is the ultrasonic induction of the phase transition due to the conversion of sound energy to heat, an eventual consequence of absorption. This induction is of interest since liposome membranes are very permeable to ions and small molecules only in the vicinity of this transition (Bangham, 1981).

REFERENCES

Adamson, A. W. (1973). A Textbook of Physical Chemistry, Academic Press, New York.

Bangham, A. D. (1981). "Introduction", in Liposomes: from Physical Stucture to Therapeutic Applications, C. G. Knight, ed., Elsevier/North-Holland Biomedical Press, New York, ch. 1.

Bangham, A. D., M. M. Standish, and J. C. Watkins (1965). "Diffusion of Univalent Ions across the Lamellae of Swollen Phospholipids", J. Mol. Biol., 13: 238-252.

Bergelson, L. D. (1978). "Paramagnetic Hydrophilic Probes in NMR Investigatons of Membrane Systems", in Methods in Membrane Biology, Vol. IX, E. D. Korn, ed., Plenum Press, New York, ch. 4.

Beyer, R. T. and S. V. Letcher (1969). Physical Ultrasonics, Academic Press, New York.

Boyd, J. F. (1971). "An Experimental Study of a Two Crystal Acoustic Interferometer", M. S. Thesis, University of Houston.

Chapman, D. and D. T. Collin (1965). "Differential Thermal Analysis of Phospholipids", Nature, 206: 189.

Chong, C. S. and K. Colbow (1976). "Light Scattering and Turbidity Measurements on Lipid Vesicles", Biochim. Biophys. Acta, 436: 260-282.

Collins, M. (1983). University of Illinois, personal communication.

Deamer, D. and A. D. Bangham (1976). "Large Volume Liposomes by an Ether Vaporization Method", Biochim. Biophys. Acta, 443: 629-634.

Del Grosso, V. A. and E. J. Smura (1953). "Materials Suitable for Sound Applications I. Ultrasonic Velocities and Impedances of Selected Liquids", NRL Report 4191, Washington D. C.

Eggers, F. (1968). "Eine Resonatormethode zur Bestimmung von Schall-Geschurndigkeit und Dampfung an geringen Flussigkeitsmengen", Acustica, 19: 323-329.

Eggers, F. and Th. Funck (1973). "Ultrasonic Measurements with Milliliter Liquid Samples in the 0.5-100 MHz Range", Rev. Sci. Instrum., 44: 967-977.

Eggers, F. and Th. Funck (1976). "Ultrasonic Relaxation Spectroscopy in Liquids", Naturwissenschaften, 63: 280-285.

Eggers, F., Th. Funck, and K. H. Richmann (1978). "Improved Ultrasonic Resonator Cell for Liquid Samples", Acustica, 40: 273-275.

Eigen, M. and L. de Maeyer (1963). "Relaxation Methods", in Technique of Organic Chemistry, Vol. VIII, pt. 2, A. Weissberger, ed., Interscience, New York.

Fleischer, S. and L. Packer, eds. (1974). Methods in Enzymology, Vol. XXXII, B, Academic Press, New York.

Fry, W. J. (1949). "The Double Crystal Acoustic Interferometer", J. Acous. Soc. Am., 21: 17-28.

Gamble, R. C. and P. R. Schimmel (1978). "Nanosecond Relaxation Processes of Phospholipid Bilayers in the Transition Zone", Proc. Natl. Acad. Sci., 75: 3011-3014.

Gradshteyn, I. S. and I. M. Ryzhik (1965). Tables of Integrals, Series, and Products, Academic Press, New York, p. 42.

Greenspan, M. and C. E. Tschiegg (1957). "Speed of Sound in Water by a Direct Method", J. Res. Nat. Bur. Stand., 59: 249-254.

Hammes, G. G. and P. B. Roberts (1970). "Ultrasonic Attenuation Measurements in Phospholipid Dispersions", Biochim. Biophys. Acta, 203: 220-227.

Harkness, J. E. and R. D. White (1979). "An Ultrasonic Study of the Thermotropic Transition of Dipalmitoyl Phosphatidylcholine", Biochim. Biophys. Acta, 552: 450-456.

Herzfeld, K. F. and T. A. Litovitz (1959). Absorption and Dispersion of Ultrasonic Waves, Academic Press, New York.

Hinz, H.-J. and J. M. Sturtevant (1972). "Calorimetric Investigation of the Influence of Cholesterol on the Transition Properties of Bilayers Formed from Synthetic L-α-Lecithins in Aqueous Suspensions", J. Biol. Chem, 247: 3697-3700.

Huang, C. (1969). "Studies on Phosphatidylcholine Vesicle Formation and Physical Characteristics", Biochemistry, 8: 344-352.

Hubbard, J. C.(1931). "Acoustic Resonator Interferometer I: The Acoustic System and the Equivalent Electrical Network", Phys. Rev., 38: 1011-1020.

Hunter, J. L. and F. E. Fox (1950). "Resonant Acoustic Interferometry with Air-Liquid Reflecting Surface", J. Acous. Soc. Am., 22: 238-242.

Jain, M. K. (1983). "Nonrandom Lateral Organization in Bilayers and Biomembranes", in Membrane Fluidity in Biology, Vol. 1, Academic Press, New York, ch. 1.

Kanehisa, M. I. and T. Y.Tsong (1978). "Cluster Model of Lipid Phase Transition with Application to Passive Permeation of Molecules and Structure Relaxation in Lipid Bilayers", J. Amer. Chem. Soc., 100: 424-432.

Kinsler, L. E. and A. R. Frey (1962). Fundamentals of Acoustics, John Wiley and Sons, Inc., New York.

Kremkau, F. W. and E. L. Carstensen (1972). "Macromolecular Interaction in Sound Absorption", in Interaction of Ultrasound and Biological Tissues: Workshop Proceedings, J. M. Reid and M. R. Sikov, eds., HEW Publ. (FDA) 73-8008, BRH/DBE 73-1, pp. 37-42.

Labhardt, A. and G. Scharz (1976). "A High Resolution and Low Volume Ultrasonic Resonator Method for Fast Chemical Relaxation Measurements", Ber. Bunsenges., 80: 83-92.

Lehninger, A. L. (1972). Biochemistry, Worth Publishers, Inc., New York.

Leithold, L. (1968). The Calculus with Analytic Geometry, Harper and Row, Evanston.

Linden, C. D., K. L. Wright, H. M. McConnell, and C. F. Fox (1973). "Lateral Phase Separations in Membrane Lipids and the Mechanism of Sugar Transport in Escherichia Coli", Proc. Nat. Acad. Sci. USA, 70: 2271-2275.

Mabrey-Gaud, S. (1981). "Differentional Scanning Calorimetry of Liposomes", in Liposomes: from Physical Structure to Therapeutic Applications, C. G. Knight, ed., Elsevier/North-Holland Biomedical Press, New York, ch. 5.

Magin, R. L. and J. N. Weinstein (1984). "The Design and Characterization of Temperature-Sensitive Liposomes", in Liposome Technology, Vol. III, G. Gregoriadis, ed., CRC Press, Inc., Boca Raton, FL., ch. 10.

Markham, J. J., R. T. Beyer, and R. B. Lindsay (1951). "Absorption of Sound in Fluids", Rev. Mod. Phys., 23: 353-411.

Maxwell, J. C. (1867). Trans. Roy. Soc. (London), 157: 49.

Melchior, D. L. and J. M. Steim (1976). "Thermotropic Transitions in Biomembranes", Ann. Rev. Biophys. Bioeng., 5: 205-238.

Mitaku, S. and K. Okano (1981). "Ultrasonic Measurements of Two-Component Lipid Bilayer Suspensions", Biophys. Chem., 14: 147-158.

Mitaku, S., A. Ikegami, and A. Sakanishi (1978). "Ultrasonic Studies of Lipid Bilayer. Phase Transitions in Synthetic Phosphatidylcholine Liposomes", Biophys. Chem., 8: 295-304.

Niesman, M. R. (1983). University of Illinois, personal communication.

Olson, F., C. A. Hunt, F. C. Szoka, W. J. Vail, and D. Papahadjopoulos (1979). "Preparation of Liposomes of Defined Size Distribution by Extrusion Through Polycarbonate Membranes", Biochim. Biophys. Acta, 557: 9-23.

Overath, P. and H. Träuble (1973). "Phase Transitions in Cells, Membranes, and Lipids of Escherichia Coli. Detection by Flourescent Probes, Light Scattering, and Dilatometery", Biochemistry, 12: 2625-2637.

Papahadjopoulos, D. (1976). in Lipids, Vol. 1, Biochemistry, R. Paoletti, G. Porcellati, and G. Jacini, eds., Raven, New York, pp. 187-195.

Papahadjopoulos, D. and H. K. Kimelberg (1973). "Phospholipid Vesicles (Liposomes) as Models for Biological Membranes: their Properties and Interactions with Cholesterol and Proteins", in Prog. Sur. Sci., Vol. 4, pt. 2, S. G. Davison, ed., Pergamon Press, New York, pp. 141-232.

Papahadjopoulos, D. and N. Miller (1967). "Phospholipid Model Membranes I. Structural Characteristics of Hydrated Liquid Crystals", Biochim. Biophys. Acta, 135: 624-638.

Pauley, H. and H. P. Schwan (1971). "Mechanism of Absorption of Ultrasound in Liver Tissue", J. Acous. Soc. Am., 50: 692-699.

Pierce, G. W. (1925). Proc. Am. Acad. Arts Sci., 60: 271.

Sano, T., J. Tanaka, T. Yasunaga, and Y. Toyoshima (1982). "Studies on the Phase Transition in Single Lamellar Liposomes. 5. The Rapid Process of the Phase Transition", J. Phys. Chem., 86: 3013-3016.

Sessa, G. and G. Weissmann (1968). "Phospholipid Spherules (Liposomes) as a Model for Biological Membranes", J. Lipid Res., 9: 310-318.

Sheetz, M. P. and S. I. Chan (1972). "Effect of Sonication on the Structure of Lecithin Bilayers", Biochemistry, 11: 4573-4581.

Stier, A. and E. Sackmann (1973). "Spin Labels as Substrates: Heterogeneous Lipid Distribution in Liver Microsomal Membranes", Biochim. Biophys. Acta, 311: 400-408.

Stokes, G. G. (1845). Trans. Cambridge Phil. Soc., 8: 287.

Strom-Jensen, P. R. (1983). "Ultrasonic Absorption in Solutions of Proteins and Peptides and in Suspensions of Liposomes", Ph. D. Thesis, University of Illinois, Urbana.

Strom-Jensen, P. R., R. L. Magin, and F. Dunn (1984). "Ultrasonic Evidence for Structural Relaxation in Large Unilamellar Liposomes", Biochim. Biophys. Acta, in press.

Symon, K. R. (1971). Mechanics, Addison-Wesley Publishing Co., Reading, MA.

Szoka, F., Jr. and D. Papahadjopoulos (1978). "Procedure for Preparation of Liposomes with Large Internal Aqueous Space and High Capture by Reverse-Phase Evaporation", Proc. Natl. Acad. Sci., 75: 4194-4198.

Szoka, F., Jr. and D. Papahadjopoulos (1980). "Comparative Properties and Methods of Preparation of Lipid Vesicles (Liposomes)", Ann. Rev. Biophys. Bioeng., 9: 467-508.

Träuble, H. and D. H. Haynes (1971). "The Volume Change in Lipid Bilayer Lamellae at the Crystalline-Liquid Crystalline Phase Transition", Chem. Phys. Lipids, 7: 324-335.

Van Dijck, P. W. M., B. de Kruijff, P. A. M. M. Aarts, A. J. Verkleij, and J. de Gier (1978). "Phase Transitions in Phospholipid Model Membranes of Different Curvature", Biochim. Biophys. Acta, 506: 183-191.

Watts, A., D. Marsh, and P. F. Knowles (1978). "Characterization of Dimyristoylphosphatidylcholine Vesicles and Their Dimensional Changes Through the Phase Transition: Molecular Control of Membrane Morphology", Biochemistry, 17: 1792-1801.

White, R., personal communication.

VITA

Valerie Marie Maynard was born in Elgin, IL on April 29, 1952. She graduated as the valedictorian from Central High School, Burlington, IL, and then graduated magna cum laude with a Bachelor of Arts degree in physics from Bradley University, Peoria, IL. This was followed by graduate study in biophysics at the University of Illinois, Urbana-Champaign, where she held a University Fellowship, a Radiation Oncology Traineeship from the National Institutes of Health, a Teaching Assistantship from the Department of Physiology and Biophysics, and a Research Assistantship from the Department of Electrical and Computer Engineering. Ms. Maynard is a member of Phi Kappa Phi and the American Physical Society.